RESONANCE OF ELECTROMAGNETIC WAVES ON CROSS-MONOPOLE WIRE STRUCTURES

Robert Cornelius Spencer

NAVAL POSTGRADUATE SCHOOL
Monterey, California

THESIS

RESONANCE OF ELECTROMAGNETIC WAVES ON CROSS-MONOPOLE WIRE STRUCTURES

by

Robert Cornelius Spencer

June 1975

Thesis Advisor: Robert W. Burton

REPORT DOCUMENTATION PAGE

READ INSTRUCTIONS BEFORE COMPLETING FORM

1. REPORT NUMBER

2. GOVT ACCESSION NO.

3. RECIPIENT'S CATALOG NUMBER

4. TITLE (and Subtitle)

Resonance of Electromagnetic Waves on Cross-Monopole Wire Structures

5. TYPE OF REPORT & PERIOD COVERED
Master's Thesis; June 1975

6. PERFORMING ORG. REPORT NUMBER

7. AUTHOR(s)

Robert Cornelius Spencer

8. CONTRACT OR GRANT NUMBER(s)

9. PERFORMING ORGANIZATION NAME AND ADDRESS

Naval Postgraduate School
Monterey, California 93940

10. PROGRAM ELEMENT, PROJECT, TASK AREA & WORK UNIT NUMBERS

11. CONTROLLING OFFICE NAME AND ADDRESS

Naval Postgraduate School
Monterey, California 93940

12. REPORT DATE
June 1975

13. NUMBER OF PAGES
124

14. MONITORING AGENCY NAME & ADDRESS(if different from Controlling Office)

Naval Postgraduate School
Monterey, California 93940

15. SECURITY CLASS. (of this report)
Unclassified

15a. DECLASSIFICATION/DOWNGRADING SCHEDULE

16. DISTRIBUTION STATEMENT (of this Report)

Approved for public release; distribution unlimited

17. DISTRIBUTION STATEMENT (of the abstract entered in Block 20, if different from Report)

18. SUPPLEMENTARY NOTES

19. KEY WORDS (Continue on reverse side if necessary and identify by block number)

20. ABSTRACT (Continue on reverse side if necessary and identify by block number)

This investigation experimentally determines the input impedance characteristics of cylindrical monopole and cross-monopole antenna structures of various lengths at 2-12 GHz

frequencies. The analyses of the wire structures include a physical reasoning of resonance effects contributed by various members of the cross-monopoles.

Resonance of Electromagnetic Waves on Cross-Monopole Wire Structures

by

Robert Cornelius Spencer
Lieutenant Commander, United States Navy
B.S. Purdue University, 1963

Submitted in partial fulfillment of the
requirements for the degree of

MASTER OF SCIENCE IN ELECTRICAL ENGINEERING

from the

NAVAL POSTGRADUATE SCHOOL
June 1975

ABSTRACT

This investigation experimentally determines the input impedance characteristics of cylindrical monopole and cross-monopole antenna structures of various lengths at 2-12 GHz frequencies. The analyses of the wire structures include a physical reasoning of resonance effects contributed by various members of the cross-monopoles.

TABLE OF CONTENTS

I. INTRODUCTION ---------- 14

II. NATURE OF THE PROBLEM ---------- 16

III. THEORY ---------- 18

A. MONOPOLES ---------- 18

B. CROSS-MONOPOLES ---------- 24

IV. EXPERIMENTAL APPARATUS ---------- 33

A. WIRE STRUCTURES ---------- 33

B. TEST FIXTURE ---------- 35

C. ANECHOIC CHAMBER ---------- 37

D. MEASUREMENT SYSTEM ---------- 37

1. Configuration ---------- 37

2. Operation ---------- 38

3. Calibration ---------- 43

a. Preparation ---------- 43

b. Warm-Up ---------- 43

c. Load Orientation ---------- 44

V. DATA DISPLAY ---------- 46

A. FORMAT ---------- 46

B. BANDWIDTH (B) AND QUALITY FACTOR (Q) ---------- 46

VI. PRESENTATION OF DATA ---------- 54

A. THE MEASURING SYSTEM ---------- 54

B. TEST FIXTURE ---------- 54

1. APC-7 to N Female Adapter---------- 54

2. Ground Plane Assembly---------- 58

C. MONOPOLES---------- 65

1. 6 mm Monopole---------- 65

2. 12 mm Monopole---------- 67

3. 18 mm Monopole---------- 69

4. 21 mm Monopole---------- 71

5. 24 mm Monopole---------- 73

6. 30 mm Monopole---------- 73

7. 36 mm Monopole---------- 76

8. 42 mm Monopole---------- 76

D. MONOPOLE LENGTH VS FREQUENCY---------- 79

E. CROSS-MONOPOLES---------- 81

1. Cross-Monopole Case 1A ---------- 81

2. Cross-Monopole Case 1B ---------- 86

3. Cross-Monopole Case 2A ---------- 88

4. Cross-Monopole Case 2B ---------- 92

5. Cross-Monopole Case 2C ---------- 96

6. Cross-Monopole Case 2D ---------- 98

7. Cross-Monopole Case 3 ---------- 103

8. Cross-Monopole Case 4 ---------- 105

9. Cross-Monopole Case 5 ---------- 109

10. Cross-Monopole Case 6A ---------- 112

11. Cross-Monopole Case 6B---------- 116

VII. CONCLUSIONS---------- 120

VIII. RECOMMENDATIONS---------- 121

BIBLIOGRAPHY---------- 122

INITIAL DISTRIBUTION LIST---------- 124

LIST OF ILLUSTRATIONS

Figure		Page
1.	Current and charge distributions on a quarter-wave monopole	18
2.	Smith Chart with impedance of monopoles near resonance f_r and antiresonance f_a	20
3.	Current and charge distributions on a three-quarter wave monopole	21
4.	Current and charge distributions on a half-wave monopole	22
5.	Arm loaded monopole	24
6.	Current and charge distributions on cross-monopole #1	27
7.	Current and charge distributions on cross-monopole #2	28
8.	Current and charge distributions on cross-monopole #3	29
9.	Current and charge distributions on cross-monopole #4	29
10.	Cross-Monopole Structure	30
11.	Photograph of wire structures and calibration short	33
12.	Drawing of wire structures and calibration short	34
13.	Feed point	35
14.	Drawing of test fixture	36
15.	Photograph of test fixture	36
16.	Photograph of anechoic chamber	37

		Page
17.	Photograph of HP-8410S Microwave Network Analyzer - Wang 600 Calculating and Plotting System	38
18.	Block diagram of HP-8410S Microwave Network Analyzer - Wang 600 Calculating and Plotting System	39
19.	Block diagram of Interface System	42
20.	Photograph of Hewlett-Packard Calculator-Plotter System	43
21.	Equivalent circuit of wire structure alone	49
22.	Equivalent circuit of wire structure with losses	50
23.	Equivalent circuit of wire structure imperfectly coupled	50
24.	Quality Factor loci of structure equivalent circuits	52
25.	Adapter and Test Unit impedance vs frequency	55
26.	Equivalent circuit of Reflection/Transmission Test Unit	56
27.	Equivalent circuit of adapter	58
28.	Ground plane and Adapter impedance vs frequency	59
29.	Ground planewith feed point	61
30.	Equivalent circuit of ground plane	63
31.	Ground plane impedance vs frequency	64
32.	6 mm Monopole impedance vs frequency	66
33.	12 mm Monopole impedance vs frequency	68
34.	18 mm Monopole impedance vs frequency	70
35.	21 mm Monopole impedance vs frequency	72

		Page
36.	24 mm Monopole impedance vs frequency	74
37.	30 mm Monopole impedance vs frequency	75
38.	36 mm Monopole impedance vs frequency	77
39.	42 mm Monopole impedance vs frequency	78
40.	Monopole resonant length vs frequency	80
41.	Cross-Monopole Case 1A impedance vs frequency	82
42.	Current and charge distributions on cross-monopole Case 1A at 5.40 GHz	83
43.	Current and charge distributions on cross-monopole Case 1A at 10.80 GHz	84
44.	Cross-Monopole Case 1B impedance vs frequency	87
45.	Cross-Monopole Case 2A impedance vs frequency	89
46.	Current and charge distributions on cross-monopole Case 2A at 3.26 GHz	90
47.	Current and charge distributions on cross-monopole Case 2A at 5.80 GHz	91
48.	Cross-Monopole Case 2B impedance vs frequency	93
49.	Current and charge distributions on cross-monopole Case 2B at 2.93 GHz	94
50.	Current and charge distributions on cross-monopole Case 2B at 5.46 GHz	94
51.	Current and charge distributions on cross-monopole Case 2B at 9.25 GHz	95
52.	Cross-Monopole Case 2C impedance vs frequency	97
53.	Current and charge distributions on cross-monopole Case 2C at 8.70 GHz	98
54.	Cross-Monopole Case 2D impedance vs frequency	99
55.	Current and charge distributions on cross-monopole Case 2D at 3.73 GHz	100

		Page
56.	Current and charge distributions on cross-monopole Case 2D at 9.00 GHz	101
57.	Cross-Monopole Case 3 impedance vs frequency	102
58.	Current and charge distributions on cross-monopole Case 3 at 2.93 GHz	103
59.	Current and charge distributions on cross-monopole Case 3 at 9.00 GHz	104
60.	Cross-Monopole Case 4 impedance vs frequency	106
61.	Current and charge distributions on cross-monopole Case 4 at 3.73 GHz	107
62.	Current and charge distributions on cross-monopole Case 4 at 5.58 GHz	107
63.	Current and charge distributions on cross-monopole Case 4 at 9.75 GHz	108
64.	Cross-Monopole Case 5 impedance vs frequency	110
65.	Current and charge distributions on cross-monopole Case 5 at 5.32 GHz	109
66.	Current and charge distributions on cross-monopole Case 5 at 9.75 GHz	111
67.	Cross-Monopole Case 6A impedance vs frequency	113
68.	Current and charge distributions on cross-monopole Case 6A at 3.38 GHz	112
69.	Current and charge distributions on cross-monopole Case 6A at 5.44 GHz	114
70.	Current and charge distributions on cross-monopole Case 6A at 10.80 GHz	115
71.	Cross-Monopole Case 6B impedance vs frequency	117

		Page
72.	Current and charge distributions on cross-monopole Case 6B at 2.80 GHz	118
73.	Current and charge distributions on cross-monopole Case 6B at 9.00 GHz	118

ACKNOWLEDGEMENT

I wish to express my appreciation to Professor R.W. Burton for his inspiration, invaluable aid, and councel during the preparation of this thesis. His academic leadership is unsurpassed.

In addition, I want to thank my wife, Beverly, and son, Scott, for their continuing support, assistance, and self denial without which, this study would not have been possible.

I. INTRODUCTION

The characteristics of straight cylindrical antennas are well known.[1] These parameters have been theoretically derived and experimentally measured by many antenna students and professional investigators. The fundamental theory relates to a perfectly conducting wire with zero radius over a lossless infinite ground plane, the unit driven by a perfect sinusoidal source with a matched impedance through a perfect feed point. Extensions of the basic theory account for deviations from these ideal conditions. Experimental measurements of practical antenna systems have confirmed the theory to a high degree of accuracy.

Subsequently, a large body of literature has built up concerning the parameters of more complex antenna structures. The primary purpose of this investigation is to add to the data bank of experimental measurements the input impedance characteristics of cylindrical monopole and cross-monopole antenna structures at microwave frequencies with emphasis on the resonance of structure members. The impedance

---

[1] King, D.D., "Measured Impedance of Cylindrical Dipoles", Journal of Applied Physics, p. 844, Vol. 17, 1946.

characteristics of the measuring system output and the test fixture used were also established as references for analysis. The analysis of wire structures also include an identification of current and charge distributions, and physical reasoning of resonance effects contributed by various members of the cross-monopoles.

II. NATURE OF THE PROBLEM

The crossed-dipole receiving antenna has been used as a model for the prediction of electromagnetic pulse (EMP) effects on aircraft. At some specific frequencies of excitation, some members of the structure can support resonance with attendent large amplitude standing waves of current and/or charge in such a way that maximums or minimums in these waves may occur at the junction of the cross.[2]

Thin wire antenna theory utilizes assumptions of boundary conditions in the vicinity of the junction based on rotational symmetry. However, this assumption is not valid in the region closer than $\lambda/10$ from the junction; hence, measured values differ significantly from predicted results.[2]

Professional investigators are continuing to produce theory and measurements of cross-wire structures as receiving

---

[2] Burton, R.W., "The Crossed-Dipole Structure of Aircraft in an Electromagnetic Pulse Environment", Proceedings of The Conference on Electromagnetic Noise, Interference and Compatibility Advisory Group for Aerospace Research and Development (AGARD) NATO, pp. 30-1 thru 30-15, Paris, France, October 1974.

antennas.[3] The electrical resonances of structure members have come to be recognized as important parameters. Therefore, this study attempts to identify resonance phenomena through the swept frequency impedance characteristics of various cross-wire configurations.

---

[3] Burton, R.W. and King, R.W.P., "Measured Currents and Charges in Thin Crossed Antennas in a Plane Wave Field," IEEE Transactions on Antennas and Propagation (to be published).

III. THEORY

A. MONOPOLES

A monopole antenna over a perfectly conducting ground plane infinite in extent, the unit driven by a sinusoidal source, is assumed to have sinusoidal charge and current distributions along the monopole length. If the monopole is electrically one-quarter wavelength long at the driven frequency, the current is assumed to be zero at the end and therefore maximum at the feed point; the opposite being assumed for the charge. This is depicted in Figure 1.

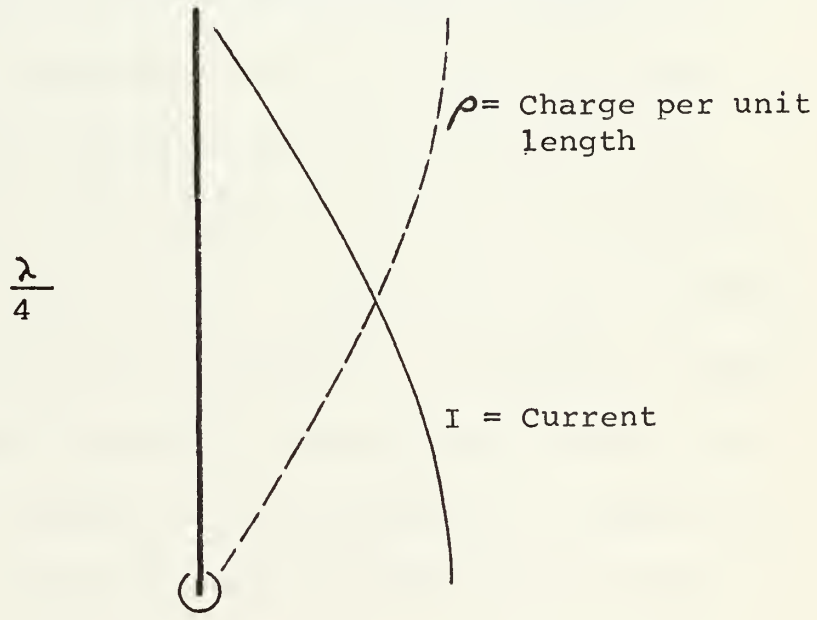

Figure 1

Current and charge distributions on a quarter-wave monopole

It should be noted that the zero current assumption at the end of a monopole is strictly true only for a

monopole with zero radius.[4] For thicker antennas, the current does not approach zero at the ends since the end caps can support radial currents. In addition, the current and charge distributions with length are not strictly sinusoidal although nearly so.[4] However, for visualization purposes, these assumptions will be continued throughout this discussion.

For the quarter-wave monopole at the resonant frequency, f_r, the current is in time phase with the voltage at the feed point and the impedance is real and minimum.[5] This impedance is labelled f_r on the Smith Chart in Figure 2. At slightly lower frequencies, the same monopole is electrically shorter than a quarter-wave, the current at the feed point is less and the voltage is more with the current leading the voltage which causes a capacitive input impedance. This is the impedance at f_1 in Figure 2. At slightly higher frequencies, the same monopole is electrically longer than a quarter-wave, the current at the feed point is less and the voltage is more with the voltage leading the current

---

[4] King, Ronald W.P., The Theory of Linear Antennas, pp. 86-87, Harvard University Press, 1956.

[5] King, R.W.P., The Theory of Linear Antennas, pp. 152-153, Harvard University Press, 1956.

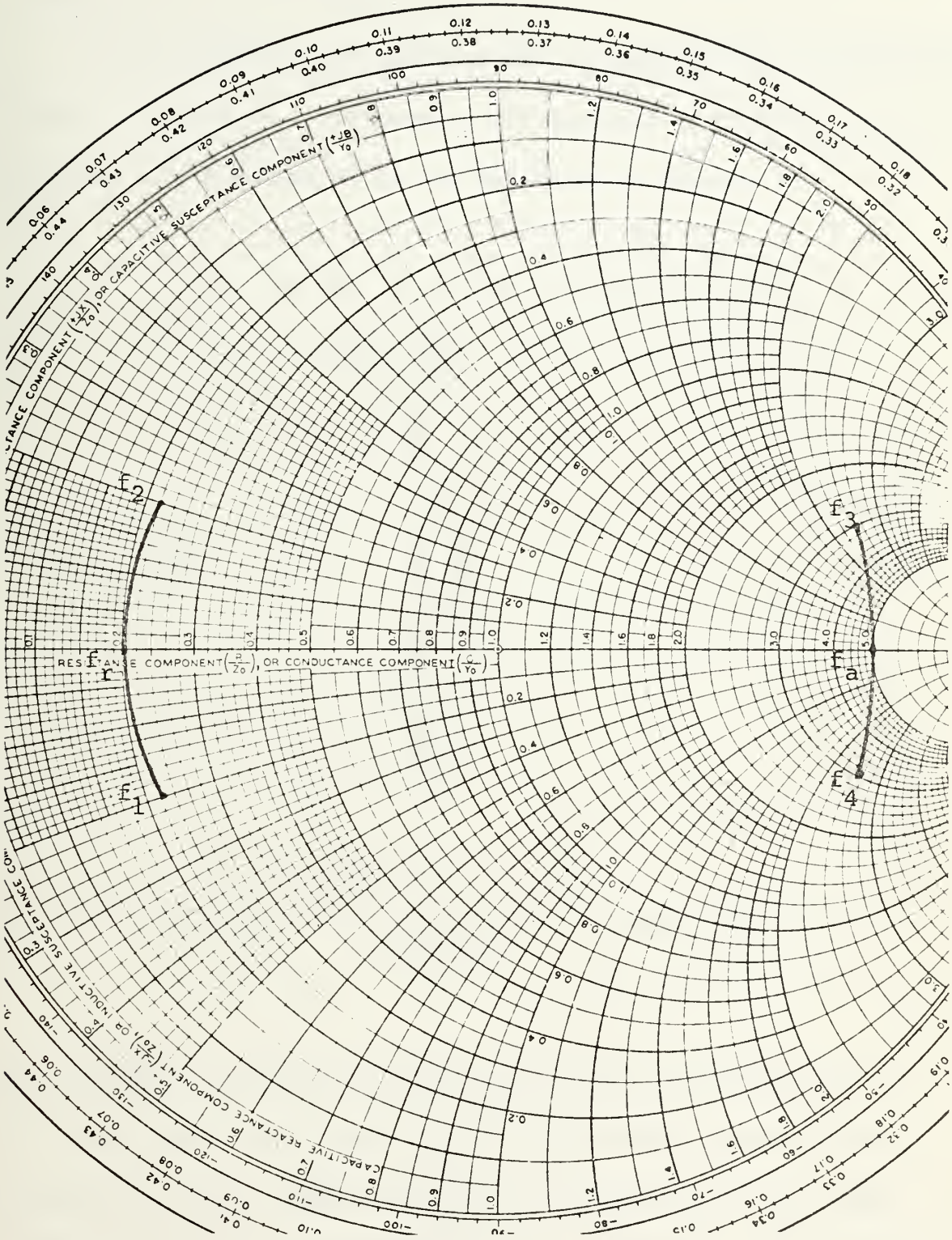

Figure 2
Smith Chart with impedance of monopoles near resonance f_r and antiresonance f_a

which causes an inductive input impedance. This is the impedance at f_2 in Figure 2.

If the monopole is electrically three-quarters wavelength long at the driven frequency, the current and charge distributions are assumed to be as depicted in Figure 3.

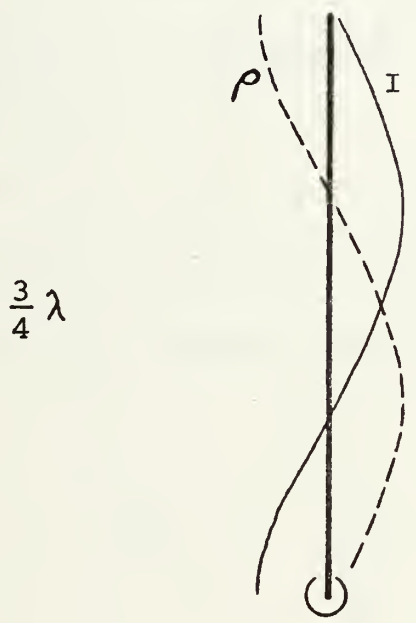

Figure 3
Current and charge distributions on a three-quarter wave monopole

The descriptions of the current, voltage, and impedance at the feed point are identical to that of the quarter-wave monopole and the impedance may be visualized as the same curve, f_1 to f_2, on the Smith Chart in Figure 2 but translated to the left to account for the lower resonant

resistance of the longer element. The same description would apply to any monopole which is electrically an odd number of quarter wavelengths long at the driven frequency; that is if

$$H = n\frac{\lambda}{4} \quad , \; n \text{ odd}$$

where H is the length of the monopole and λ is the wavelength on the monopole, which is the condition defining input resonance.[5] Any monopole of such a length is said to be current fed.

On the other hand, if the monopole is electrically one-half wavelength long at the driven frequency, the current and charge distributions are assumed to be as depicted in Figure 4.

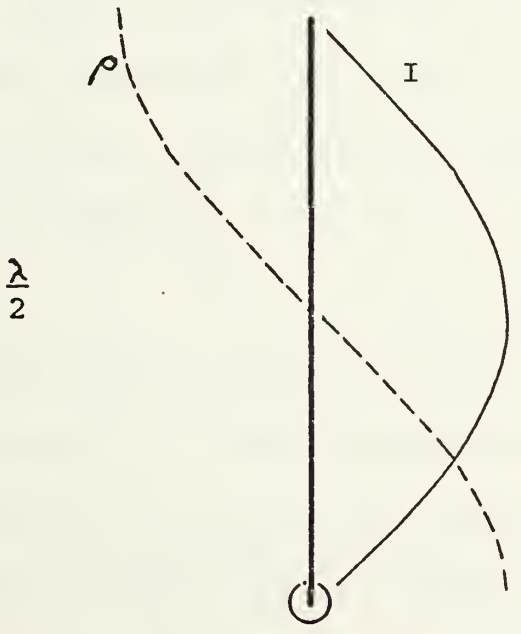

Figure 4

Current and charge distributions on a half-wave monopole

At this antiresonant frequency, at the feed point, the current is minimum and in-phase with the voltage which is maximum causing an input impedance which is real and maximum.[5] This is the impedance at f_a in Figure 2. At slightly lower frequencies, the same monopole is electrically shorter, the current at the feed point is greater and the voltage is less with the voltage slightly leading the current causing an inductive input impedance. This impedance is labelled f_3 in Figure 2. At slightly higher frequencies, the same monopole is electrically longer, the current at the feed point is greater and the voltage is less with the current slightly leading the voltage causing a capacitive input impedance. This is the impedance at f_4 in Figure 2.

The same description would apply to any monopole which is electrically an integer number of half-wavelengths long at the driven frequency; that is if

$$H = m \frac{\lambda}{2} \quad , \text{ m an integer}$$

which is the condition defining input antiresonance.[5] The input impedance of all such monopoles may be visualized as the same curve, f_3 to f_4, on the Smith Chart in Figure 2 but translated to the left to account for the lower antiresonant resistance of the longer element. Any monopole of such a length is said to be voltage fed.

For the ideal conditions assumed in this discussion, and near the resonant or antiresonant frequency, it may also be assumed that a small increase in length of a monopole at a fixed frequency is equivalent to a small increase in frequency with a fixed length monopole. Of course, a decrease in length is also equivalent to a decrease in frequency. This assumption will be useful in the analysis of more complex structures.

B. CROSS-MONOPOLES

The analysis of a monopole with an arm attached perpendicular to its length is somewhat more complicated. Such a structure is shown in Figure 5.

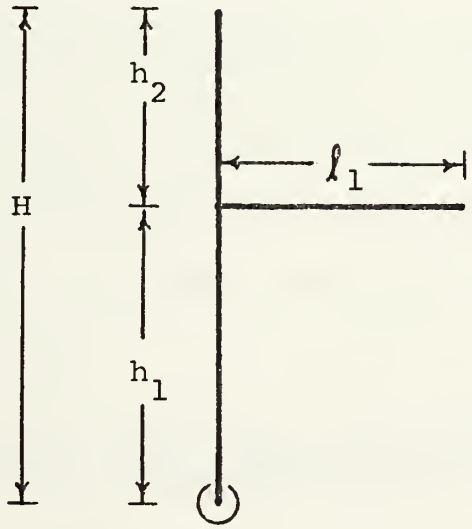

Figure 5
Arm loaded monopole

Mathematical methods and associated computer programs have been applied to this analysis problem with some success

as related to the limited experimental measurements available. For example, C.D. Taylor reported on scattering from thin crossed wires in 1970.[6] Chao and Strait followed in 1971 with some related work on the thin crossed wire problem.[7] In 1972, C. M. Butler reported using piecewise sinusoidal current basis functions in the analysis of thin crossed wires.[8] Related thin wire computer programs such as the Syracuse University Program by Chao and Strait, the Antenna Modeling Program (AMP) by Miller, the Ohio State Program by Richmond, the TCI Program by Tanner, and the Bigant Program by Arens, have been applied to the junction problem.

In good cylindrical conductors, conduction electrons are assumed to reside on the surface, and surface current to flow almost entirely in the axial direction, constant circumferentially at a given cross section.[9]

---

[6] Taylor, C.D., Lin, S.M., and McAdams, H.V., "Scattering from Crossed Wires", IEEE Transactions on Antennas and Propagation, Vol. 18, pp. 133-136, January 1970.

[7] Chao, H.H. and Strait, B.J., "Radiation and Scattering by Configurations of Bent Wires with Junctions", IEEE Transactions on Antennas and Propagation, Vol. 19, pp. 701-702, September 1971.

[8] Butler, C.M., "Currents Induced on a Pair of Skew Crossed Wires", IEEE Transactions on Antennas and Propagation, Vol. 20, pp. 731-736, November 1972.

[9] Ramo, S., Whinnery, J.R., and VanDuzer, T.V., Fields and Waves in Communications Electronics, pp. 254-293, Wiley, 1965.

Therefore, at a junction, the charge is assumed to be equally divided between the connecting conductors, the surface of the junction being equipotential.

$$\rho_{h_1} = \rho_{h_2} = \rho_{\ell_1} \qquad \text{at the junction}$$

This charge distribution was analyzed by King and Wu.[10] Further, Kirchoff's Current Law applied at the junction states that the summation of currents into the connecting members must equal zero.

$$I_{h_1} + I_{h_2} + I_{\ell_1} = 0 \qquad \text{at the junction}$$

These assumptions, although not all exact, are valid for the purposes of this study.

One simplistic view of such a cross-monopole as seen from the feed point, is as a loaded vertical monopole. The loading causes the presumed monopole to appear longer than the length of the vertical member and to have a smaller resonant radiation resistance. At the junction, the current is afforded an additional path in which to flow and the charge is provided an additional conductor on which to accumulate.

---

[10] King, R.W.P. and Wu, T.T., "Analysis of Crossed Wires in a Plane-Wave Field," Tech. Rept. No. 653, Division of Engineering and Applied Physics, Harvard University, Cambridge, Mass., July 1974.

Another view of the cross-monopole considers the electrical length of each member and the current and voltage phases at the junction. For example, consider the simple three-quarter wave monopole shown in Figure 3 with its current and charge distributions. If an arm is attached one-quarter wavelength from the top of the monopole and assuming no distortion of the distributions, the arm would be fed from a maximum current and minimum charge point. If the arm were one-quarter wavelength long at the driven frequency, then the quarter-wave monopole distribution of Figure 1 could be assumed in that arm. Maximum loading effects could thus be expected. This combination of distributions is shown in Figure 6.

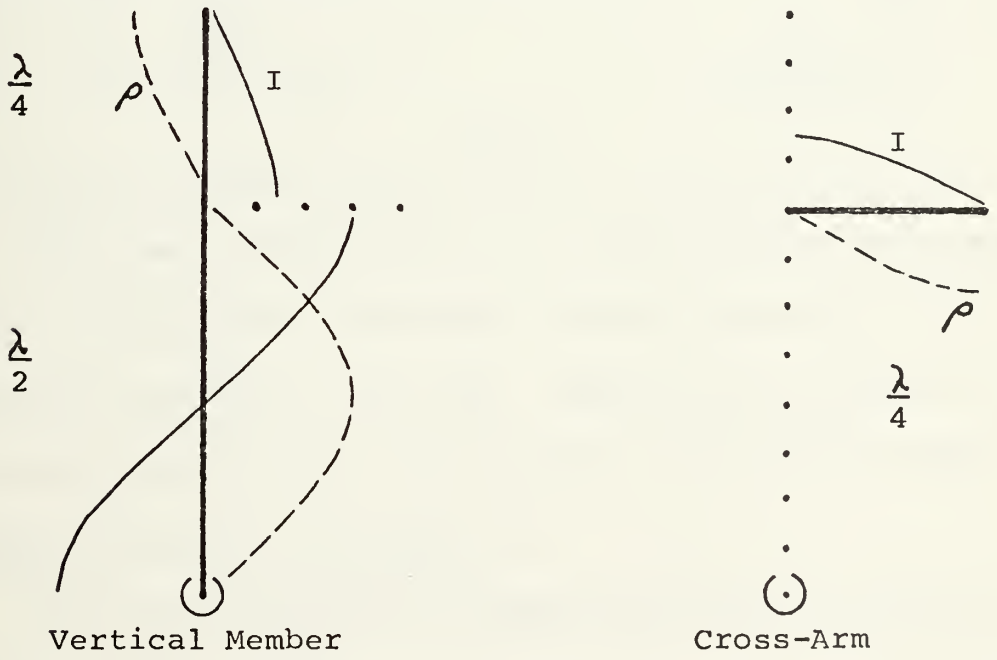

Figure 6

Current and charge distributions on cross-monopole #1

If the arm were attached one-quarter wavelength from the feed point and again assuming no distortion of the distributions, the arm would be fed from a maximum charge and minimum current point. This combination of distributions is shown in Figure 7.

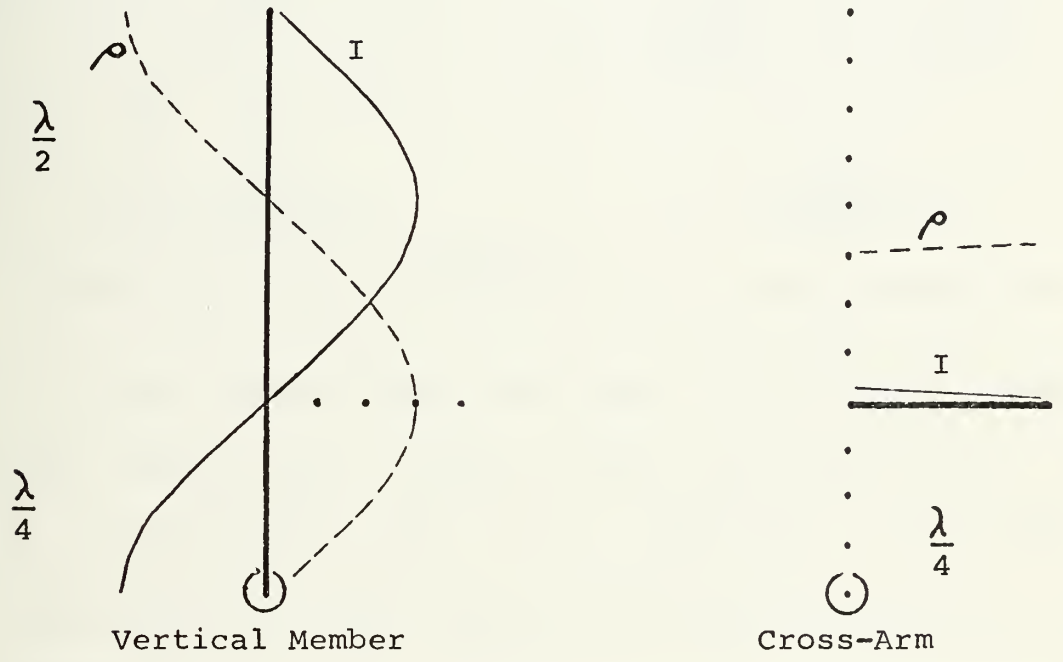

Figure 7
Current and charge distributions on cross-monopole #2

In this case, although the arm is one-quarter wavelength long at the driven frequency, the feed conditions do not support resonance in the arm. Under this condition, the loading effect of the arm would be expected to be much less than in the case of Figure 6.

Consider a monopole to which two arms of different lengths are attached at the same position. Such a structure is shown in Figure 8 along with the assumed current and charge distributions.

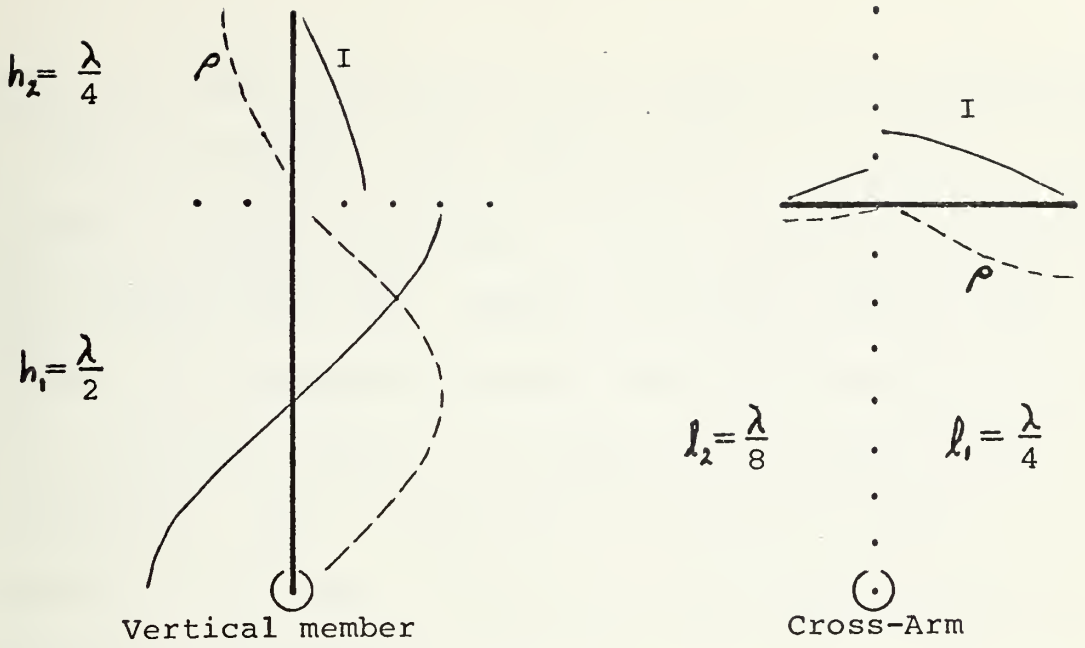

Figure 8
Current and charge distributions on cross-monopole #3

It is seen that although both arms are fed from the same point; hence, from a common current and charge point, arm ℓ_1 is resonant but ℓ_2 is not. Therefore, ℓ_1 provides heavy loading at this frequency but ℓ_2 provides only light loading.

However, if the same structure were driven with twice the frequency, the analysis would be as indicated in Figure 9.

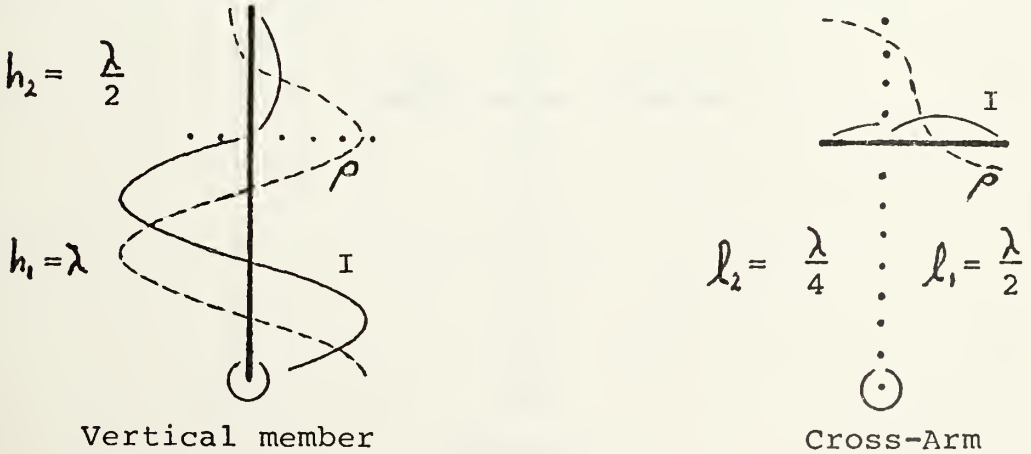

Figure 9
Current and charge distributions on cross-monopole #4

In this case, the current at the junction is minimum and the charge is maximum. Even though arm ℓ_2 is a quarter wavelength long, the necessary driving current is not available to resonate this arm. However, arm ℓ_1, being a half wavelength long, requires minimum current and maximum charge at the junction; hence, is half-wave antiresonant at the driven frequency. From a comparison of Figures 8 and 9, it can be seen that the same structure can react quite differently at different frequencies.

Up to this point, structure member lengths have been constrained to be multiples of quarter-wavelengths. However, in general, at a given driving frequency, none of the members are necessarily of resonant length.

Assume a structure of the form shown in Figure 10 with $h_1 > \ell_1 > h_2 > \ell_2$.

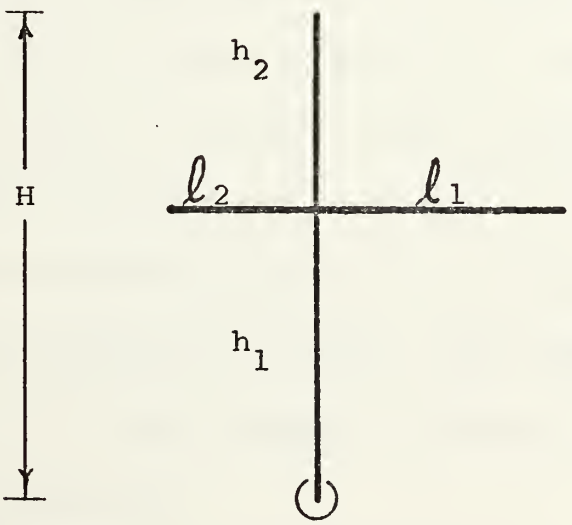

Figure 10

Cross-monopole structure

As the driving frequency is increased from a low value, a frequency will be reached at which the structure is resonant; that is, at which the input impedance is real and minimum. A quarter-wave monopole which was resonant at the same frequency would have length H' > H. Now, as the frequency is further increased, another point will be reached at which $h_1+\ell_1$ is a quarter-wavelength on the structure. This should provide some positive re-enforcement to the driving frequency and cause the current to favor the ℓ_1 member at the expense of the h_2 and ℓ_2 members. Although the input impedance is, in general, complex at this frequency, some perturbation in linearity might be expected due to the change in current distribution between the members at the junction. A similar condition will obtain at higher frequencies when the frequency is such that $h_1 + h_2$ quarter-wave resonant, or at multiples of these frequencies. Another condition will occur when h_1, h_2, ℓ_1, or ℓ_2 is quarter-wave resonant. Although these members are not terminated at the junction, an impedance mismatch exists at that location which should cause a wave reflection of small magnitude. Hence, a slight perturbation in input impedance linearity might be expected at these frequencies.

Some structures may include two or more members which are the same length. Under this condition, these members

should resonate at the same frequency. Since all of the members of the structure are coupled, greater perturbations in input impedance linearity might be expected in this situation.

As a consequence of the foregoing qualitative analysis of a simple cruciform structure, seven frequencies exist at which nonlinearities in input impedance may occur as well as multiples of these frequencies.

IV. EXPERIMENTAL APPARATUS

A. WIRE STRUCTURES

American (B&S) gauge 17 solid, annealed, copper wire was used in the construction of the monopoles and cross-monopoles used in this study. The nominal diameter of this wire is 1.15 mm with an ohmic resistance of 1.663×10^{-5} Ω/mm at 20°C. However, the use of fine-grade steel wool in the removal of insulating varnish from the wire reduced its diameter to 1.10 mm. The wires, at the junctions, were shaped to maintain uniform dimensions and joined by 3AG60SN solder. Length dimensions were controlled to within ± 0.1 mm.

Eight monopoles and eleven cross-monopoles were constructed. A photograph of the actual structures used is shown in Figure 11. Drawings of the wire structures and a calibration short are shown in Figure 12.

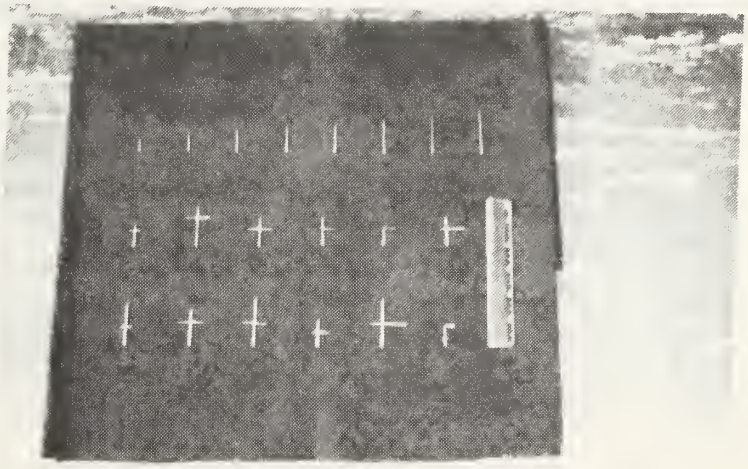

Figure 11

Photograph of wire structures and calibration short

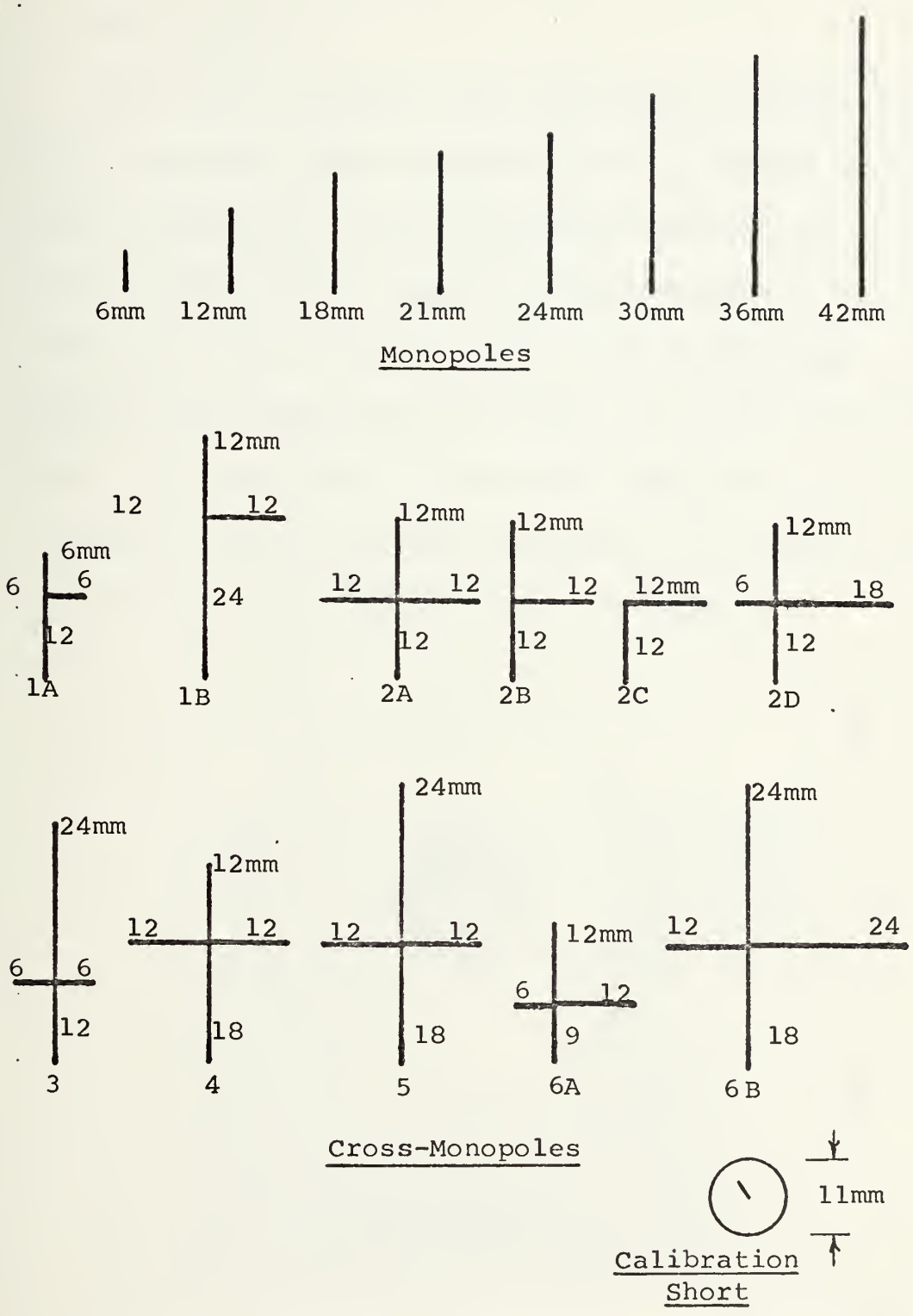

Figure 12

Drawing of wire structures and calibration short

B. TEST FIXTURE

Each wire structure to be measured was inserted 5.5 mm into the hollow center conductor of an Amphenol UG/U 58 panel receptacle. The receptacle was mounted on an aluminum ground plane using a copper stand-off block to maintain the feed point flush with the face of the ground plane. The ground plane measurements were 30.5 cm x 30.5 cm square and 3 mm in thickness. The center feed point aperture in the ground plane was 6 mm in diameter. An enlarged sketch of the feed point region is shown in Figure 13.

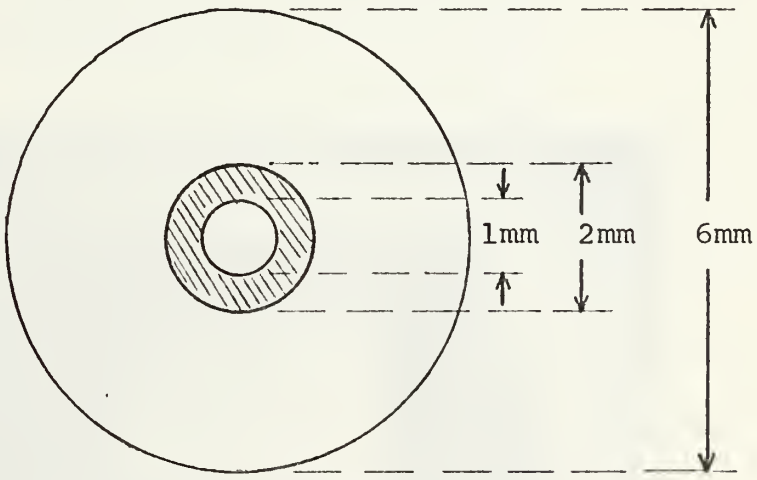

Figure 13

Feed point

The panel receptacle was then connected to the signal source by means of an HP-11524A APC-7 to N Female Adapter. A cross section view of this assembly with the calibration

short installed is shown in Figure 14.

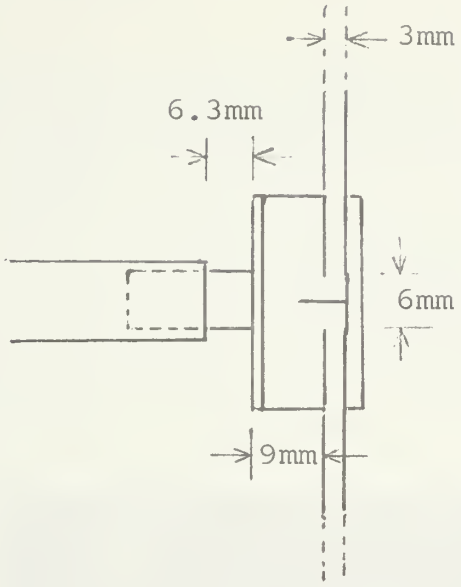

Figure 14

Drawing of test fixture

The signal source side of the assembly is shown in the photograph in Figure 15.

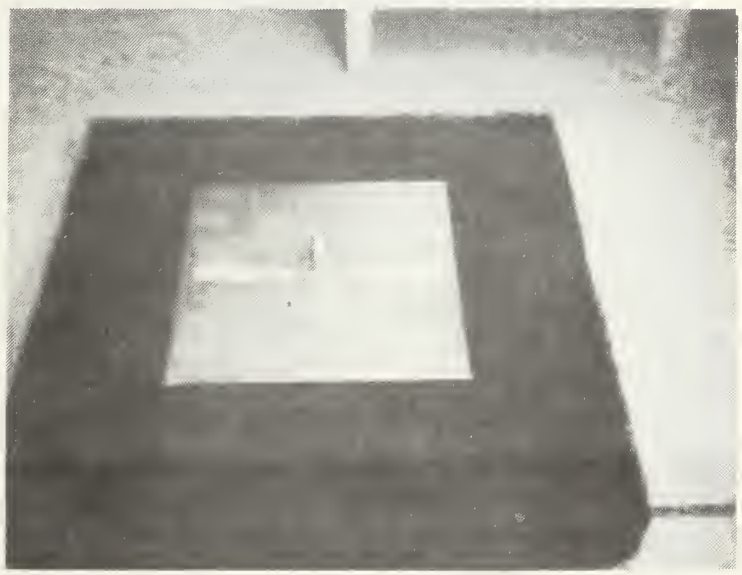

Figure 15

Photograph of test fixture

C. ANECHOIC CHAMBER

In order to prevent the return of radiated energy during measurement, the test fixture was immersed in an anechoic chamber. The internal dimensions of the chamber were 61 x 48 x 38 cm and was constructed of 10 cm thick Eccosorb H radar absorbing material. A photograph of the chamber interior is shown in Figure 16.

Figure 16
Photograph of anechoic chamber

D. MEASUREMENT SYSTEM

1. Configuration

Impedance measurements were facilitated by use of the HP-8410S Microwave Network Analyzer-Wang 600 Calculating and Plotting System. The results of the measurements was impedance data in the form of a Smith Chart and in tabulated

numerical form. Figure 17 is a photograph and Figure 18 is a block diagram of this system.

Figure 17

Photograph of HP-8410S Microwave Network Analyzer-Wang 600 Calculating and Plotting System

2. Operation

The Microwave Network Analyzer System is composed of three major units. The HP-8690B Sweep Oscillator with the HP-8690B series RF plug-in provides the voltage signal to the HP-8743A Reflection-Transmission Test Unit. This signal is split into the reference and test channels. The test channel signal is output to the test fixture with its installed wire structure. When this signal is reflected from the structure, a standing wave pattern is distributed along the transmission line dependent on the relationship of the load impedance to the line impedance. This standing wave pattern is composed of the sum of the incident

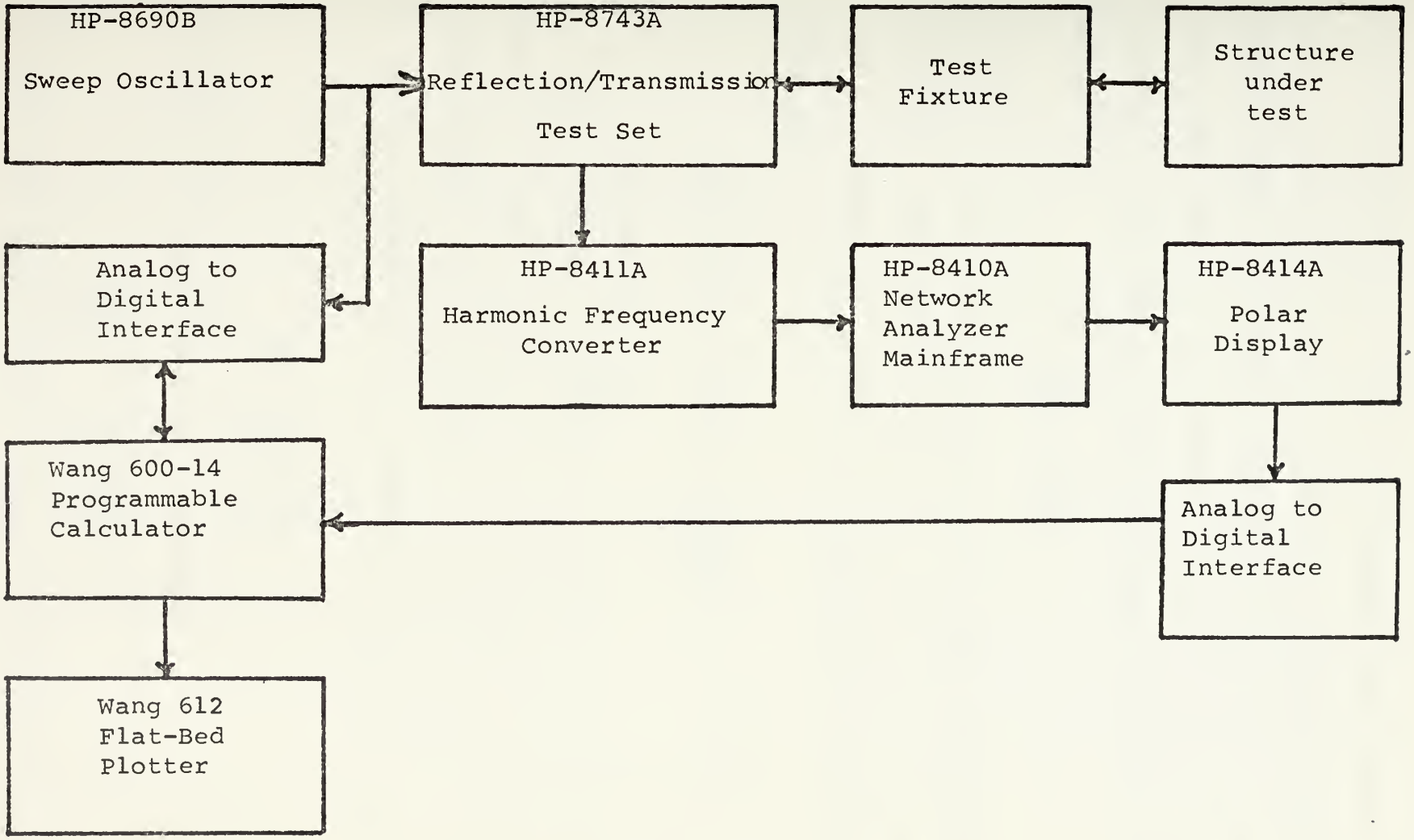

Figure 18

Block diagram of HP-8410S Microwave Network Analyzer-Wang 600 Calculating and Plotting System

wave on the load, V_i, and the reflected wave from the load, V_r. At the load, the ratio of V_r to V_i and the phase angle between them are uniquely determined by the load impedance, given that there is no radiated energy returned to the structure. This ratio is the reflection coefficient, Γ, defined by

$$\Gamma = \frac{V_r}{V_i} = \rho \angle \phi$$

where ρ is the magnitude and ϕ is the phase relationship of the ratio. The standing wave ratio (SWR) and the return loss are defined in terms of the magnitude in the following relations.

$$\text{Standing Wave Ratio} = \frac{1 + \rho}{1 - \rho}$$

$$\text{Return Loss} = \frac{1}{\rho}$$

The reflection coefficient is determined in the HP-8410A Network Analyzer Mainframe and is displayed on the HP-8414A Polar Display. This parameter, in terms of the load impedance, Z_L, and the characteristic impedance of the line, Z_o, is

$$\Gamma = \frac{Z_L - Z_o}{Z_L + Z_o}$$

Therefore, the normalized load impedance is

$$\frac{Z_L}{Z_o} = \frac{1 + \Gamma}{1 - \Gamma}$$

Since this relationship defines the Smith Chart, an overlay so inscribed can be placed over the polar display

for direct visual interpretation as normalized impedance. Every position on the polar display therefore, not only represents a unique reflection coefficient, but also a unique load impedance.

In order to communicate the impedance at a specific frequency to the calculator, the Sweep Oscillator is tuned to the desired frequency in the continuous wave (CW) mode. The X and Y deflection voltages on the polar display are sampled by matched HP-3470lA Digital Voltmeters. The frequency is measured by an HP-5340A Frequency Counter and converted from serial to parallel. These three digital signals; X deflection, Y deflection, and frequency, are read by the Wang 600 calculator through the interface system and the Input/Output Buffer shown in Figure 19. For each data set input, the calculator computes the resistance, R, and the reactance, X, and stores these values in memory. Upon command, the calculator prints the frequency, resistance, and reactance of each data set in memory and commands the Wang 612 Flat-Bed Plotter to print a point representing each data set at the appropriate position on a Smith Chart.

The data thus produced by the measuring system is processed and reproduced as resistance and reactance curves as functions of frequency by use of the HP-9821A Calculator-HP-9862A Plotter System shown in the photograph in Figure 20.

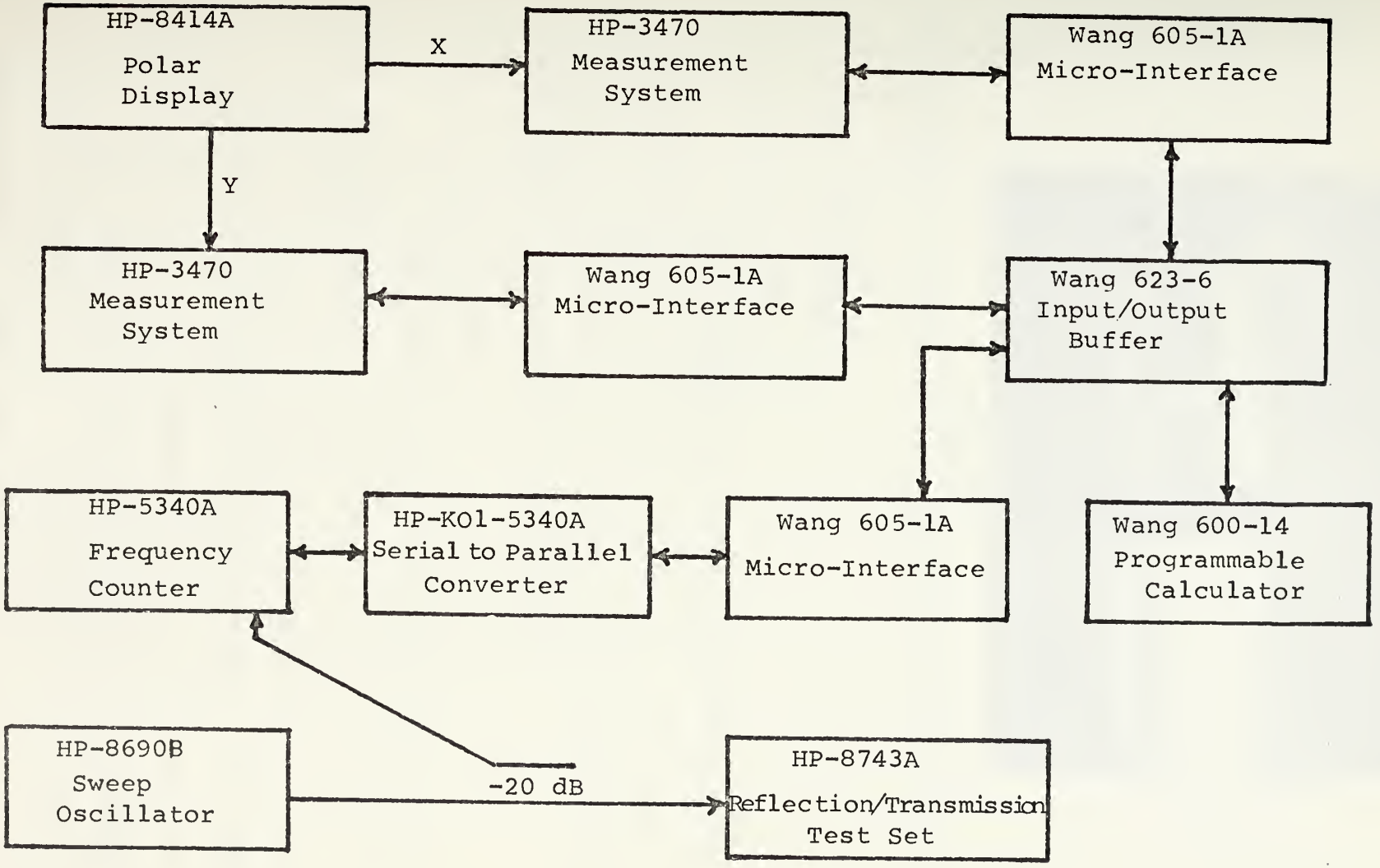

Figure 19

Block diagram of Interface System

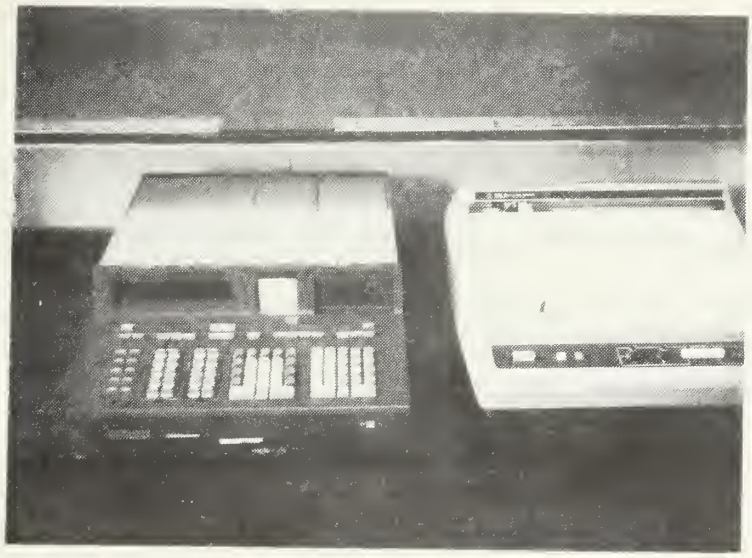

Figure 20

Photograph of Hewlett-Packard Calculator-Plotter System

3. Calibration

a. Preparation

The preparation of the measurement system for impedance measurements deserves mention. Although the system is internally stable over a broad range of frequencies, some special preparations are necessary.

b. Warm-Up

The warm-up time to achieve stability was found to vary with system components. It was found to be prudent to keep the Frequency Counter energized except for periods of preventive maintenance and calibration. The Sweep Oscillator had to be energized two to four hours prior to use. The longer periods were required for the higher frequency RF plug-ins. The remaining units of the system stabilized in a short time period.

c. Load Orientation

After prescribed intrasystem calibration, the measurement system had to be calibrated to a known load at the feed point in order to measure reflection coefficients and impedances accurately. Although an open circuit with reflection coefficient, $\Gamma = 1 \angle 0^{\circ}$, and impedance, $Z = \infty + j\,0$, would be the best load to which to calibrate, such loads are extremely difficult to fabricate at microwave frequencies because of capacitive end effects. Even short circuits with $\Gamma = 1 \angle 180^{\circ}$ and $Z = 0 + j\,0$ are difficult to achieve but not impossible. Such a calibration short was fabricated for the purposes of this study and is shown, with dimensions, in Figure 11.

The short was designed to be installed in the same position as the wire structures. The center conductor was inserted 5 mm into the panel receptacle with the 11 mm circular disk flush against the feed point on the ground plane. The disk thus covered the aperture at the feed point and contacted the ground plane over a 2.5 mm radius.

During calibration, the short was pressure fitted for minimum contact resistance. The performance of the calibration short thus installed was comparable to the manufacturer's short over frequency ranges less than 300 KHz.

With the Sweep Oscillator in the sweep mode and limited to a range less than 300 KHz, the reference plane extension and polar display calibrations were adjusted to achieve a reflection coefficient near 1 $\angle 180^{\circ}$ over the frequency range; that is, a short circuit. The short was then removed, the Sweep Oscillator placed in the CW mode, the structure under test installed in the test fixture, the fixture immersed in the anechoic chamber, and measurements commenced. Of course, a similar calibration procedure was required for each range of frequencies, the total extending from 2.00 to 12.00 GHz. To achieve the most accurate measurements at resonance, antiresonance, and frequencies above 8.00 GHz, calibrations were often made at single frequencies with the Sweep Oscillator in the CW mode.

V. DATA DISPLAY

A. FORMAT

The format of the presentation of wire structure impedance characteristics was chosen to exhibit all points of interest. The rectangular graphs of resistance and reactance as functions of frequency present continuous values and emphasize peaks, nulls, and zero crossings as well as major nonlinearities. The Smith Charts present the resonant and anti-resonant points of the total structure as well as emphasizing the nonlinearities which occur when the natural frequencies of the cross-monopole members lock-in with the driven frequency of the structure. Key points are labelled for frequency identification. A sketch of the wire structure represented is included in each presentation. In the cross-monopole graphs, the impedance of an equal length vertical monopole is included for comparison purposes. This permits characteristics of the added cross-arm, as coupled to the vertical member and the ground plane, to be identified in the analysis.

B. BANDWIDTH (B) AND QUALITY FACTOR (Q)

The half-power points (f_i), bandwidths (B), and quality factor (Q) near resonance and antiresonance can be determined

from the Smith Chart in each case by a simple geometric construction technique.[11]

Near resonance, a structure may be represented as a simple shunt resonant circuit characterized by a loaded $Q = Q_L$, where

$$\frac{1}{Q_L} = \frac{1}{Q_o} + \frac{1}{Q_{ext}}$$

Q_o being the unloaded Q characteristic of the structure itself, and $\frac{1}{Q_{ext}}$ the loading due to the external circuits. The Q of a structure, like the Q of any resonant circuit, is proportional to the ratio of the energy stored to the energy lost to ohmic losses and to radiation per cycle.[12]

$$Q = 2\pi \frac{\text{Maximum energy stored}}{\text{Energy lost per cycle}}$$

A large Q indicates a large amount of stored energy near the structure in proportion to the energy radiated per cycle, assuming ohmic losses are negligible. A large Q also means that the structure acts like a sharply tuned circuit. Since the bandwidth is inversely proportional to

---

[11] Hewlett-Packard Application Note 117-1, Microwave Network Analyzer Applications, pp. 8.7-8.9, June 1970.

[12] King, R.W.P., The Theory of Linear Antennas, pp. 171-173, Harvard University Press, 1956.

Q in the relationship

$$B \doteq \frac{fo}{Q}$$

a large Q is clearly not desirable if a broader bandwidth is needed but may be very appropriate for certain military applications.

The useful bandwidth of a structure depends, in general, on both its radiation pattern and its impedance characteristics.[12] For a thin wire monopole, the bandwidth is usually determined by the impedance variation since the pattern changes less rapidly with frequency, length, or radius of wire. However, with a very thick cylindrical antenna, the impedance characteristics may be satisfactory over so wide a bandwidth that the pattern variation with frequency determines one or both of the half-power frequencies. In all cases under this study, structure member lengths vary from 6 mm to 42 mm and all wire radii are 0.55 mm for a length to radius ratio from 11 to 76 which is not thin but not in the category of very thick. Therefore, in this study, the bandwidth may be determined by impedance variations alone as frequency varies. The bandwidth can then be arbitrarily specified by the frequency limits, f_1, and f_2, at which the standing wave ratio (SWR) on the transmission line exceeds a value at which the power radiated is reduced to half the maximum value.

Reference /5/ provides a method to develop half power, or Q, loci on a Smith Chart of impedance for resonant cavities. Reference /8/ interprets antennas in terms of resonant structures. The following development of Q loci is based on the information in reference /5/ and /8/ as well as the conclusions from the previous paragraphs.

The quality factor, Q_o, of the wire structure alone can be determined from the equivalent circuit shown in Figure 21.

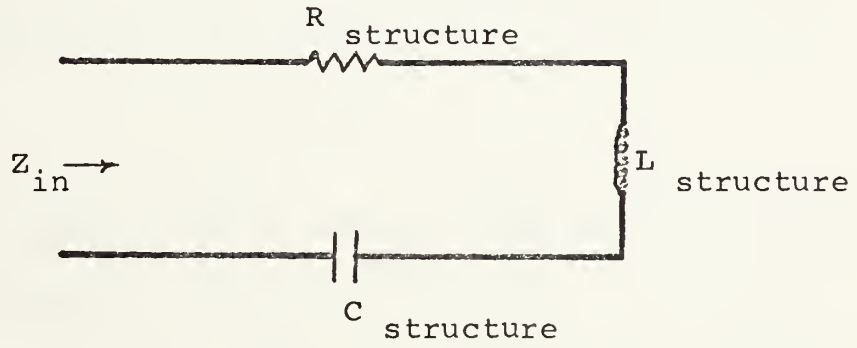

Figure 21
Equivalent circuit of wire structure alone

The quality factor, Q_L, of the entire system, including all sources of energy loss, with the structure perfectly coupled to the transmission line, can be determined from the equivalent circuit shown in Figure 22 where Z_o is the characteristic impedance of the transmission line and V_s is the source voltage.

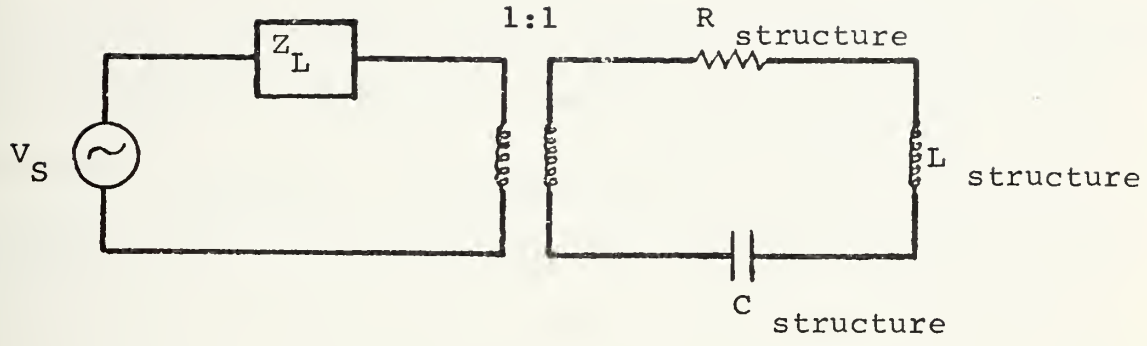

Figure 22

Equivalent circuit of wire structure with losses

The quality factor, Q_{ext}, of the external system assuming the structure has no Q of its own (R=0), with the losses due to the external load only, and with the structure imperfectly coupled to the transmission line, can be determined from the equivalent circuit shown in Figure 23.

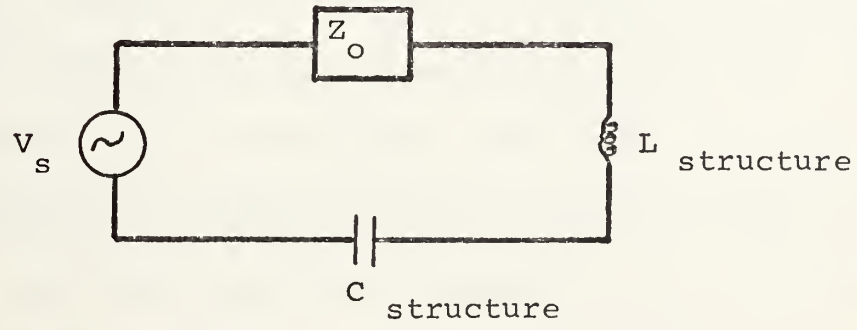

Figure 23

Equivalent circuit of wire structure imperfectly coupled

An analysis of the equivalent circuits shown in Figures 21, 22, and 23, with the solutions normalized and translated to the Smith Chart, permits Q loci to be constructed as shown in Figure 24. The Q_o arcs connect the points at which $R_{Structure} = \pm X_{Structure}$ and are the half-power points of the structure alone. The centers of the arcs are at $Z = 0 \pm j\ 1$, each with a radius established by the distance to the point $Z + 0 \pm j\ 0$. The Q_L loci are straight lines connecting the point $Z = 0 \pm j\ 0$ to $Z = 0 + j\ 1$ and to $Z = 0 - j\ 1$ and are the half-power points at which $X_{Structure} = R_{Structure} + Z_o$. The Q_{ext} arcs are centered at the intersection of the tangents to the Smith Chart at $Z = 0 \pm j\ 0$ and $Z = 0 \pm j\ 1$, each with a radius equal to the value such that the arcs go through these points. The Q_{ext} arcs describe the half-power points at which $X_{Structure} = Z_o$.

The frequencies at which an impedance curve intersects a given Q loci are then the associated half power frequencies. For example, for the impedance curve shown in Figure 24, and considering the structure alone, the antiresonant frequency is f_a, the lower half-power frequency is f_1, and the upper half-power frequency is f_2. The calculated bandwidth of the structure is then

$$B = f_2 - f_1$$

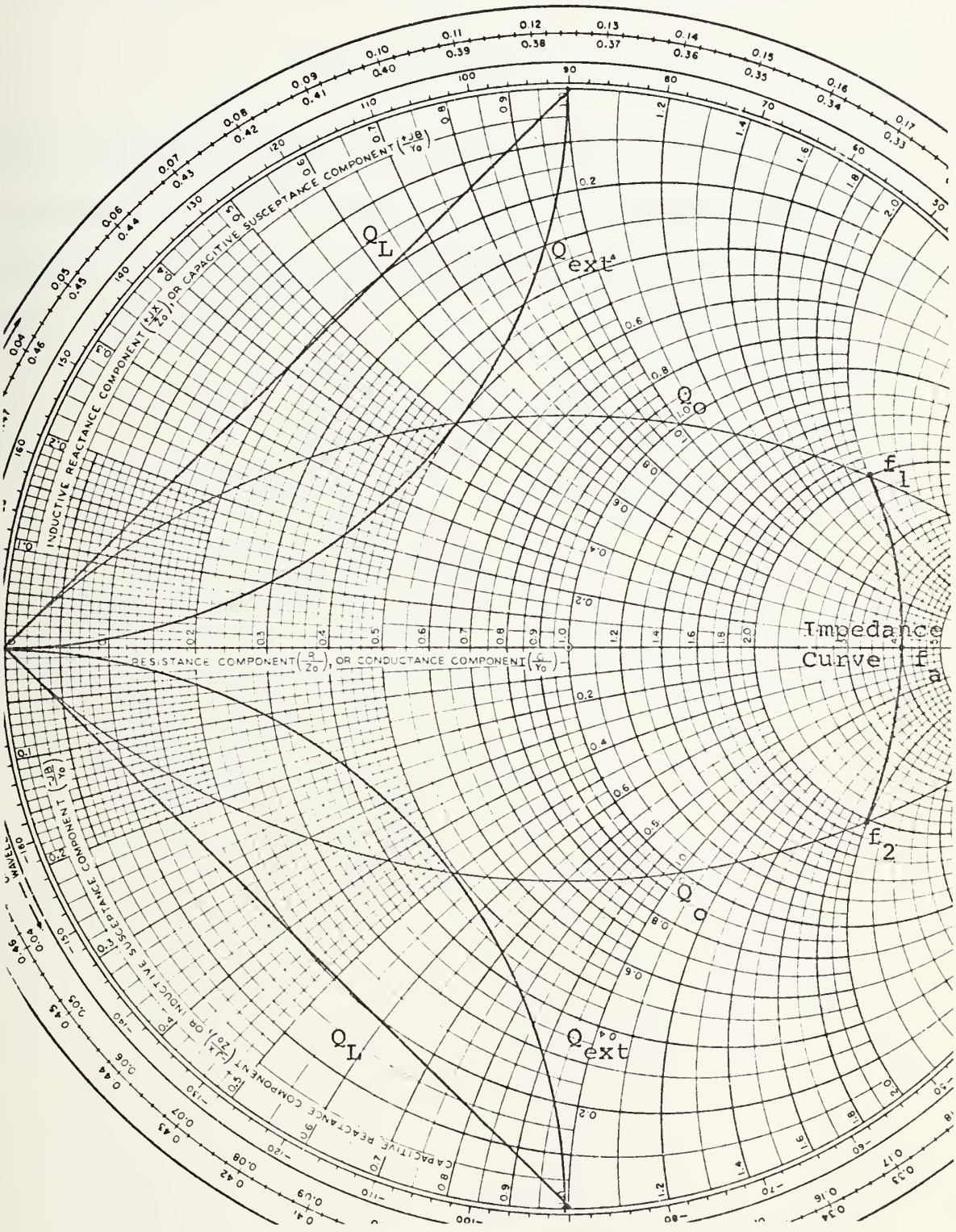

Figure 24

Quality factor loci of structure equivalent circuits

and Q_o of the structure is

$$Q_o = \frac{f_a}{f_2 - f_1}$$

The half-power frequencies may be located with a drawing compass on the Smith Charts of impedance measurements to establish the bandwidth and Q of any structure near resonance or antiresonance.

VI. PRESENTATION OF DATA

A. THE MEASURING SYSTEM

Before attempting to interpret the results of impedance measurements of the wire structures, it is desirable to examine the characteristics of the Microwave Network Analyzer System as well as the test fixture used in the measurements. Therefore, a full range of measurements were made on the unloaded output port of the Reflection/Transmission Test Unit, on the output port loaded with the open test fixture adapter; and finally, on the output port loaded with the adapter and the ground plane with its open panel receptacle.

B. TEST FIXTURE

1. APC-7 To N Female Adapter

Figure 25 compares the measured impedance of the open adapter with that of the open output port of the test unit for frequencies from 2.00 to 12.00 GHz. Each of the impedance characteristics was measured while radiating into the anechoic chamber after calibration to an HP-11512A Male Coaxial Short. Due to data point bunching, the Smith Chart in Figure 25 shows only the impedance envelopes, general trends, and key points.

For the output port, it is seen that the resistance is higher at the lower frequencies than at the higher

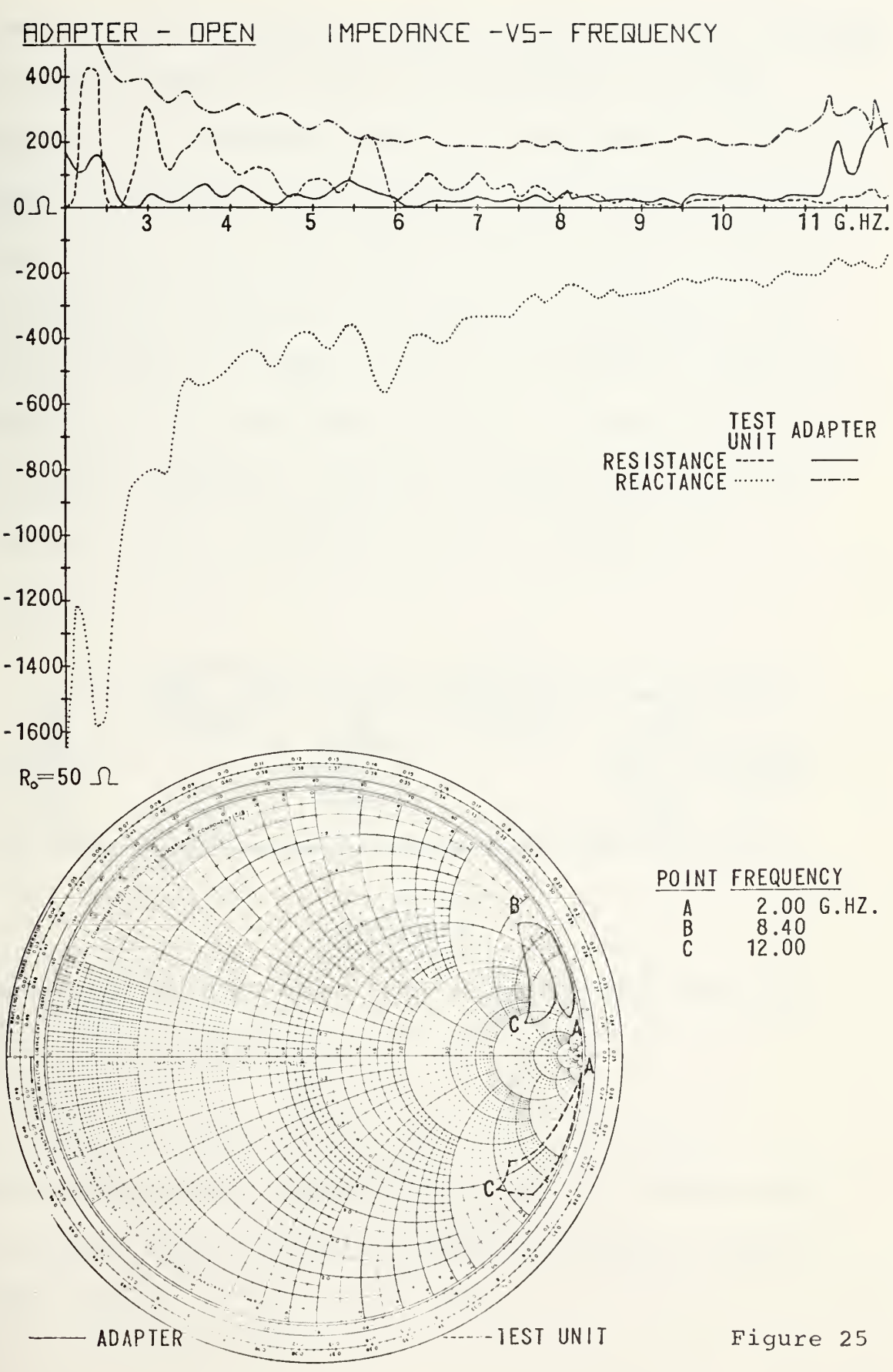

POINT	FREQUENCY
A	2.00 G.HZ.
B	8.40
C	12.00

Figure 25

frequencies, with peaks occurring at about 700 KHz intervals, the highest peak at 2.3 GHz. The reactance is highly capacitive at the lower frequencies and less capacitive at the higher frequencies as it should be. The reactance characteristic exhibits the same peaking phenomena as the resistance. An equivalent circuit of the Reflection/Transmission Test Unit as seen at the open output port is shown in Figure 26 where V_s is the ideal swept frequency voltage source, Z_s is the source impedance, and the pie network represents the impedance of the transmission line and output port.

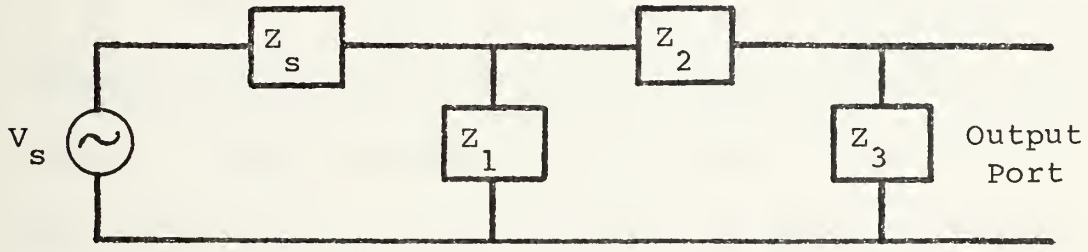

Figure 26

Equivalent circuit of Reflection/Transmission Test Unit

The impedances are complicated and are not representable by lumped circuit elements across the frequency range of measurements.

For the adapter, the resistance is relatively high at the high and low frequencies and low at the intermediate frequencies with the characteristic peaks of the output port. The high resistance at the higher frequencies is clearly attributable to the adapter and its interaction with the output port since the high resistance was not present before the adapter was added. The maximum resistance at the lower frequencies is less than half that of the unloaded output port; hence, the adapter has effectively added an impedance in parallel with the output port in this frequency range.

The reactance of the adapter is inductive at all frequencies between 2.00 and 12.00 GHz with relatively high values at lower frequencies and a small increase above 10.5 GHz. The reactance also exhibits the peaking phenomena characteristic of the output port. Comparing the reactance of the adapter-loaded output with the output alone, it can be deduced that the adapter has added a highly inductive component to the system.

It should also be noted that the frequency at which minimum reactance occurs is 8.4 GHz. This reversal in phase trend, characteristic of the adapter, will be seen to dominate the impedance measurements of all attached structures as will be pointed out later.

An equivalent circuit as seen at the open adapter is shown in Figure 27.

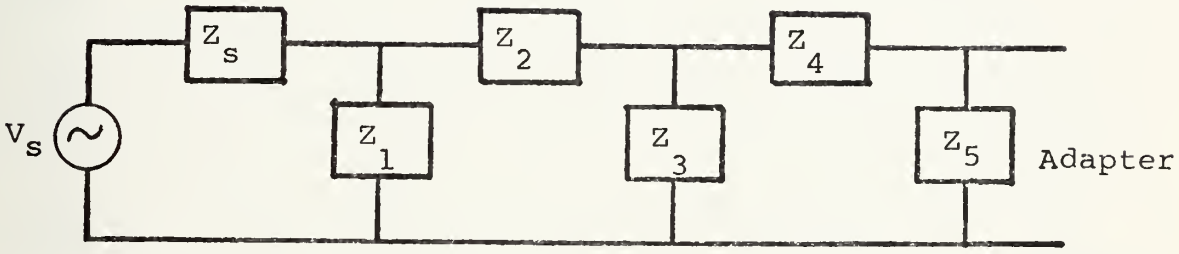

Figure 27

Equivalent circuit of adapter

Again, the impedances are complicated and cannot be represented by lumped circuit elements across the frequency range of measurements.

2. Ground Plane

Figure 28 compares the measured impedance of the open ground plane with that of the open, adapter-loaded, output port. The impedance characteristic of the open ground plane, as well as all wire structures, was measured while radiating into the anechoic chamber after calibration to the fabricated short shown in Figure 11, at the feed point. Again, due to data point bunching, the Smith Chart in Figure 28 shows only the impedance envelopes and general trends.

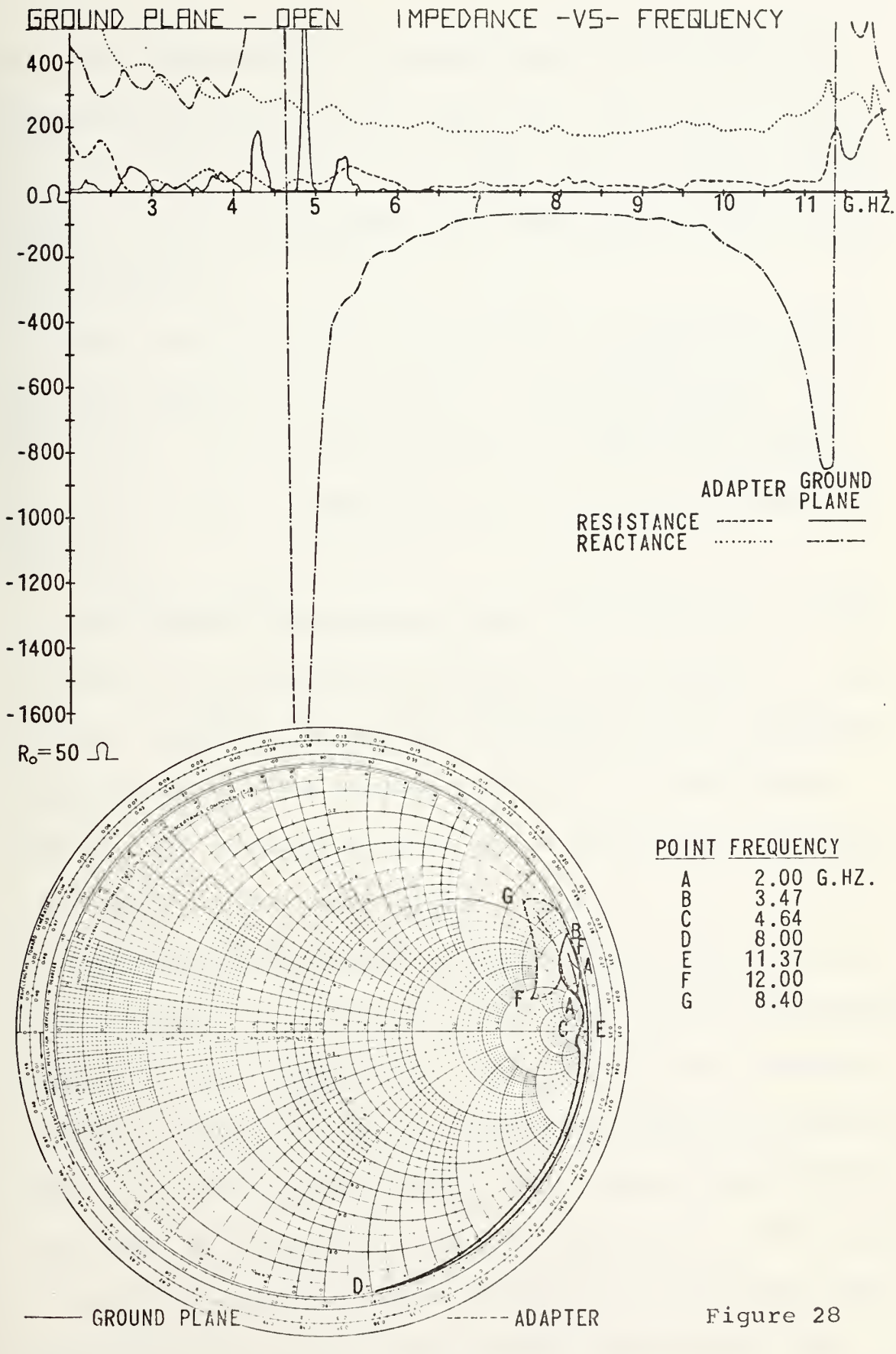

POINT	FREQUENCY
A	2.00 G.HZ.
B	3.47
C	4.64
D	8.00
E	11.37
F	12.00
G	8.40

Figure 28

The resistance of the ground plane is near zero at frequencies above 6 GHz and peaks near 4.85 GHz with oscillations characteristic of the output port. The peak resistance is seen to be several times that of the adapter at the same frequency.

The reactance of the ground plane is inductive below 4.64 GHz and above 11.37 GHz but capacitive between these two values. It is nearly constant at about 70 Ω between 6.5 and 9.5 GHz, a range of 3 GHz, where the resistance is very low.

The reactance has phase trend reversals near 3.47 and 8.00 GHz. The reversal at 8.00 GHz is undoubtedly the same reversal noted at 8.4 GHz for the adapter with a different frequency due to the loading effect of the ground plane. However, the reversal at 3.47 GHz is evidently a characteristic added by the ground plane itself.

The reactance is seen to peak to large magnitudes on either side of the zero crossings, characteristic of resonant circuits. The slopes of the curves through zero reactance are very steep due to the low resistive component indicating high Q near these frequencies. Since these characteristics were added by the addition of the ground plane to the system, the resonant and antiresonant frequencies should have some significance in terms of the physical dimensions of the

structure. This significance can be determined by an examination of the dimensions of the ground plane shown in the sketch in Figure 29.

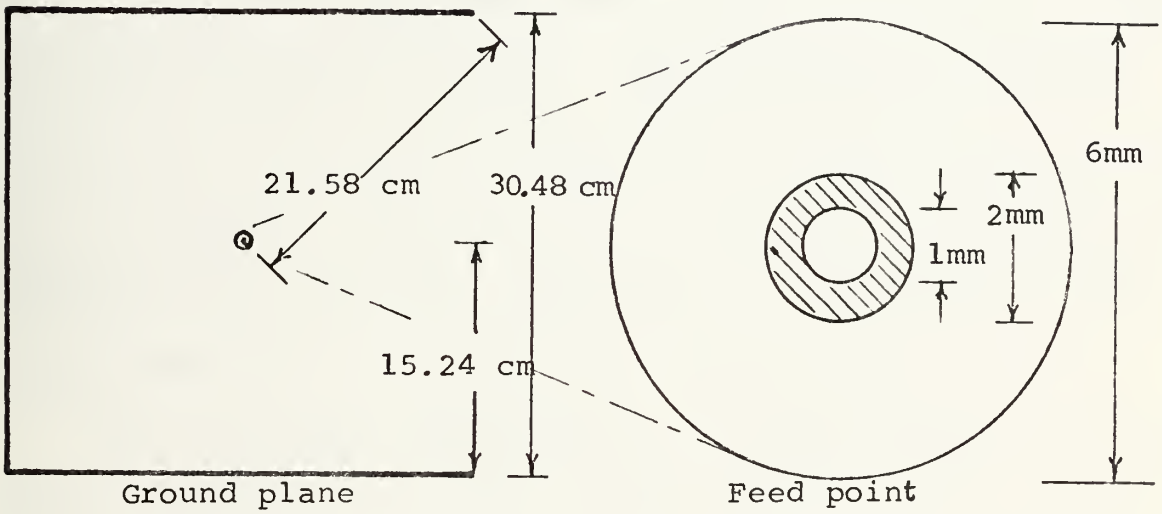

Figure 29

Ground plane with feed point

The free-space wavelength at 4.64 GHz is about 6.47 cm. Jordan shows that the phase velocity component along a conducting surface is less than the speed of light in free space.[13] Consequently, the wavelength on the ground plane is somewhat greater than 6.47 cm. Since the nearest edges of the plane are 15.24 cm and the corners are 21.58 cm

---

[13] Jordan, E.C. and Balmain, K.G., Electromagnetic Waves and Radiating Systems, pp. 202-205, Prentice-Hall Inc., 1968.

from the center, it is apparent that three wavelengths fit on the plane between the feed point and the edge near the corners. Hence, the effective radius of the plane is three-wave antiresonant providing positive re-enforcement to standing wave patterns of current. This interpretation is consistent with the change from inductive to capacitive reactance with increase in frequency which is defined as the antiresonant frequency of a structure. Therefore, antiresonance at 4.64 GHz is associated with the ground plane itself.

The free-space wavelength at 11.37 GHz is about 2.64 cm. Again considering the reduced phase velocity in the coaxial dielectric at the feed point a quarter wavelength, 2.5 mm, fits nicely between the center conductor and the edge of the aperture in the feed point. The resulting standing quarter wave is consistent with the change from capacitive to inductive reactance with increase in frequency which is defined as the resonant frequency of a structure. This resonant frequency, 11.37 GHz, is therefore associated with the feed point aperture.

King has documented this effect at the feed point.[14]

---

[14] King, R.W.P., Transmission Line Theory, pp. 430-437 McGraw Hill, 1955.

The impedance loading the end of a coaxial line is not just that of the structure attached, but also includes effects due to the finite size of the aperture at the point of excitation. The fringing effects are not negligible, and they are particularly important at antiresonance. The effects can be modeled as a small negative capacitance located at the end of the coaxial line for analysis purposes. The addition of a small fringing capacitance to that region then makes the theoretical and measured resonance occur at the same frequency. An equivalent circuit as seen at the open feed point in the ground plane is shown in Figure 30.

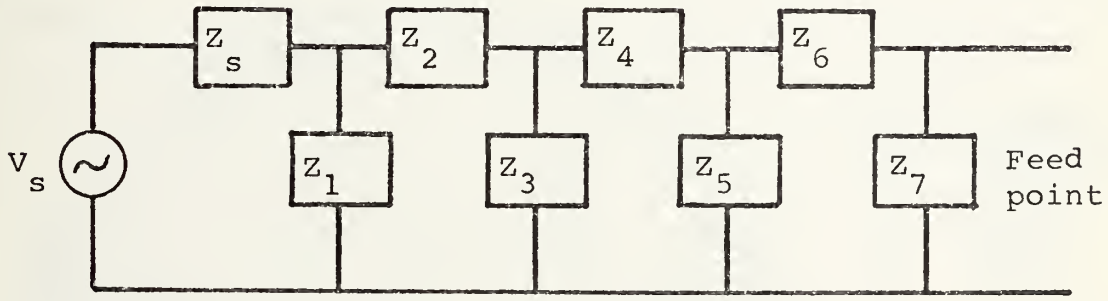

Figure 30

Equivalent circuit of ground plane

The impedances cannot be represented by lumped circuit elements due to the complexity of their frequency dependence.

The total impedance range of the test fixture alone is shown in Figure 31. This form of the characteristics will

GROUND PLANE - OPEN IMPEDANCE -VS- FREQUENCY

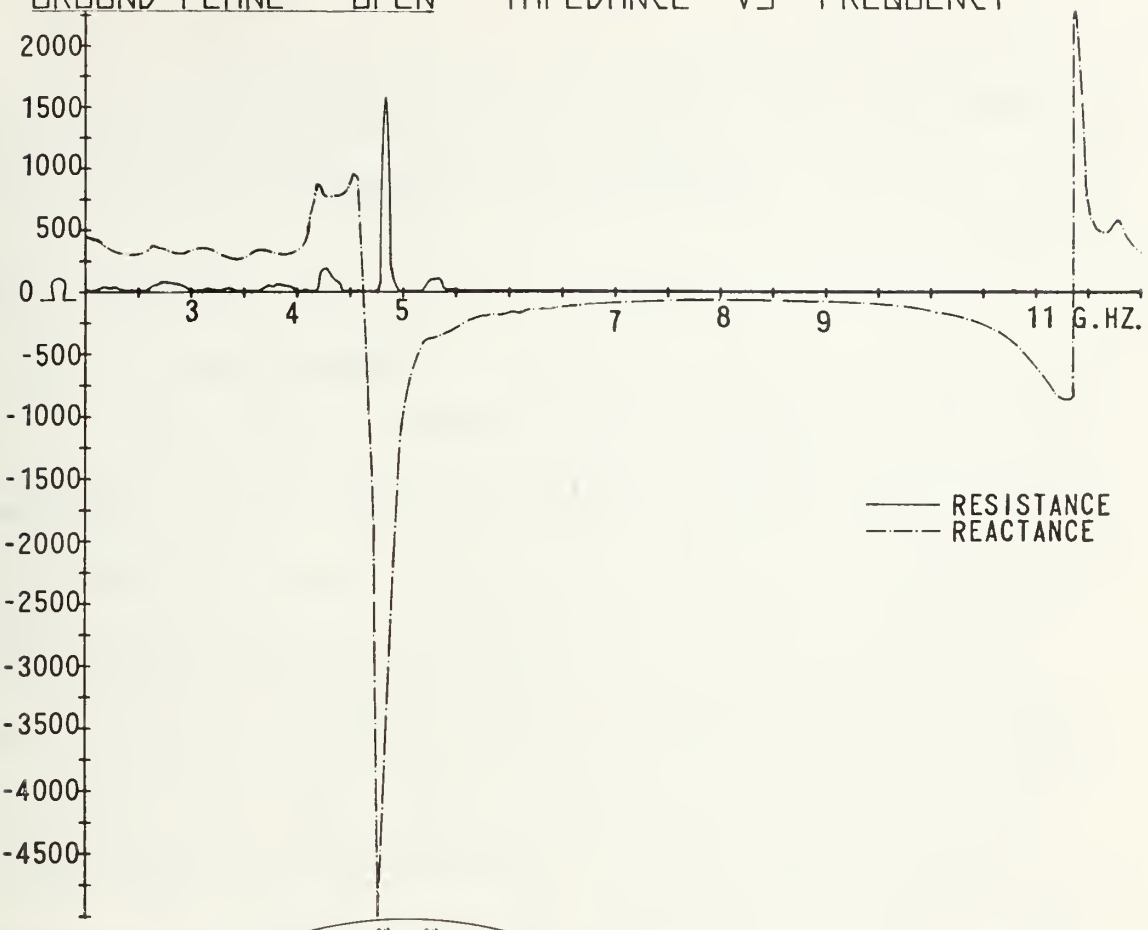

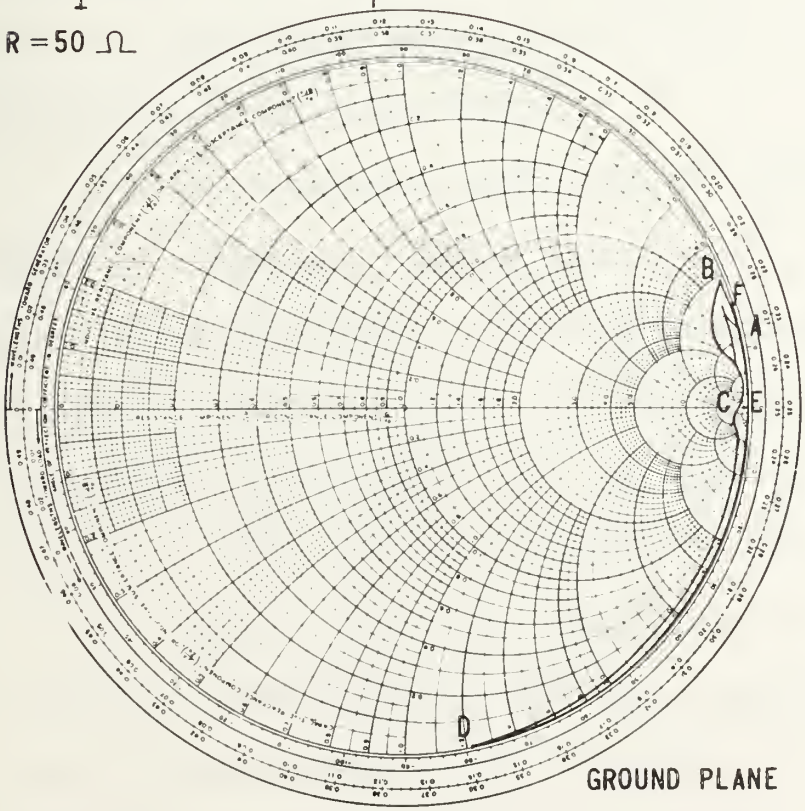

GROUND PLANE

POINT	FREQUENCY
A	2.00 G.HZ.
B	3.47
C	4.64
D	8.00
E	11.37
F	12.00

be useful as a reference when analyzing wire structure characteristics measured on this fixture.

C. MONOPOLES

1. 6 mm Monopole

The input impedance characteristics of the 6 mm monopole, as seen from the feed point of the test fixture are shown in Figure 32. All wire structures in this study have members which are multiples of the 6 mm length to facilitate the maximum number of resonant points within the 2-12 GHz range. The addition of the wire has added capacitance to the system due to the coupling between the wire and the ground plane and has added inductance to the system due to the wire length.

The resistance peaks near 2.57 GHz, undoubtedly aided by a similar characteristic of the test unit output port, but also consistent with antiresonance of the total assembly including the test fixture at this frequency. The resistance is then quite low near 2.00 GHz and above 4.00 GHz with a small increase above 10.00 GHz.

The reactance near antiresonance at 2.57 GHz exhibits the peaking and steep slope, characteristic of narrow bandwidth and high Q. However, the reactance near resonance at 10.80 GHz exhibits a shallow slope, characteristic of wide bandwidth and low Q. The resonance at 10.80

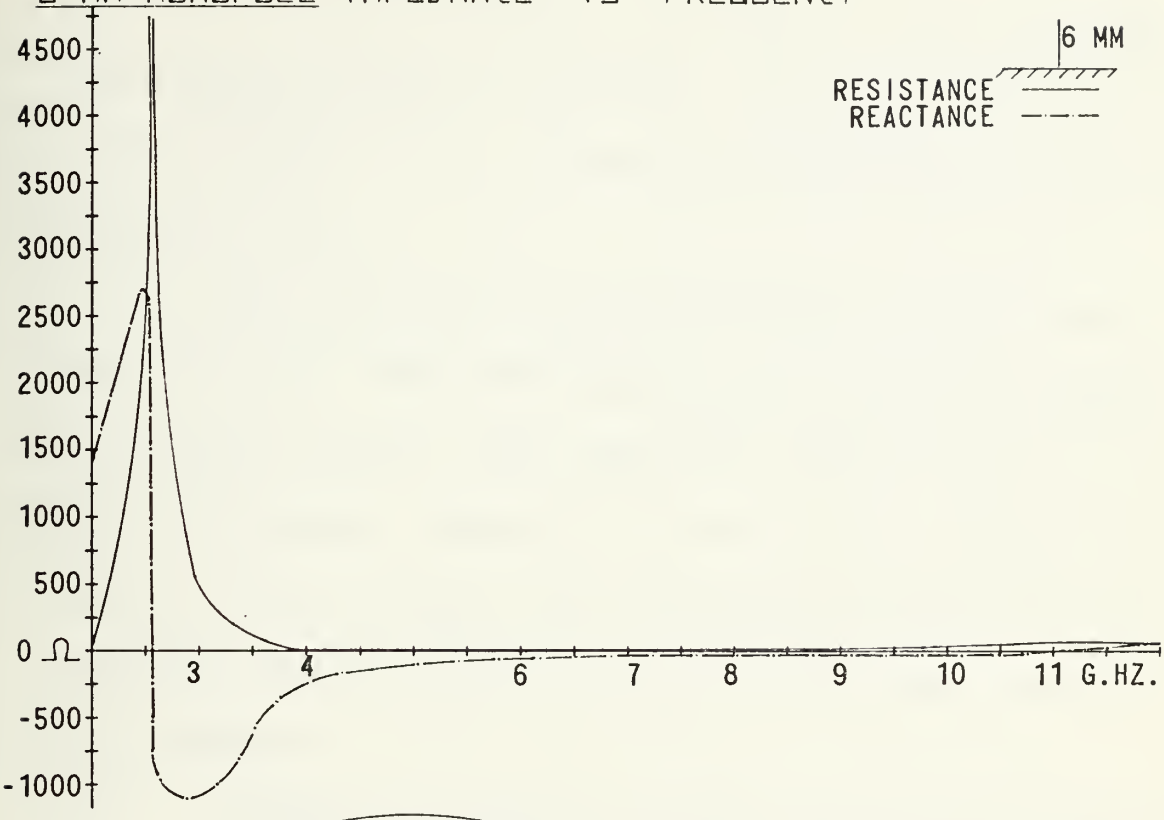

$R_o = 50\ \Omega$

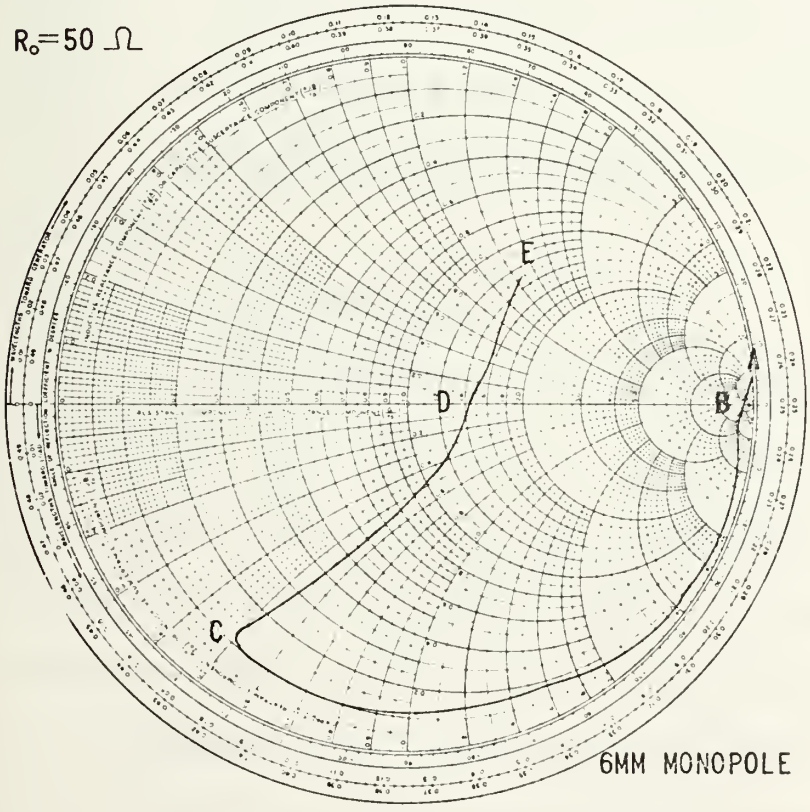

POINT	FREQUENCY
A	2.00
B	2.57
C	8.00
D	10.80
E	12.00

6MM MONOPOLE Figure 32

GHz defines the 6 mm monopole as a quarter-wave structure when coupled to the test fixture. The standing wave patterns on the monopole at this frequency are then assumed to be as shown in Figure 1.

The free space quarter-wavelength at 10.8 GHz is about 6.95 mm. This would indicate that the wave velocity on the wire is about 0.864 times the speed of light in free space as expected. However, it will be seen that the wave velocity is not constant but varies with distance from and orientation to the ground plane as well as other wires in the structure.

Finally, it should be noted that point C, 8.00 GHz, on the Smith Chart in Figure 32 is the reversal in phase trend previously identified as a characteristic of the adapter.

2. 12 mm Monopole

The impedance of the 12 mm monopole is shown in Figure 33. The oscillations in resistance below 4.0 GHz and the peak near 2.2 GHz are attributable to the measuring system and test unit output port. The perturbation in impedance linearity at point D, 8.50 GHz, on the Smith Chart is a characteristic of the adapter alone but the peak in resistance near 11.36 GHz and the attendent resonance are characteristics of the total test fixture. These forces

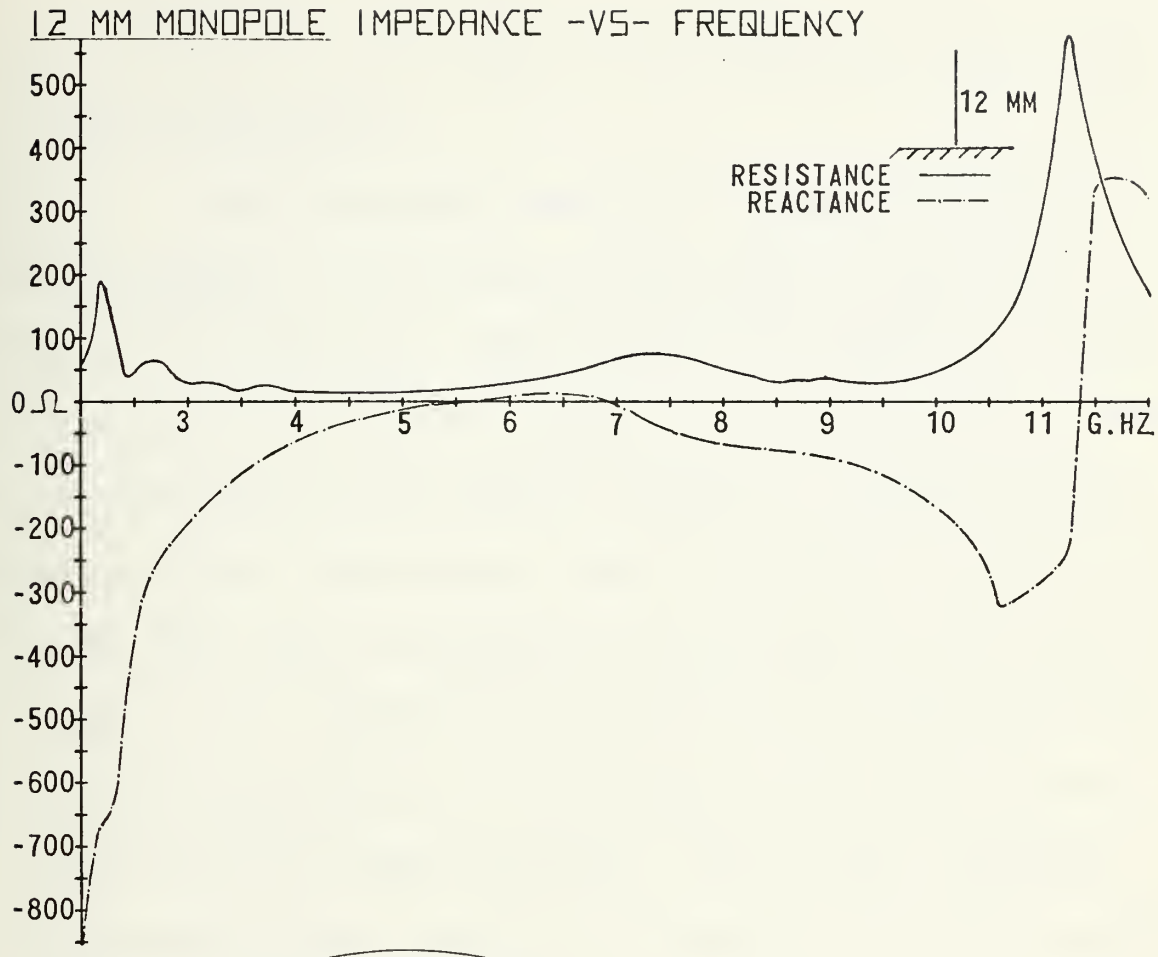

$R_o = 50\ \Omega$

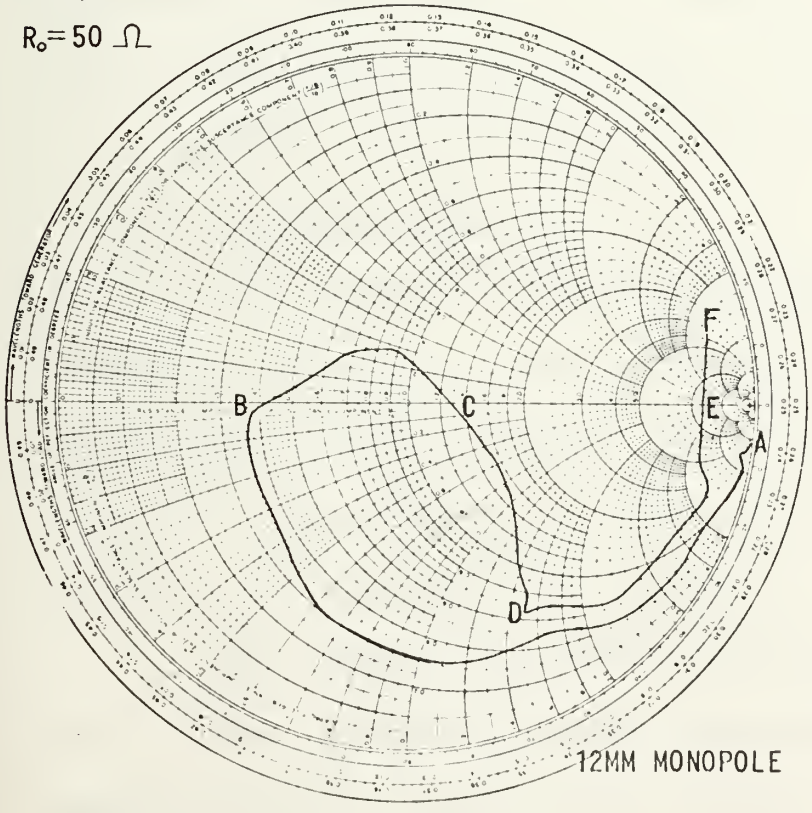

12MM MONOPOLE

POINT	FREQUENCY
A	2.00 G.HZ.
B	5.46
C	6.91
D	8.50
E	11.36
F	12.00

Figure 33

will prevail to some degree on the characteristics of all measured structures.

The resistance peak near 7.3 GHz is obviously attributable to the 12 mm monopole since it was absent on previous structures. The monopole, as coupled to the test fixture, is quarter-wave resonant at 5.46 GHz having standing wave patterns as shown in Figure 1. It would then be expected that the monopole should be half-wave resonant at about 10.9 GHz with standing wave patterns as in Figure 4. However, the impedance is dominated by the characteristics of the test fixture in this frequency range forcing antiresonance at a lower frequency. At 6.91 GHz, half-wave antiresonance does occur in the monopole but the sinusoidal form of the standing wave patterns is undoubtedly distorted due to strong coupling near the feed point.

3. 18 mm Monopole

The impedance of the 18 mm monopole is shown in Figure 34. Once again, the resistance peak near 2.2 GHz of the output port is evident. Also, the phase reversal at 8.35 GHz of the adapter and the domination of characteristics by the test fixture at high frequencies obtains.

The resonant frequency of the monopole is seen to be 3.67 GHz. At this frequency, the monopole is quarter-wave resonant with the standing wave pattern of Figure 1. The

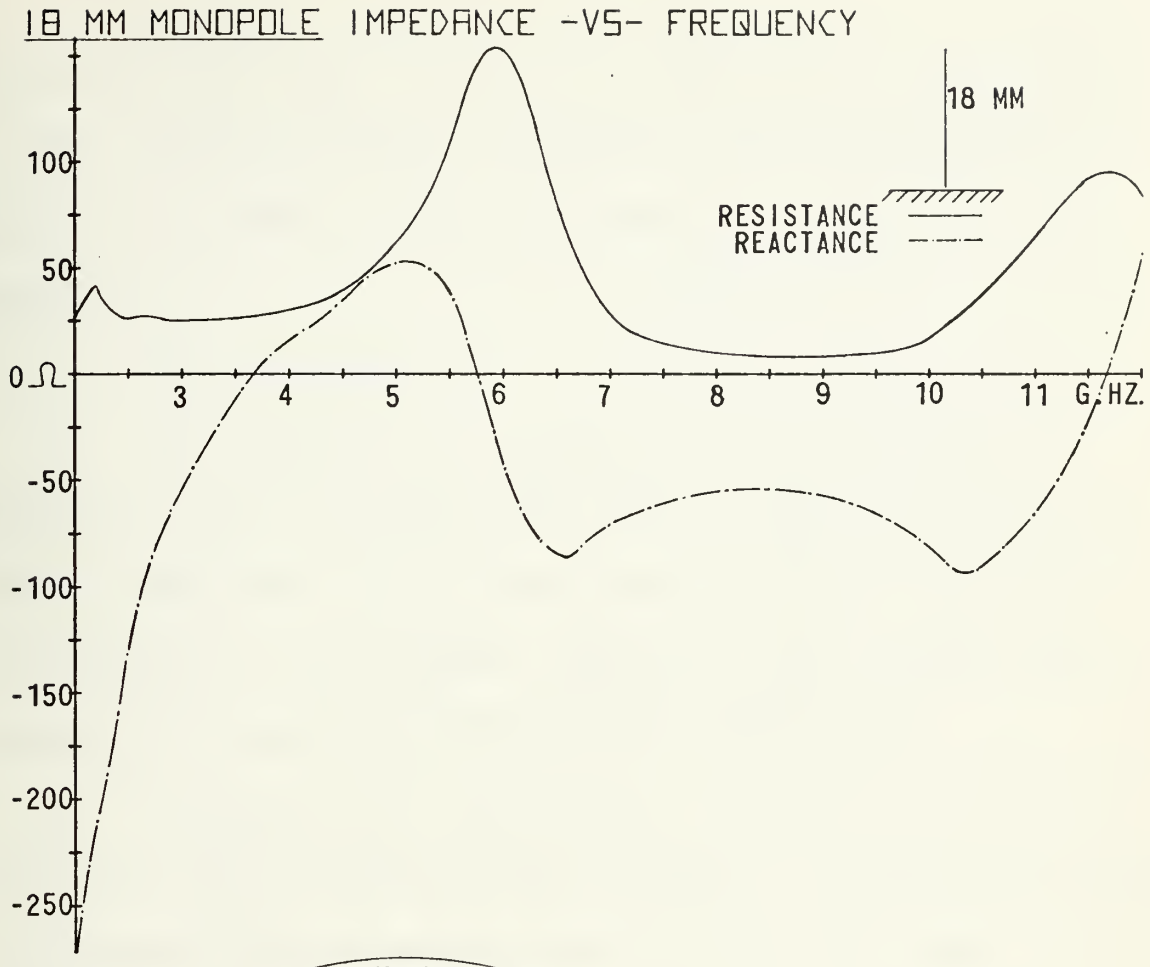

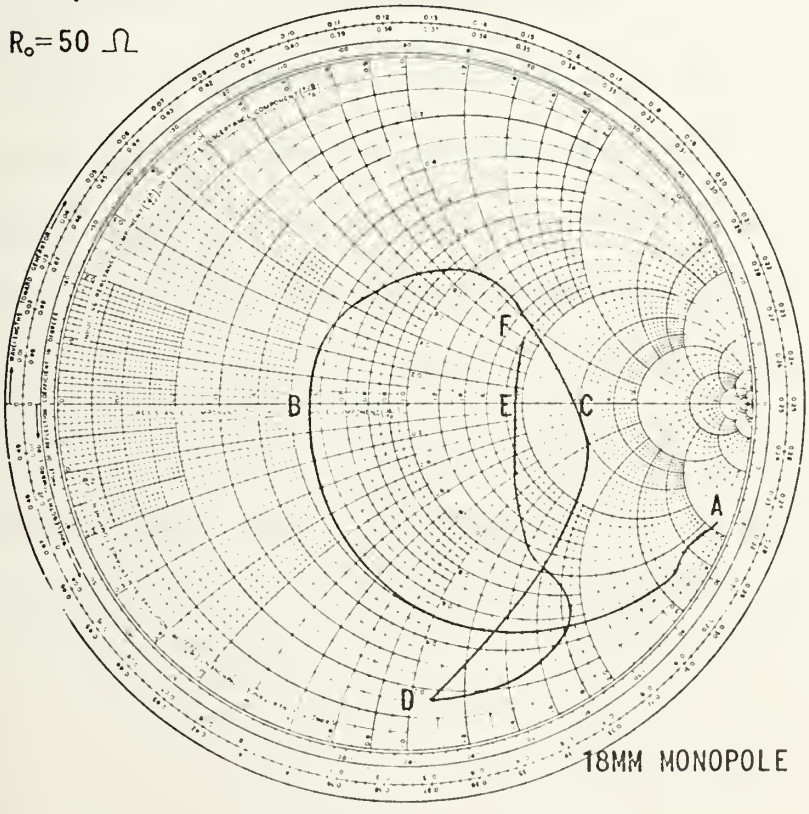

POINT	FREQUENCY
A	2.00 G.HZ.
B	3.67
C	5.75
D	8.35
E	11.66
F	12.00

18MM MONOPOLE

Figure 34

resistance peak near 5.75 and the associated antiresonance at that frequency indicates standing half-wave patterns of current and charge on the wire similar to that shown in Figure 4.

4. 21 mm Monopole

The impedance of the 21 mm monopole is shown in Figure 35. The resistance peak near 2.2 GHz caused by the output port still dominates as does the phase reversal at 8.50 GHz due to the adapter. Also, the test fixture still controls the characteristics at high frequencies.

Resonance for this monopole occurs at 3.21 GHz at which the wire is quarter-wave resonant. If the test fixture had permitted the impedance curve on the Smith Chart to continue in a clockwise progression with frequency increase, three-quarter wave resonance would have been expected at about three times the quarter-wave resonant frequency; about 9.6 GHz. Such multiples would be expected for all wire structures at both resonant and antiresonant frequencies.

The resistance peak near 5.47 GHz and the associated zero crossing of reactance at that frequency identifies the monopole as half-wave antiresonant with the associated standing wave patterns.

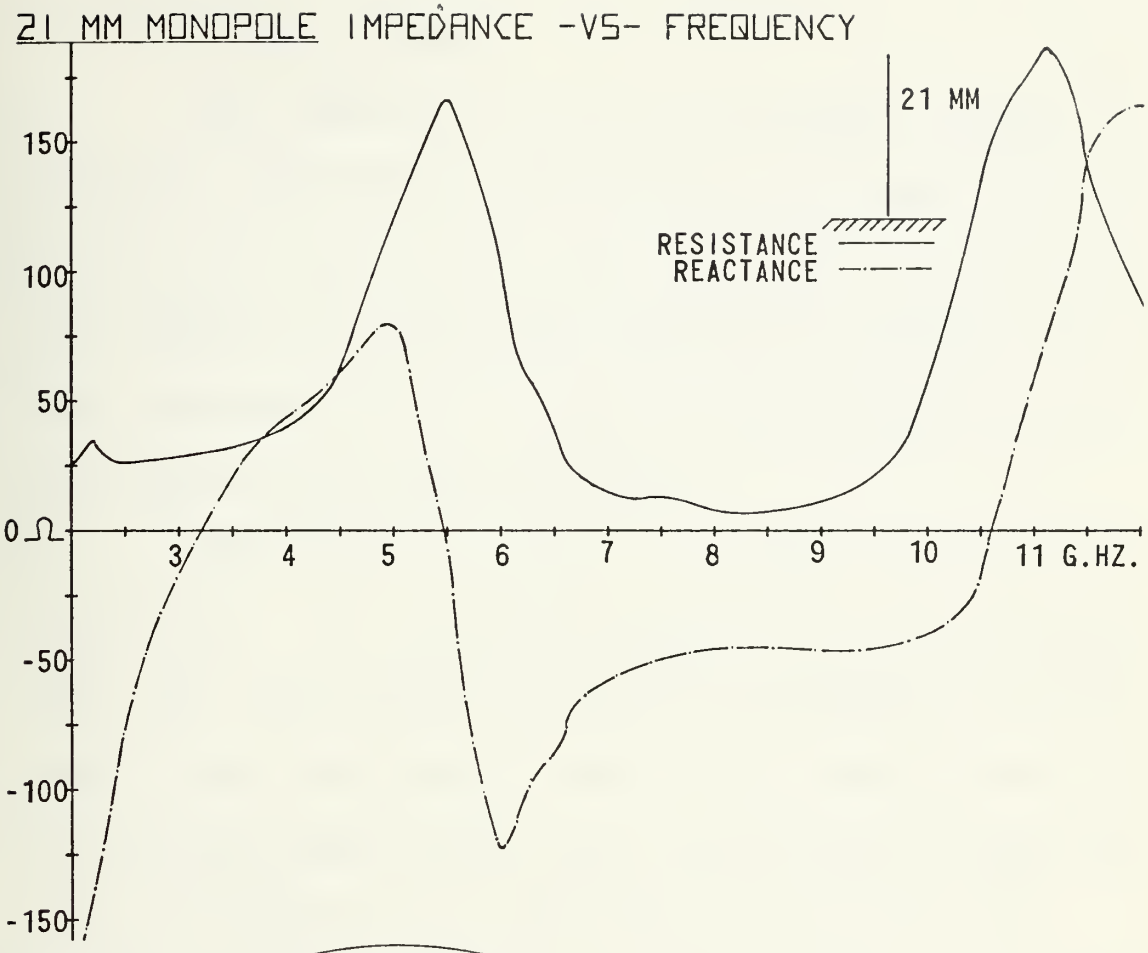

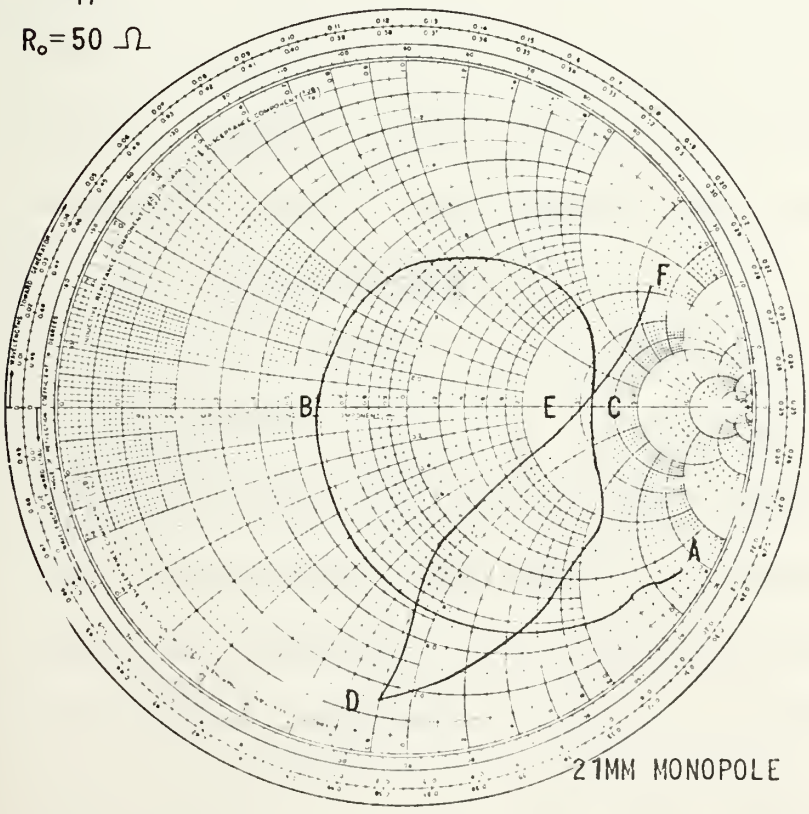

POINT	FREQUENCY
A	2.00 G.HZ.
B	3.21
C	5.47
D	8.50
E	10.60
F	12.00

21MM MONOPOLE

Figure 35

5. 24 mm Monopole

The impedance of the 24 mm monopole is shown in Figure 36. The familiar domination of the characteristics by the output port and the test fixture will be recognized. This monopole is quarter-wave resonant at 2.78 GHz and half-wave antiresonant at 5.09 GHz with the associated standing wave patterns previously described.

The peaking of reactance between 7 and 10 GHz is significant. It is clear as a result of previous measurements that the reactance is being held capacitive in this range by the feed system. However, the characteristics of the monopole alone should allow the reactance to peak inductively permitting the expected three-quarter wave resonance and full-wave antiresonance in this frequency range. It will be seen in the characteristics of longer monopoles that inductive peaking does indeed occur.

6. 30 mm Monopole

The impedance characteristics of the 30 mm monopole are exhibited in Figure 37. The monopole is quarter-wave resonant at 2.29 GHz and half-wave antiresonant at 4.52 GHz. The reactance approaches zero between 7.0 and 8.0 GHz in the range where three-quarter wave resonance and full-wave antiresonance were expected. In addition, the resistance peaks near 7.8 GHz and this is associated with the monopole's attempt to become antiresonant.

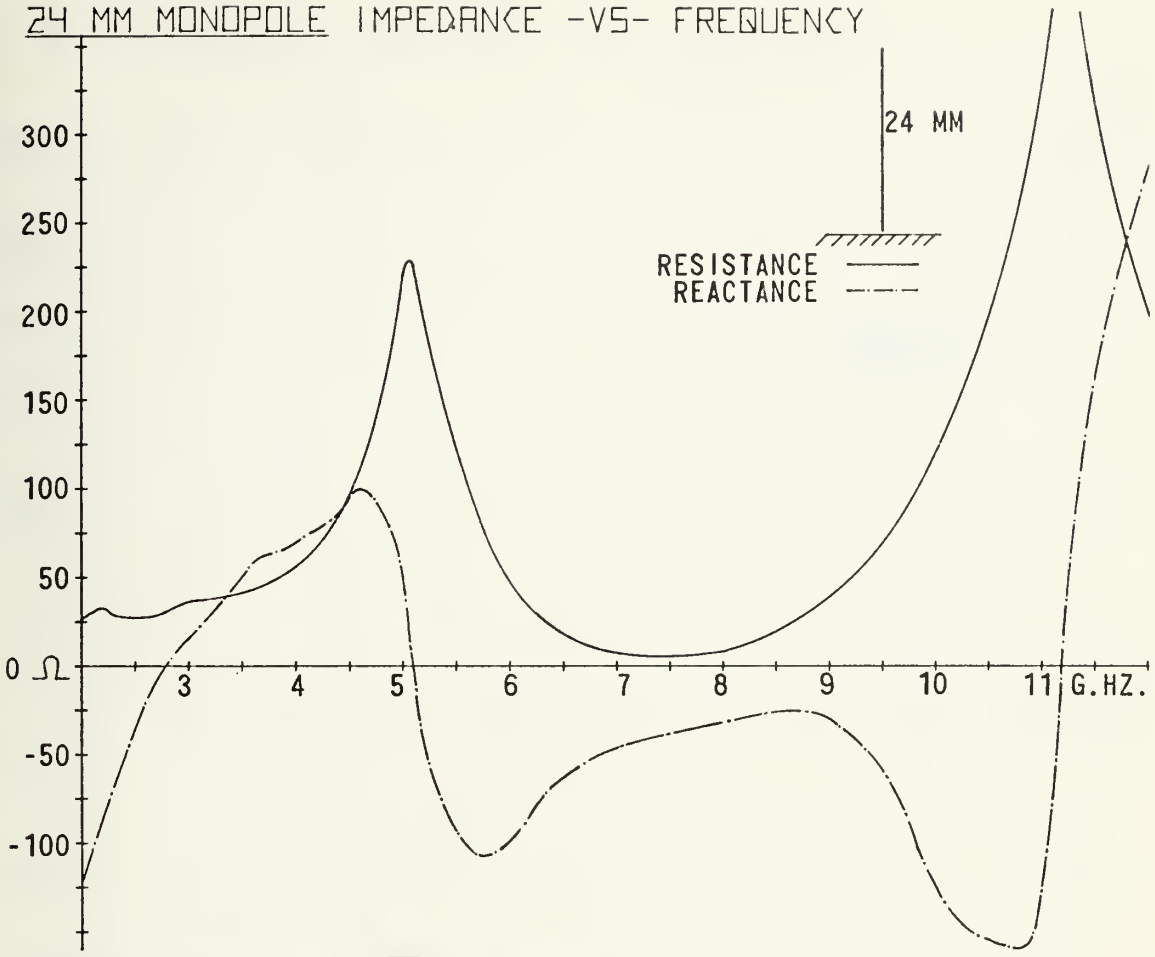

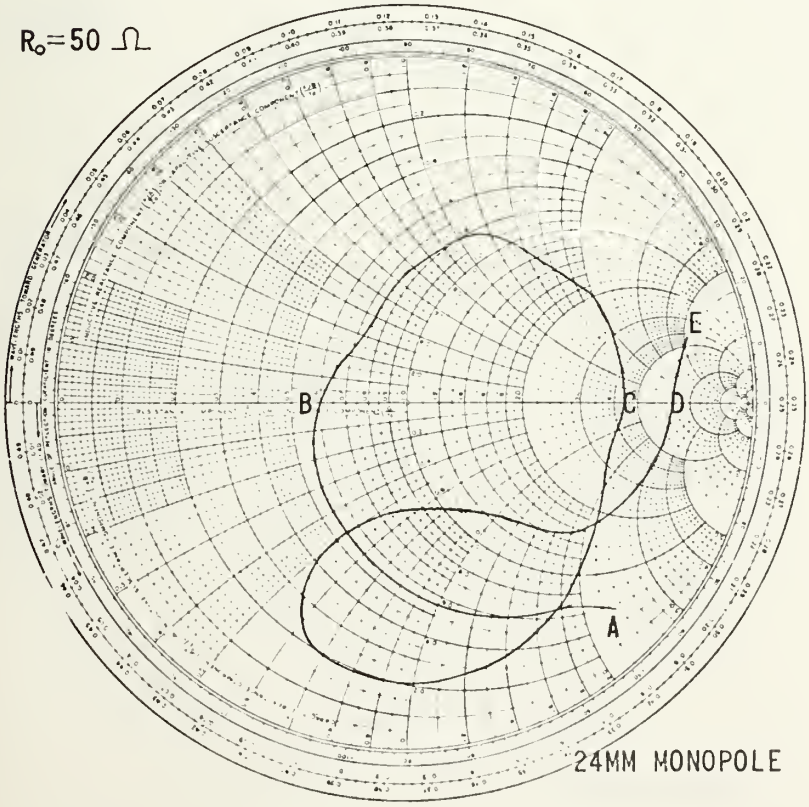

POINT	FREQUENCY
A	2.00 G.HZ.
B	2.78
C	5.09
D	11.14
E	12.00

24MM MONOPOLE

Figure 36

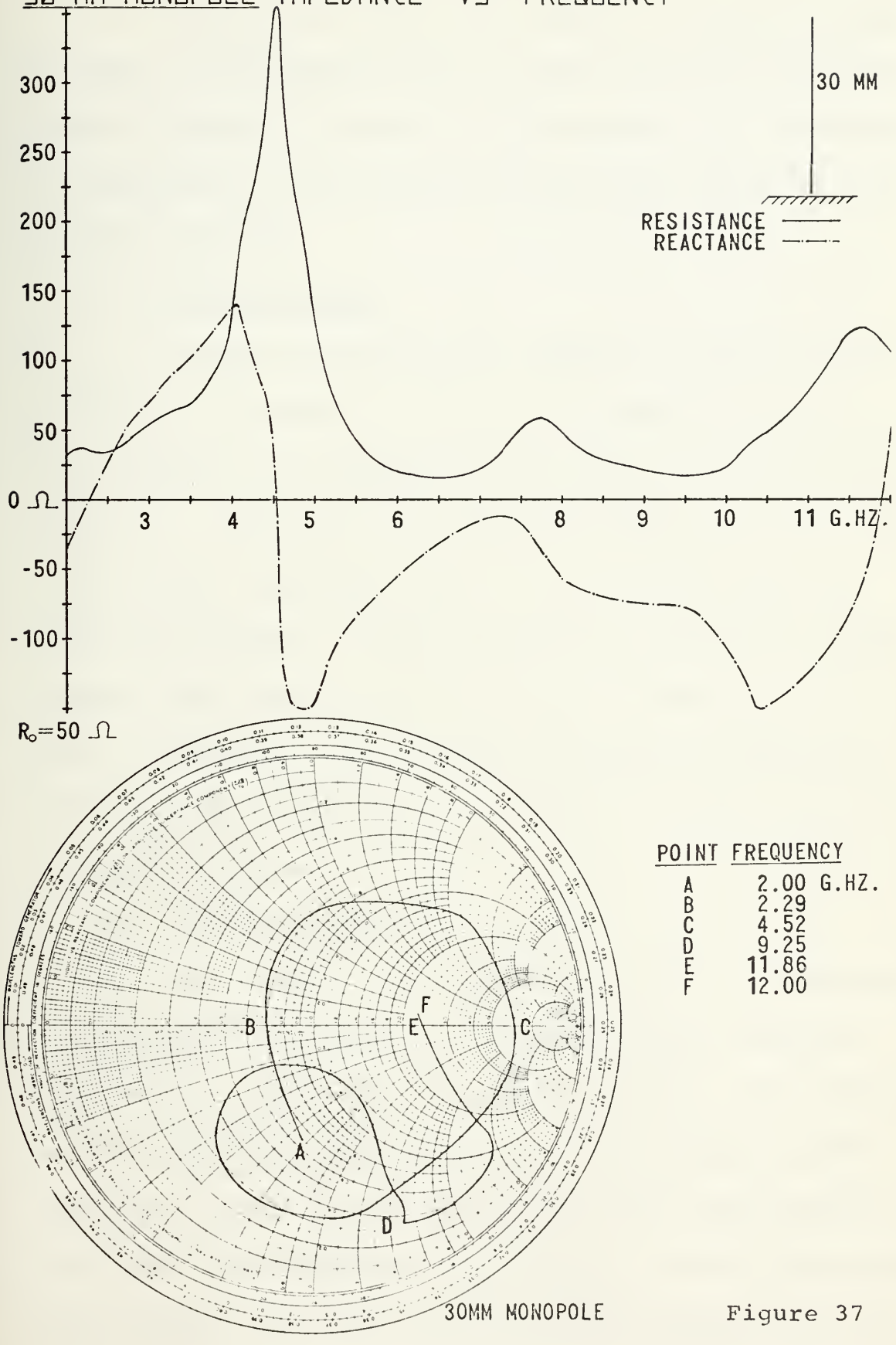

POINT	FREQUENCY
A	2.00 G.HZ.
B	2.29
C	4.52
D	9.25
E	11.86
F	12.00

Figure 37

There is an additional peaking of reactance near 9.7 GHz. This characteristic is associated with the five-quarter resonant frequency of the monopole, which resonance is suppressed by the dominance of the feed system as previously discussed.

7. 36 mm Monopole

Figure 38 displays the impedance characteristics of the 36 mm monopole. The wire is evidently quarter-wave resonant at a frequency below 2.00 GHz as was to be expected. Half-wave antiresonance occurs at 4.05 GHz with its attendant resistance peak. The reactance peaks inductively between 6.07 GHz, at which the monopole is three-quarter wave resonant, and 6.49 GHz, at which it is full-wave antiresonant. The monopole attempts to become five-quarter wave resonant near 10.0 GHz but is again restrained by the feed system.

8. 42 mm Monopole

The impedance characteristics of the 42 mm monopole are presented in Figure 39. The quarter-wave resonant frequency is well below the 2.00 GHz minimum. The half-wave antiresonant frequency is 3.64 GHz. Three-quarter wave resonance occurs at 5.14 GHz and full-wave antiresonance at 5.86 GHz. The attempt of the monopole to become five-quarter wave resonant and three-halves wave antiresonant near 8.5

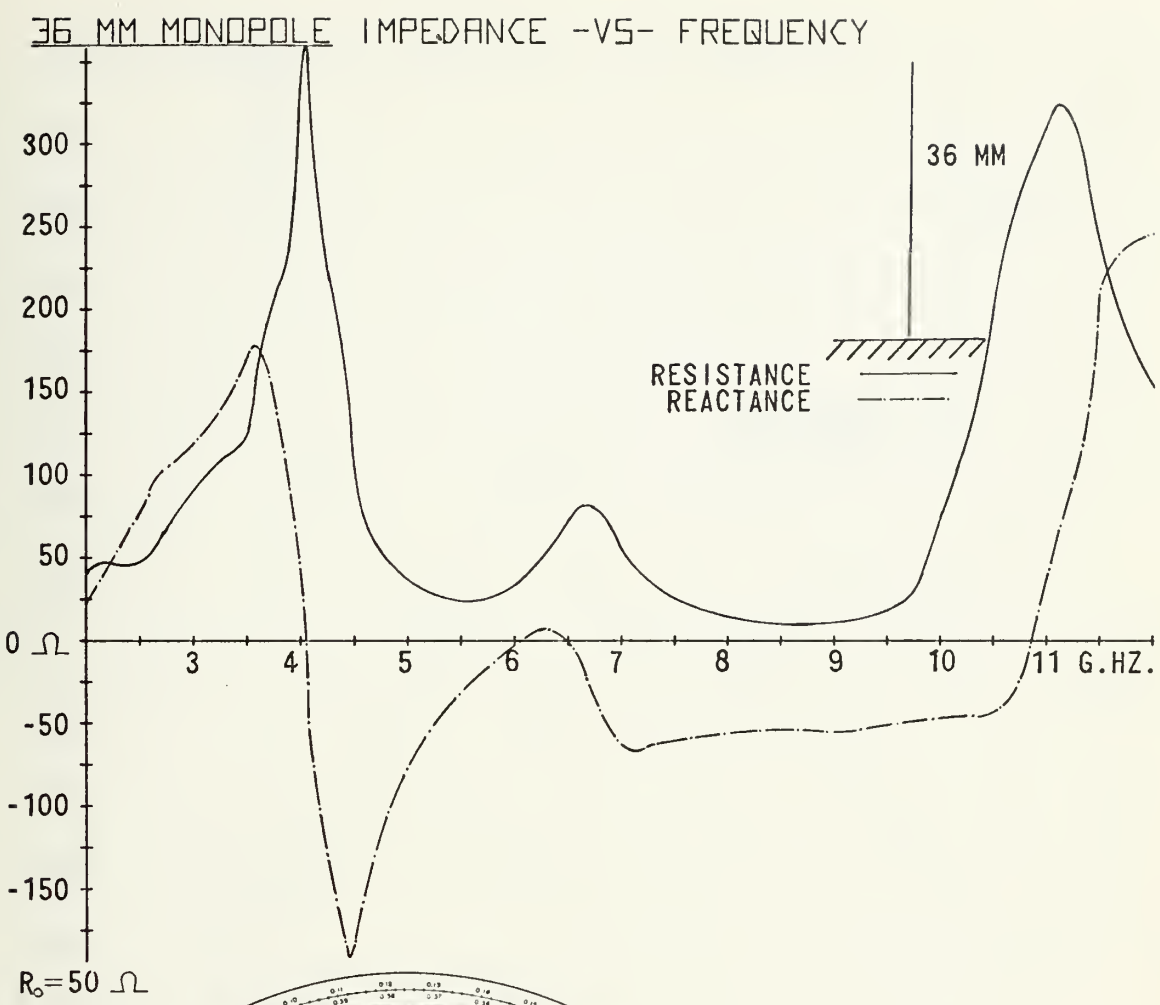

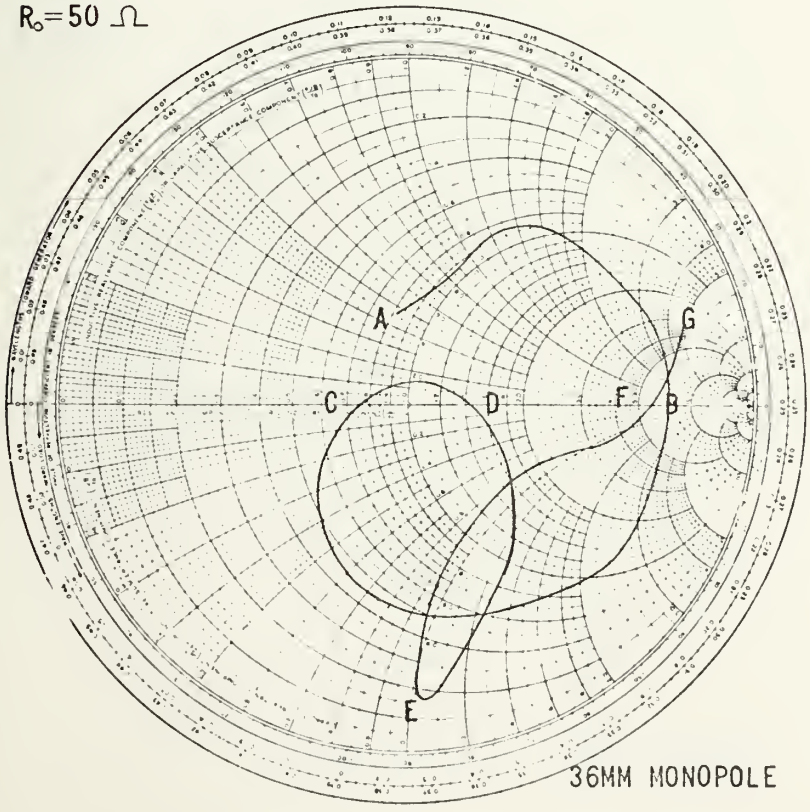

POINT	FREQUENCY
A	2.00 G.HZ.
B	4.05
C	6.07
D	6.49
E	8.50
F	10.86
G	12.00

36MM MONOPOLE

Figure 38

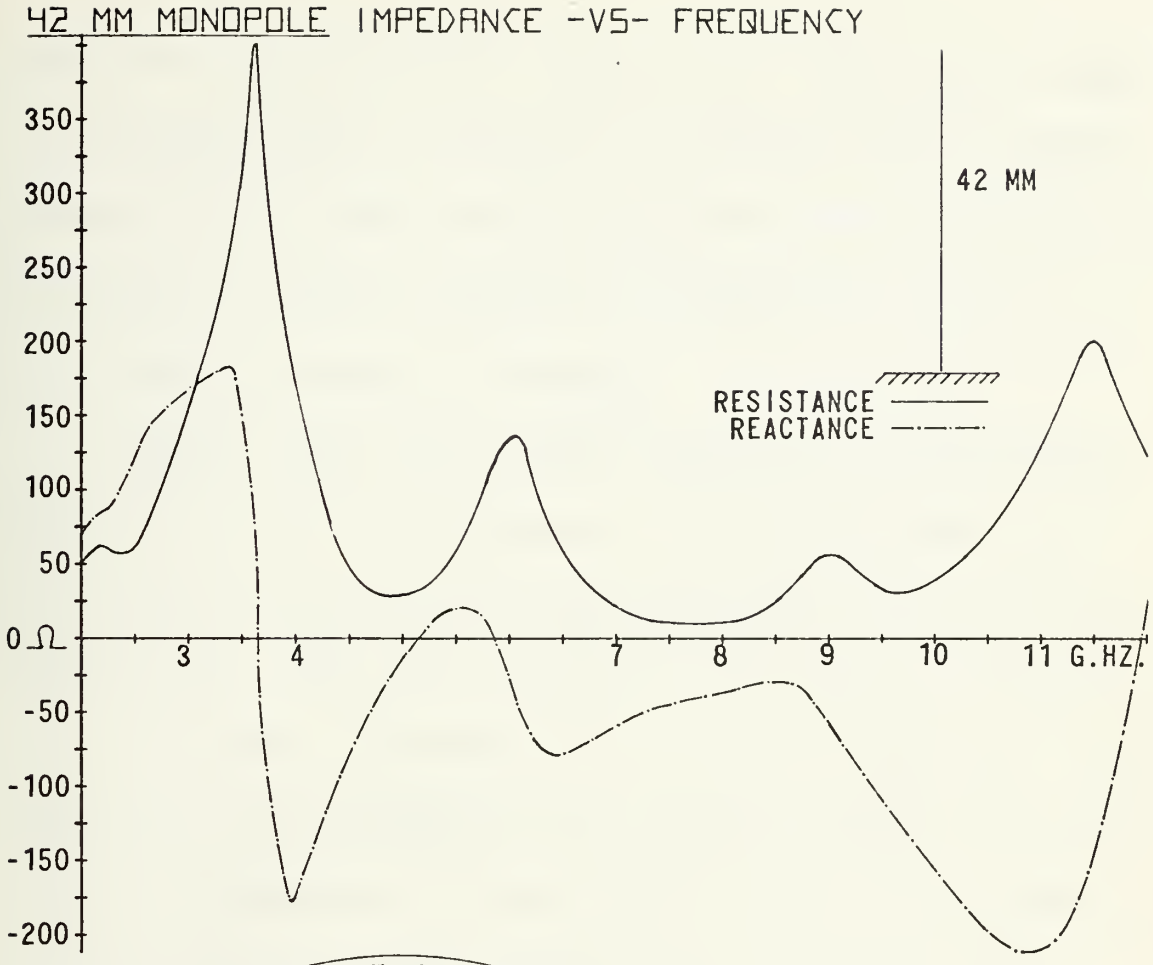

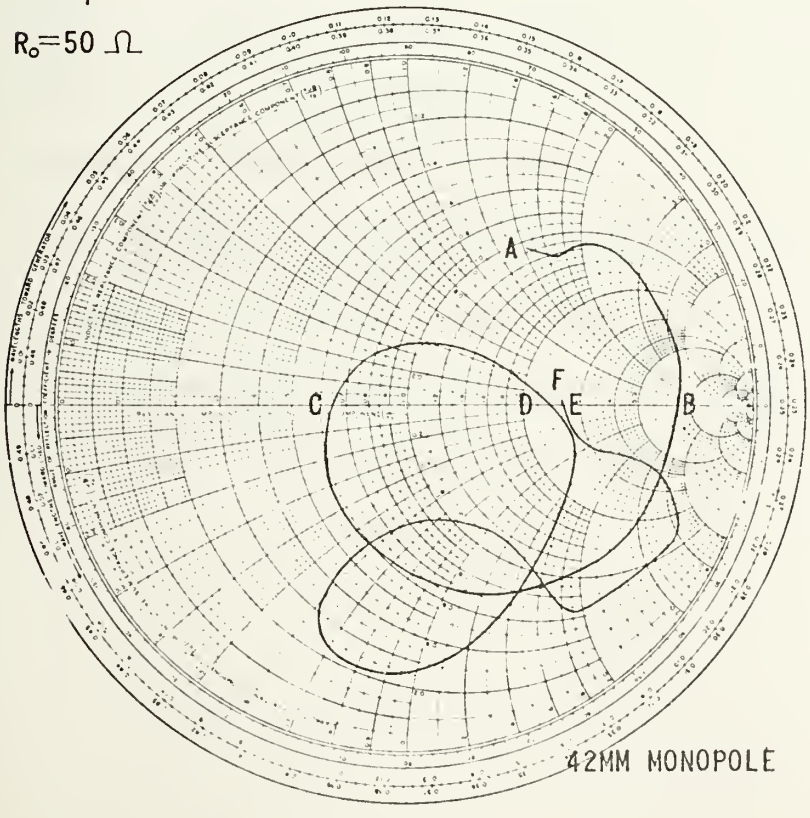

42MM MONOPOLE

POINT	FREQUENCY
A	2.00 G.HZ.
B	3.64
C	5.14
D	5.86
E	11.97
F	12.00

Figure 39

GHz is now pronounced but unsuccessful. However, the peak in resistance near 9.0 GHz is an indication that a longer monopole will indeed resonate in these modes as was seen in the case of the 30 mm monopole in Figure 37.

D. MONOPOLE LENGTH VS FREQUENCY

Resonant and antiresonant frequencies of longer monopoles up to 84 mm were measured for resonant modes up to seven-quarter wavelengths and antiresonant modes up to two-wavelengths. This data, together with similar information for the shorter monopoles, is presented in Figure 40. This graph then, is a summary of the measured resonant and antiresonant frequencies of the monopoles and will be useful in the analyses of more complex wire structures. The deviation of these curves from theory is small and is attributable to the following facts: the monopoles are not fed from an ideal, frequency independent source with a matched impedance through an ideal feed point; the monopoles have finite radii and ohmic losses; and finally, the ground plane has ohmic losses and is finite in extent.

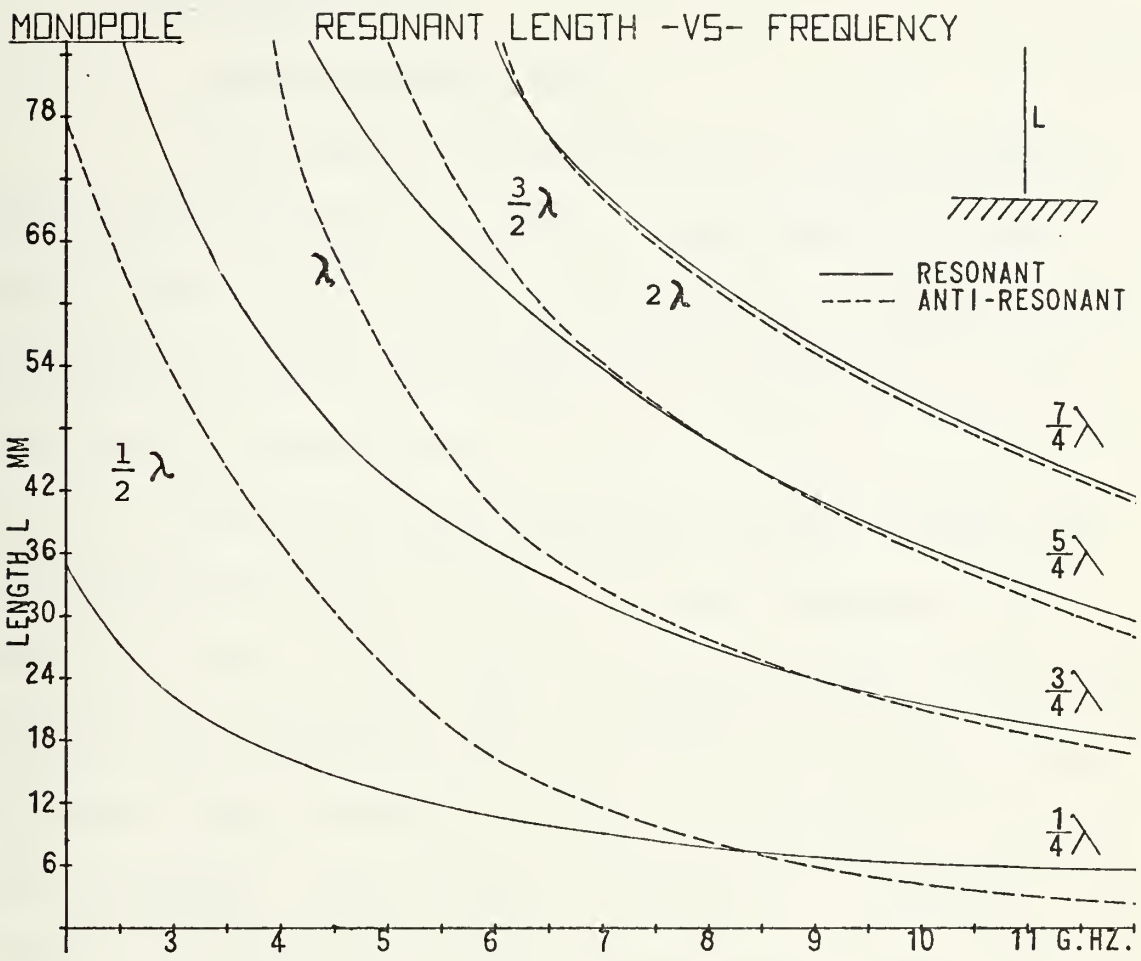
MONOPOLE
RESONANT LENGTH -VS- FREQUENCY
L
RESONANT
ANTI-RESONANT
LENGTH L MM
78
66
54
42
36
30
24
18
12
6
3
4
5
6
7
8
9
10
11 G.HZ.
1/2 λ
λ
3/2 λ
2 λ
7/4 λ
5/4 λ
3/4 λ
1/4 λ

Figure 40

E. CROSS-MONOPOLE

1. Cross-Monopole Case 1A

The impedance characteristics of cross-monopole Case 1A are presented in Figure 41 along with the simple monopole of equal height. This wire structure is composed of an 18 mm monopole with an orthogonal 12 mm cross-arm centered 12 mm from the ground plane.

From the theory developed earlier in this paper and the impedance measurements of simple monopoles, the prediction could be made that the cross-monopole, due to the loading of the cross-arm, will be resonant and antiresonant at somewhat lower frequencies than the associated 18 mm unloaded monopole. This is seen to be true. In addition, effects of the cross arm might be seen near frequencies associated with the 6, 12, and 18 mm current paths as discussed earlier.

Disregarding the previously identified characteristics of the feed system, it is seen that the structure is resonant at 3.05 GHz and antiresonant at 5.65 GHz. An examination of Figure 40 reveals that these are quarter-wave resonant and half-wave antiresonant frequencies respectively of a simple monopole about 20 mm long.

From the Smith Chart in Figure 41, it is seen that sharp perturbations in the impedance occur at 5.40 GHz and 10.80 GHz. 5.40 GHz is very near the quarter-wave

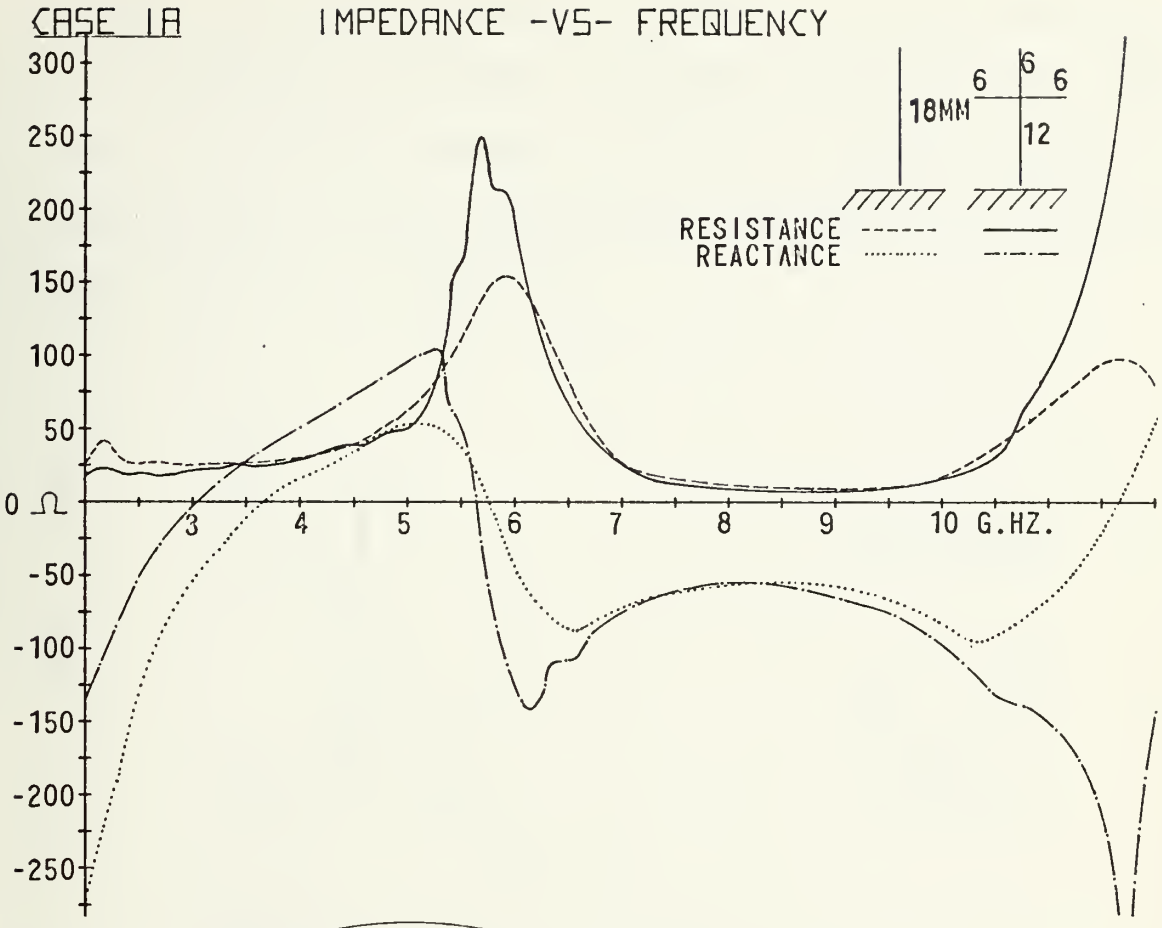

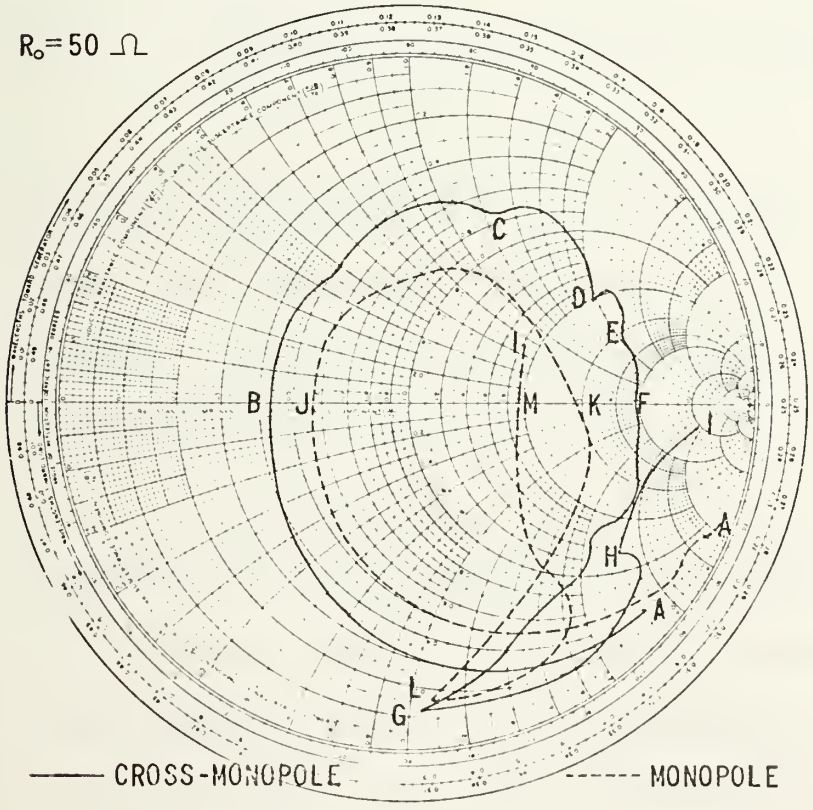

POINT	FREQUENCY
A	2.00 G.HZ.
B	3.05
C	4.38
D	5.40
E	5.55
F	5.65
G	8.50
H	10.80
I	12.00
J	3.67
K	5.75
L	8.35
M	11.66

Figure 41

resonant frequency of a 12 mm monopole. At this frequency, the 6 mm members are about one-eighth wavelength long. Therefore, the junction location is neither a current maximum nor charge minimum of the standing wave patterns on the structure which are shown in Figure 42.

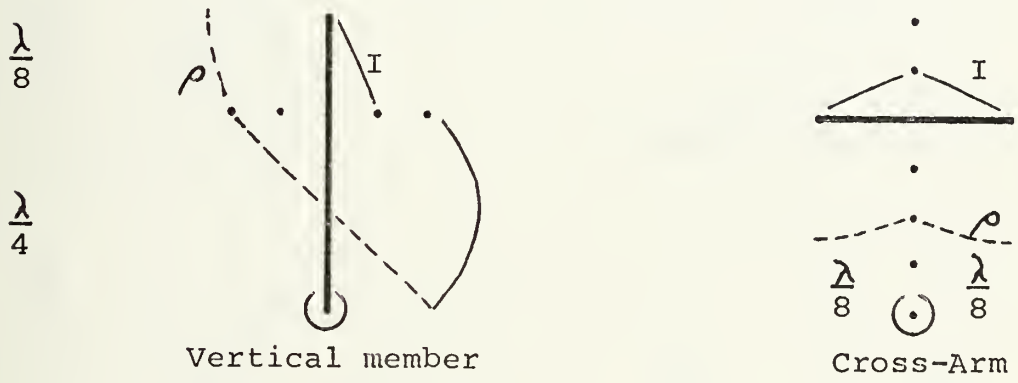

Figure 42

Current and charge distributions on cross-monopole Case 1A at 5.40 GHz

However, the current fed to the junction from the lower member is about equally divided between the three upper members. Consequently, maximum coupling occurs between the members in the junction region.

The frequency, 10.80 GHz, is the quarter-wave resonance of a 6 mm monopole and is therefore associated with the three upper members of the cross. The effect is undoubtedly enhanced by the resonation of three members rather than one. The cross-arm is located at a current

maximum and charge minimum. The current fed into the junction from the lower 12 mm member is nearly equally divided between the three upper 6 mm members. A sketch of the current and charge distributions on the structure at this frequency is shown in Figure 43.

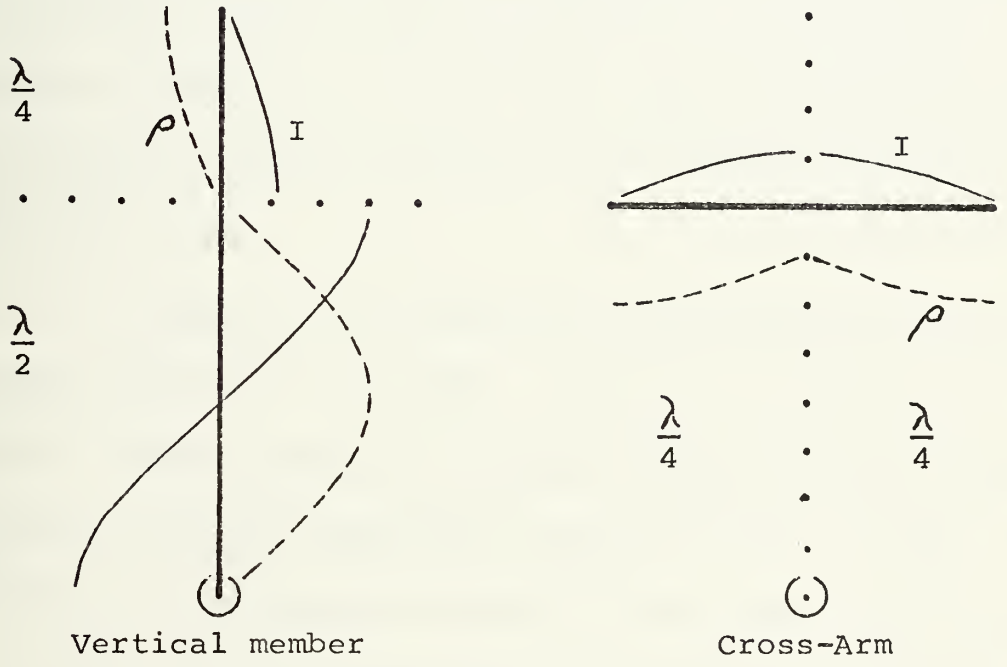

Figure 43
Current and charge distributions on cross-monopole Case 1A at 10.80 GHz

In terms of coupling, the physical structure of the cross must be considered. At the lower frequencies, all of the cross members are electrically short as compared with a wavelength. As the frequency approaches 5.40 GHz, the current in all members is maximized simultaneously at the junction resulting in the perturbation observed in the impedance characteristics. As the frequency approaches the natural quarter-wave resonant frequency of the 6 mm members,

10.80 GHz, the standing wave on all members have a maximum current near the junction. Hence, the coupling between the members is maximized exactly at 10.80 GHz supporting a frequency lock-in effect. This might be characterized by saying that the natural frequency of the members is identical to the driven frequency of the structure. As the driven frequency is further increased, the lock-in due to the coupling is broken - hence, the form of the impedance perturbation on the Smith Chart.

In terms of the reflection coefficient, Γ, as the frequency approaches 5.40 GHz, the voltage incident at the feed point reaches a relative maximum compared to the voltage reflected from the feed point reducing Γ to a minimum. The same V_r/V_i relationship occurs at 10.8 GHz. As evidenced on the Smith Chart in Figure 41, this dip in Γ is quite sharp as the frequency is swept through resonant conditions.

The analysis of Case 1A may be summarized as follows. From the feed point, at frequencies near 3.05 and 5.65 GHz, the structure resonates as if it were a 20 mm monopole. At 5.40 GHz, coupling near the junction reaches a relative maximum. At 10.80 GHz, standing quarter-wave resonances are set up in the three 6 mm members with maximum mutual coupling between the cross-arms

and the vertical member. At both resonant frequencies, 5.40 and 10.80 GHz, the reflection coefficient passes through a sharp relative minimum.

2. Cross-Monopole Case 1B

The impedance of cross-monopole Case 1B is reproduced in Figure 44. This structure is composed of a 36 mm monopole loaded with a 24 mm cross-arm centered 24 mm from the ground plane. These dimensions are exactly double those of Case 1A shown in Figure 41. Consequently, the analytic method and reasoning used in Case 1A is applied to this structure.

The structure is resonant at 6.65 GHz and anti-resonant at 4.03 and 7.29 GHz. From Figure 40, these values are seen to correspond roughly to the characteristic frequencies of a simple 36 mm monopole as expected. Major perturbations in impedance linearity occur at 2.78 and 5.75 GHz. Figure 40 reveals that 2.78 GHz corresponds to the quarter-wave resonant frequency of a 24 mm monopole. The frequency, 5.75 GHz, relates to the quarter-wave resonance of a 12 mm monopole, the length of the upper three members of the cross. The analysis of waveforms on the structure and coupling between the members near these frequencies are therefore identical to those of Case 1A. The distributions on the structure of Case 1A at the corresponding frequencies,

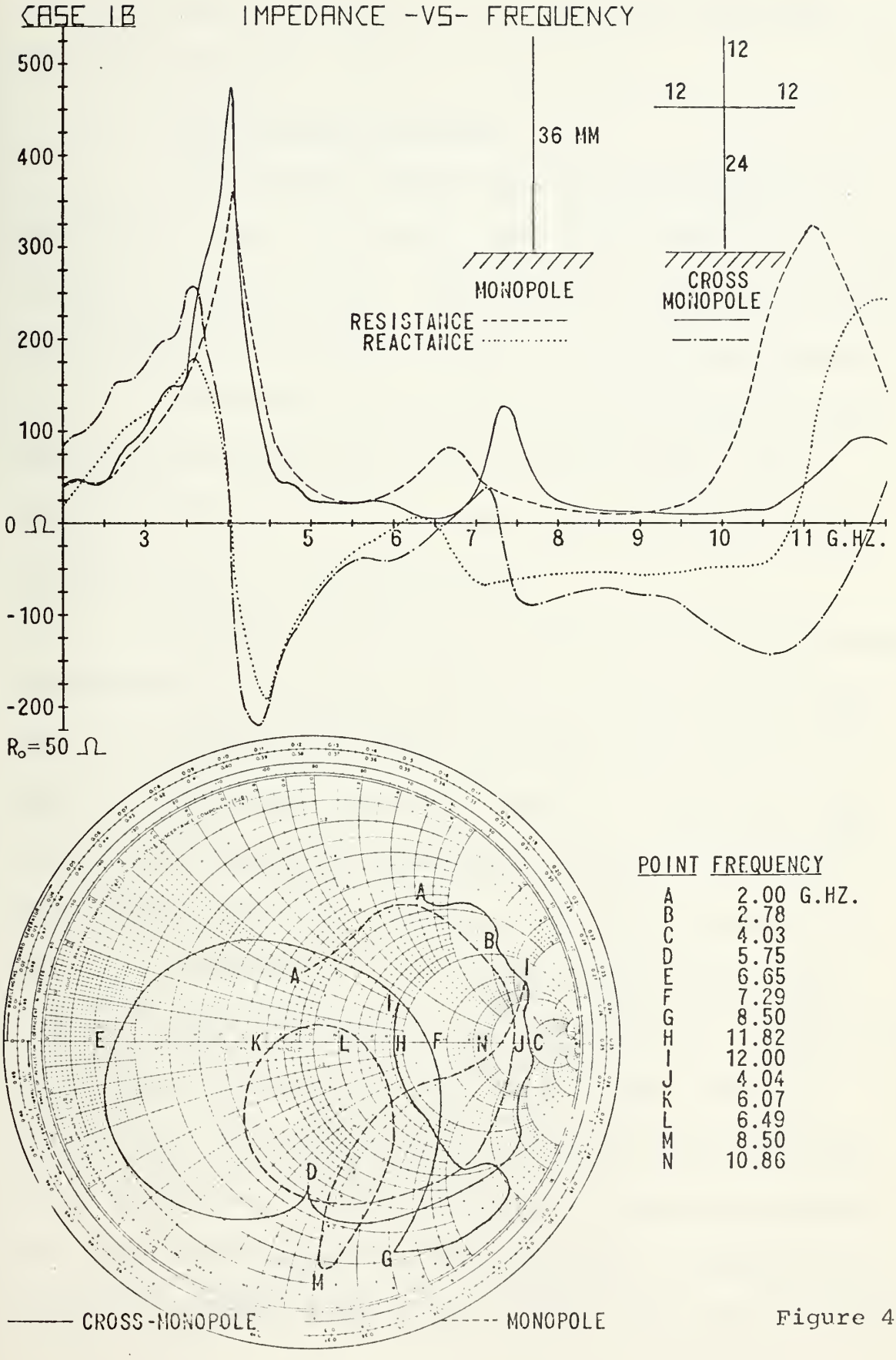

POINT	FREQUENCY
A	2.00 G.HZ.
B	2.78
C	4.03
D	5.75
E	6.65
F	7.29
G	8.50
H	11.82
I	12.00
J	4.04
K	6.07
L	6.49
M	8.50
N	10.86

Figure 44

shown in Figures 42 and 43, are thus equally applicable to Case 1B at 2.78 and 5.75 GHz respectively.

3. Cross-Monopole Case 2A

The impedance characteristics of cross-monopole Case 2A are shown in Figure 45 along with those of the simple monopole of equal height. The cross is an orthogonal arrangement of four 12 mm members as shown in the included sketch.

The resonant frequency of the structure is 2.21 GHz and the antiresonant frequency is 5.28 GHz; these characteristics corresponding approximately to the 24 mm monopole without cross-arm loading.

The characteristics in Figure 45 reveal significant perturbations in impedance linearity at 3.26 and 5.80 GHz. Near 3.26 GHz, the resistance increases while the rate of reactance change decreases with change in frequency. Near 5.80 GHz, the resistance decreases but again, reactance tends toward constancy. Another view of this anomaly is that, as the frequency is increased slightly above these critical values, the magnitude of the reflection coefficient, and thus the standing wave ratio on the line, increases sharply while the phase angle trend tends toward reversal. Stated another way; as the frequency is increased slightly above these critical values, the magnitude of the reflected voltage to incident voltage ratio at the feed point increases

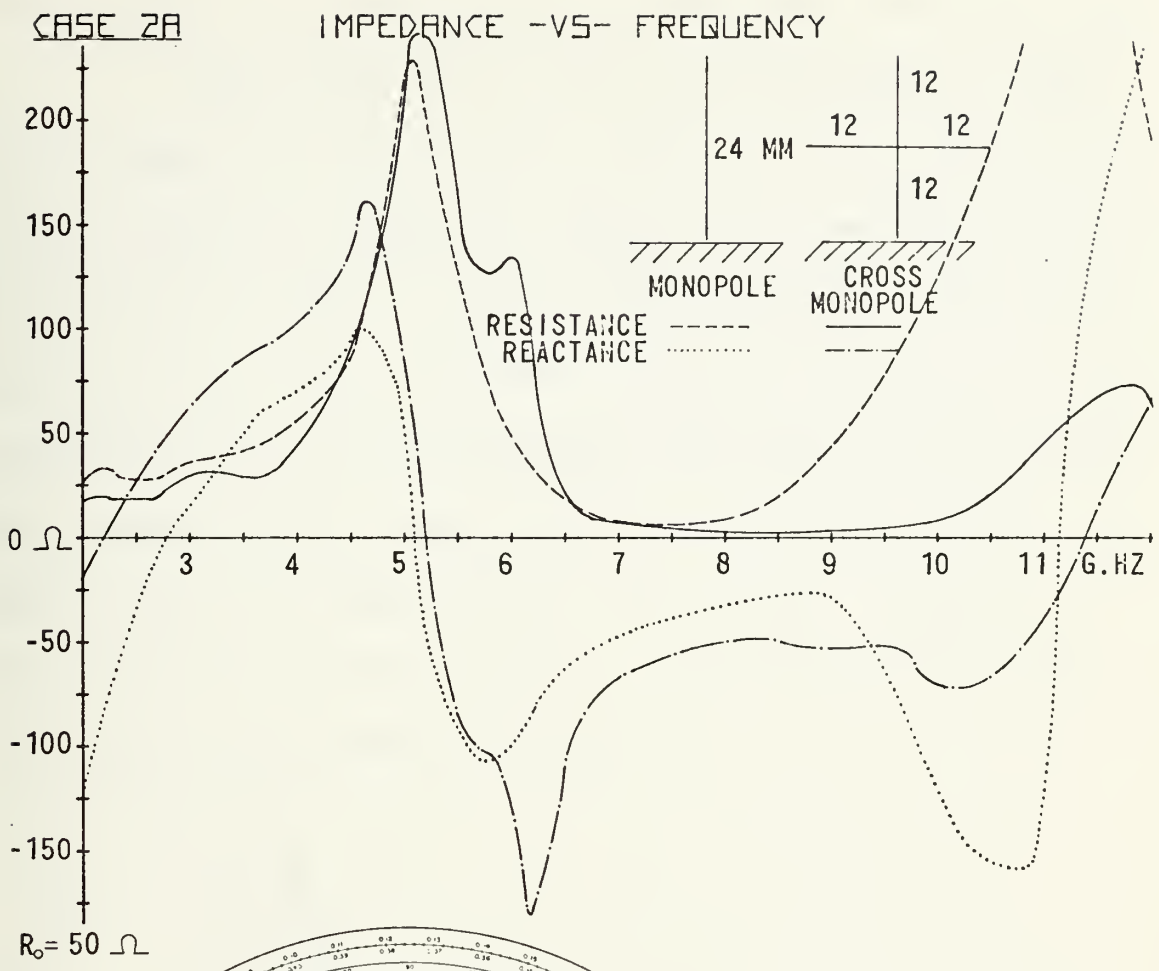

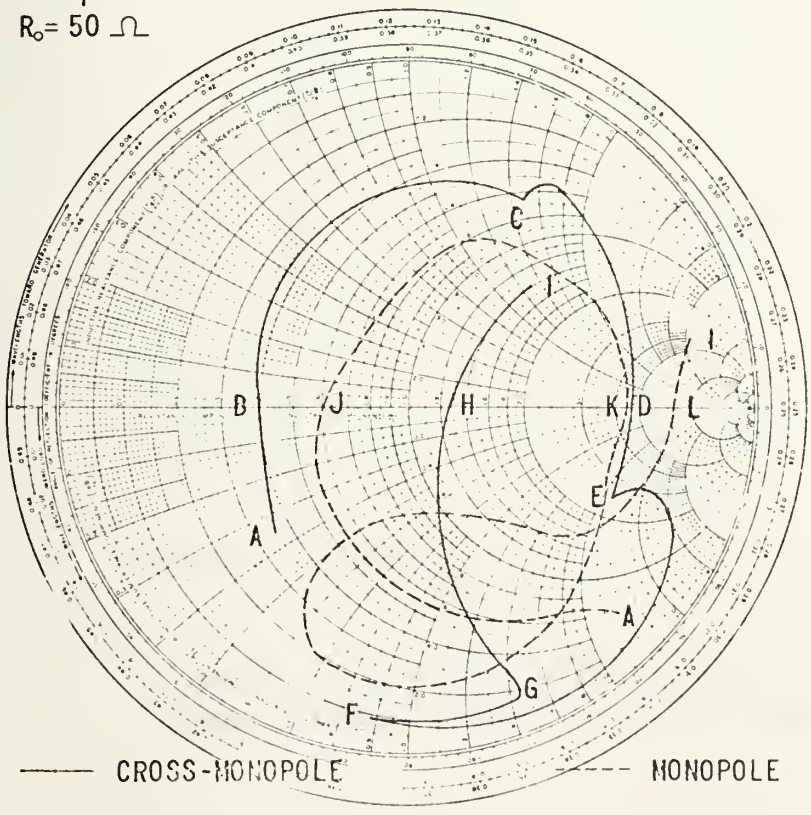

POINT	FREQUENCY
A	2.00 G.HZ.
B	2.21
C	3.26
D	5.28
E	5.80
F	8.36
G	10.10
H	11.38
I	12.00
J	2.78
K	5.09
L	11.14

Figure 45

sharply while the relative phase trend tends toward reversal.

One conclusion to these interpretations is that, at 3.26 GHz, the standing wave patterns on the cross have a current maximum and charge minimum at the feed point and the vertical 24 mm member is quarter-wave resonant. The 12 mm arms and upper vertical member, however, are only one-eighth wavelength long at this frequency and hence, do not resonate. The current fed into the junction from the lower member is split between the upper three 12 mm members. Coupling is thus enhanced near the junction. The associated standing wave patterns are shown in Figure 46.

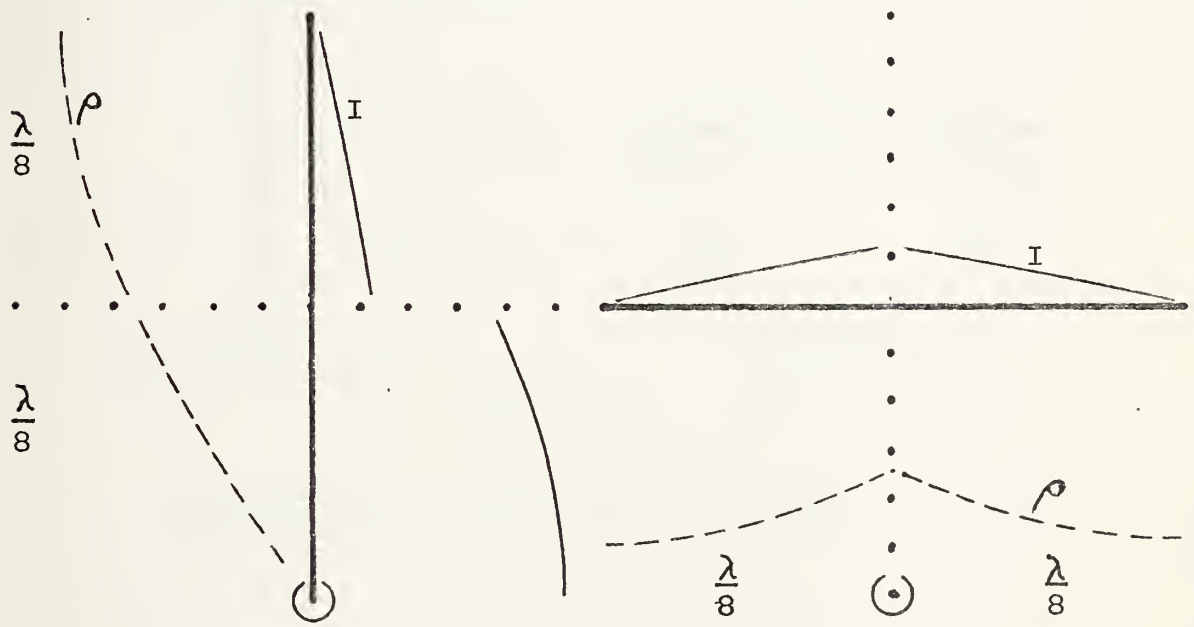

Figure 46

Current and charge distributions on cross-monopole Case 2A at 3.26 GHz

The impedance perturbation at 5.80 GHz is identified with the quarter-wave resonant frequency of a 12 mm monopole. The revealing interpretation here is that, at this frequency, the impedance is relatively high but the reflection coefficient at the feed point is small compared with higher frequencies and hence, the current is a relative minimum and the voltage is a relative maximum at that position. The related standing waves on the wire structure are then as shown in Figure 47.

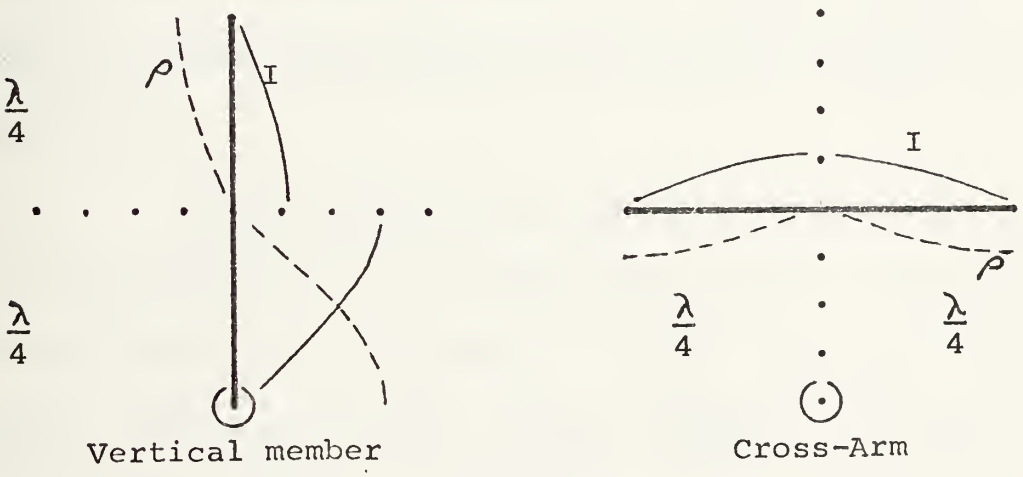

Figure 47

Current and charge distributions on cross-monopole Case 2A at 5.80 GHz

The upper three 12 mm members are all quarter-wave resonant at 5.80 GHz and the junction is located at a current maximum and charge minimum. All members thus resonate strongly with

maximum coupling near the junction.

4. Cross-Monopole Case 2B

The impedance of cross-monopole Case 2B is presented in Figure 48. The composition of this structure is a 24 mm monopole loaded with a single 12 mm arm located 12 mm from the ground plane. This structure is identical to that of Case 2A but with one 12 mm arm removed.

The resonant frequency of this structure is 2.43 GHz with antiresonance occurring at 5.20 GHz. Again, as in Case 2A, these characteristics are similar to those of a 24 mm monopole.

The perturbation in impedance linearity at 2.93 GHz is related to the 24 mm current path in the vertical member. It is in quarter-wave resonance at that frequency. The current into the junction is split between the upper two 12 mm members. Moderate coupling thus occurs in the junction region although the 12 mm members do not resonate. The standing wave patterns at this frequency are shown in Figure 49.

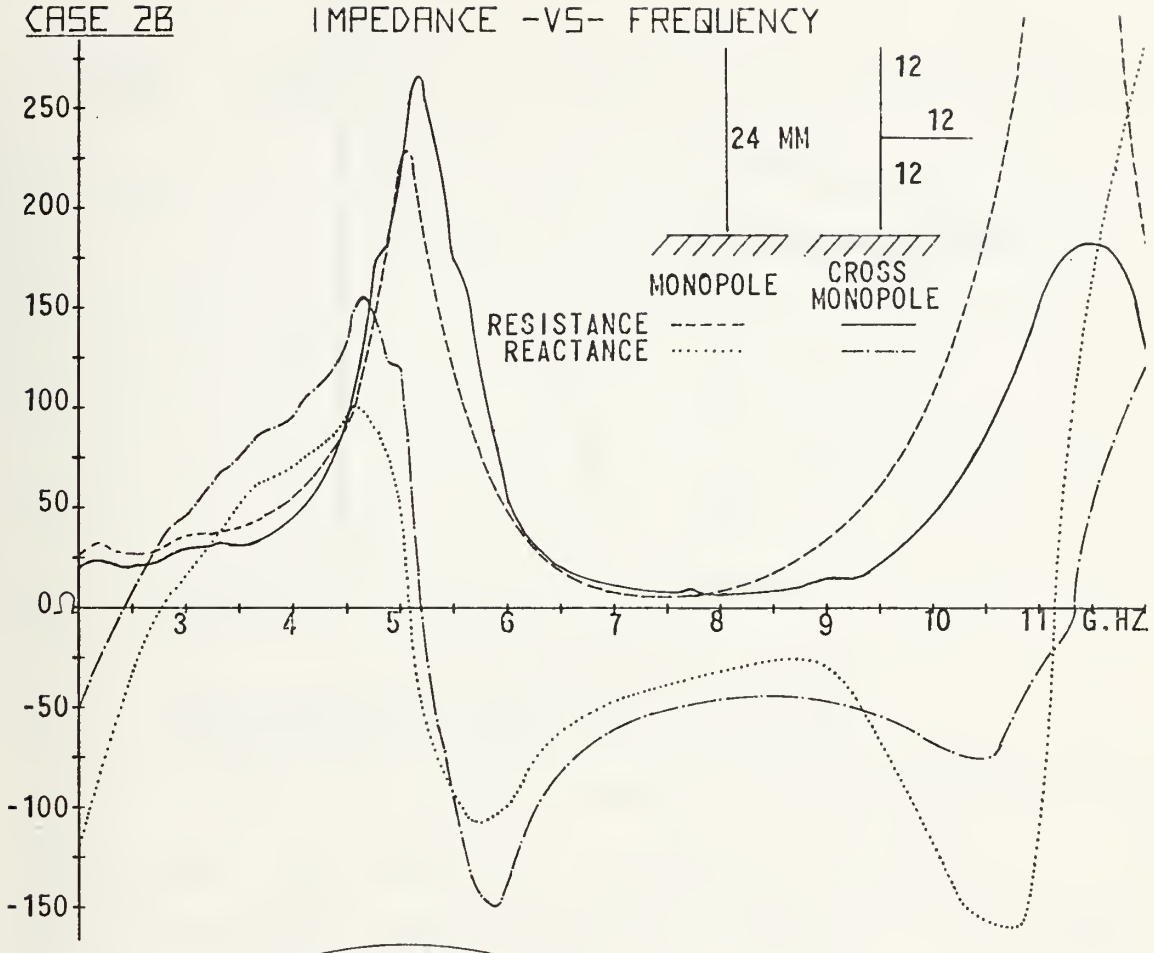

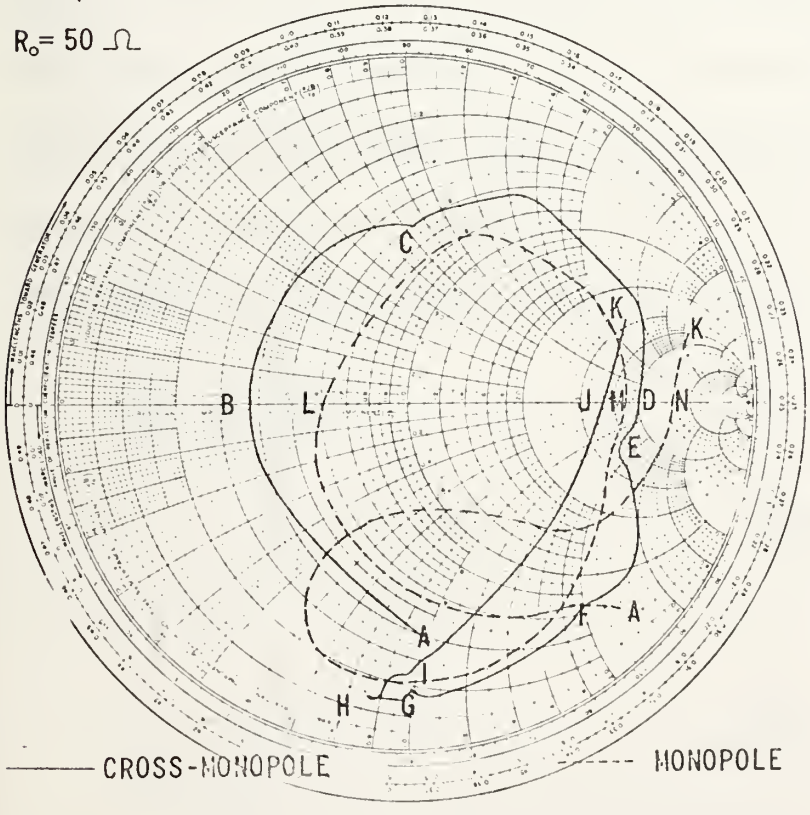

POINT	FREQUENCY
A	2.00 G.HZ.
B	2.43
C	2.93
D	5.20
E	5.46
F	6.24
G	7.65
H	8.00
I	9.25
J	11.34
K	12.00
L	2.78
M	5.09
N	11.14

Figure 48

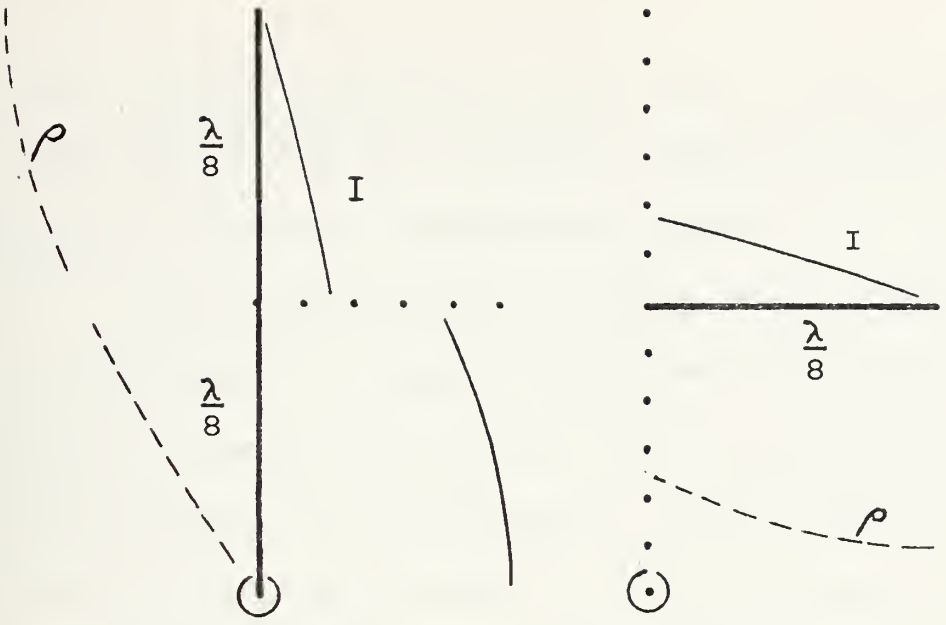

Figure 49

Current and charge distributions on cross-monopole Case 2B at 2.93 GHz

The 12 mm simple monopole was quarter-wave resonant at 5.46 GHz. Therefore, the nonlinearity at point E in Figure 48 is associated with quarter-wave resonance in the three 12 mm members of the cross. At this frequency, the current standing wave in each member has a maximum near the junction. Therefore, maximum coupling occurs in the junction region. The associated standing wave patterns are shown in Figure 50.

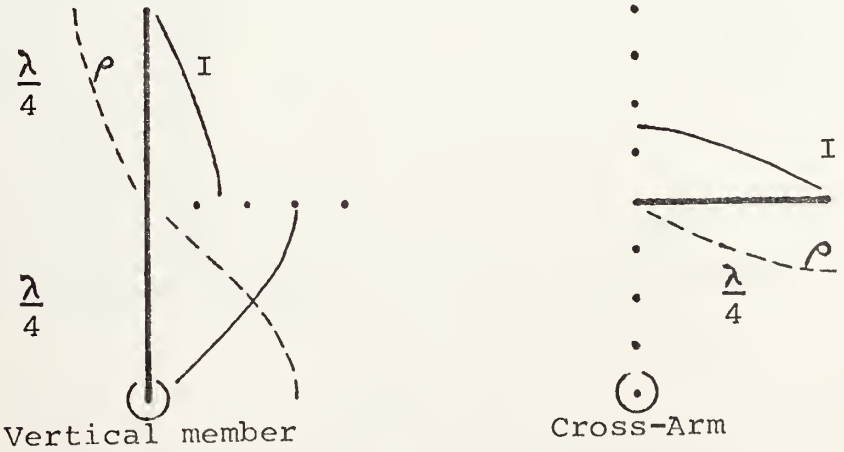

Figure 50

Current and charge distributions on cross-monopole Case 2B at 5.46 GHz

However, the lock-in effect in this case is less than for the equivalent frequency in Case 2A, shown in Figure 47, because the coupling is effectively halved.

The perturbation at 9.25 GHz, point I in Figure 48, is explainable in terms of the three-quarter wave resonance of the 24 mm vertical member of the structure. At this frequency, the 12 mm members are not resonant but the current fed to the junction is divided between the arm and upper member. The location of the cross junction is neither a current nor charge maximum nor minimum. The associated standing wave patterns are shown in Figure 51.

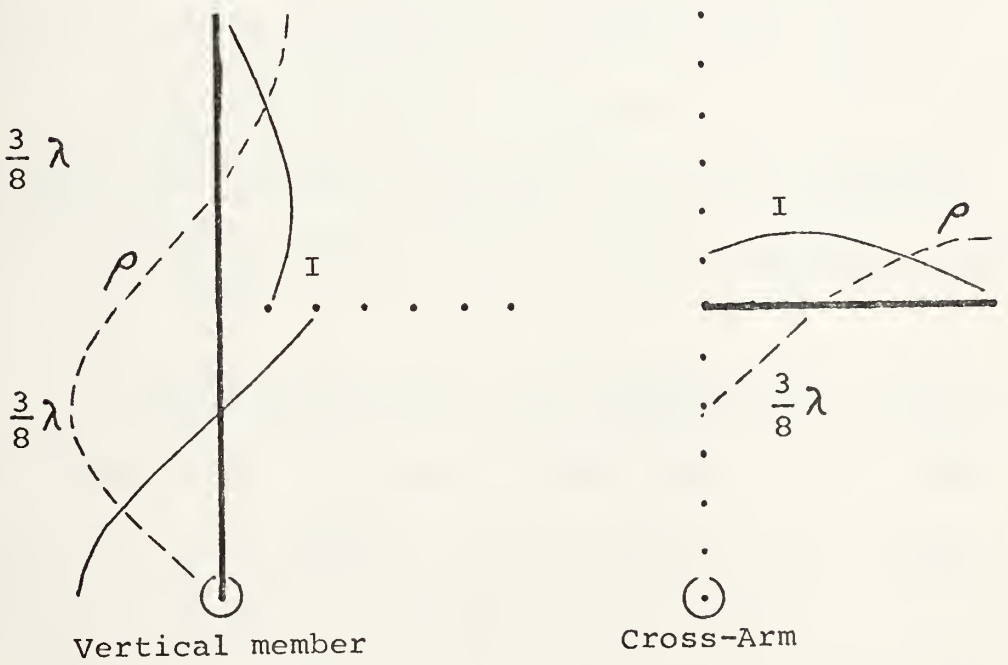

Figure 51

Current and charge distributions on cross-monopole Case 2B at 9.25 GHz

5. Cross-Monopole Case 2C

Characteristics of cross-monopole Case 2C are reproduced in Figure 52. It is seen that this structure is a 12 mm monopole top loaded with a 12 mm arm. It is thus compared with an unloaded 12 mm monopole. It may also be observed that this structure is the same as Case 2A but with the top and one 12 mm arm removed.

The resonant and antiresonant frequencies of this structure are 3.01 and 5.30 GHz respectively. These characteristics are the same as those for a simple 22 mm monopole as interpolated from Figure 40. The conclusion can be drawn that, near these frequencies, the structure looks more like a longer bent monopole than it does a shorter top-loaded monopole. In fact, the characteristics throughout the measured frequency range are remarkably similar to those of the 21 mm monopole presented in Figure 35.

The perturbation in the characteristics at 8.70 GHz is related to the 24 mm current path. At this frequency, the 24 mm length is three-quarter wave resonant. Again, the location of the junction is neither a current nor charge maximum nor minimum. The standing wave distributions are shown in Figure 53.

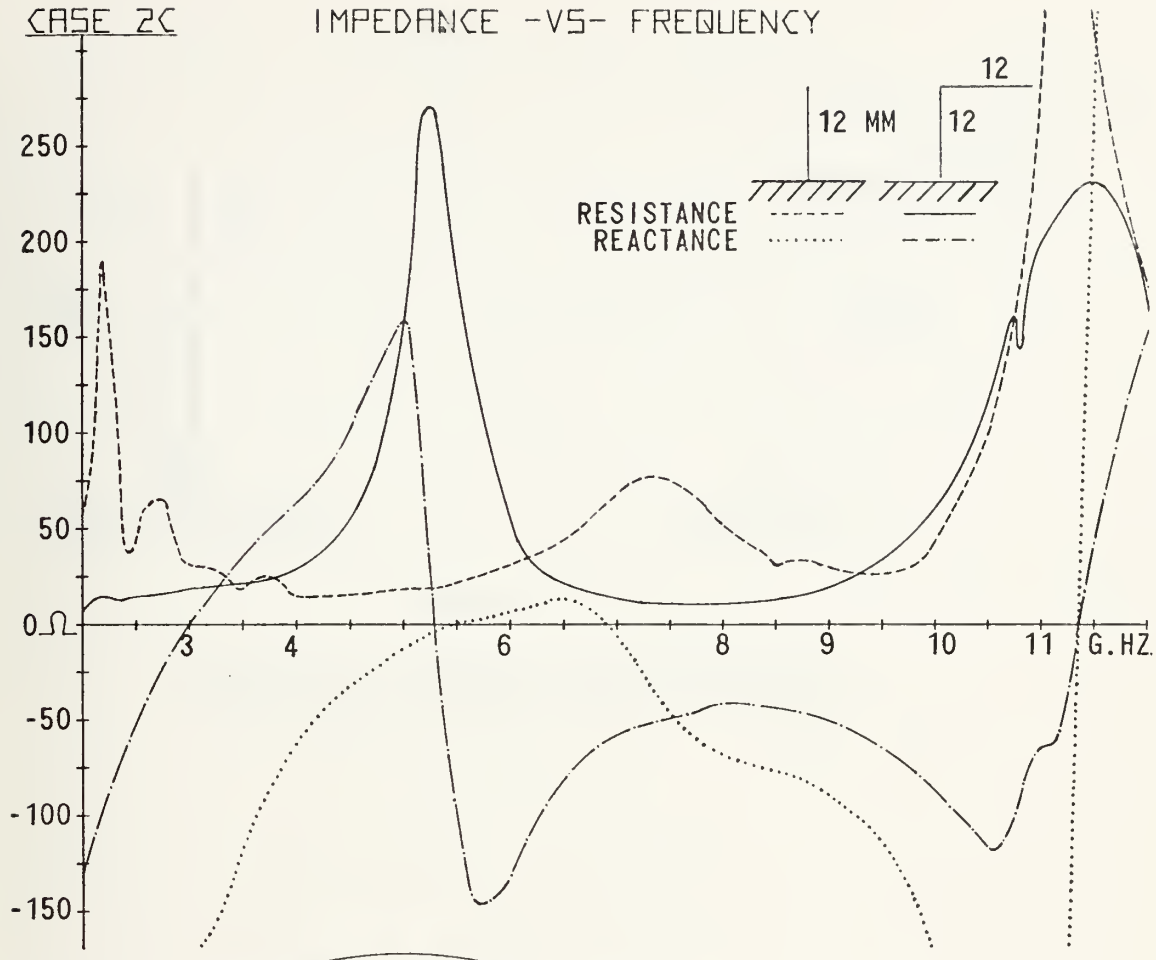

$R_o = 50\ \Omega$

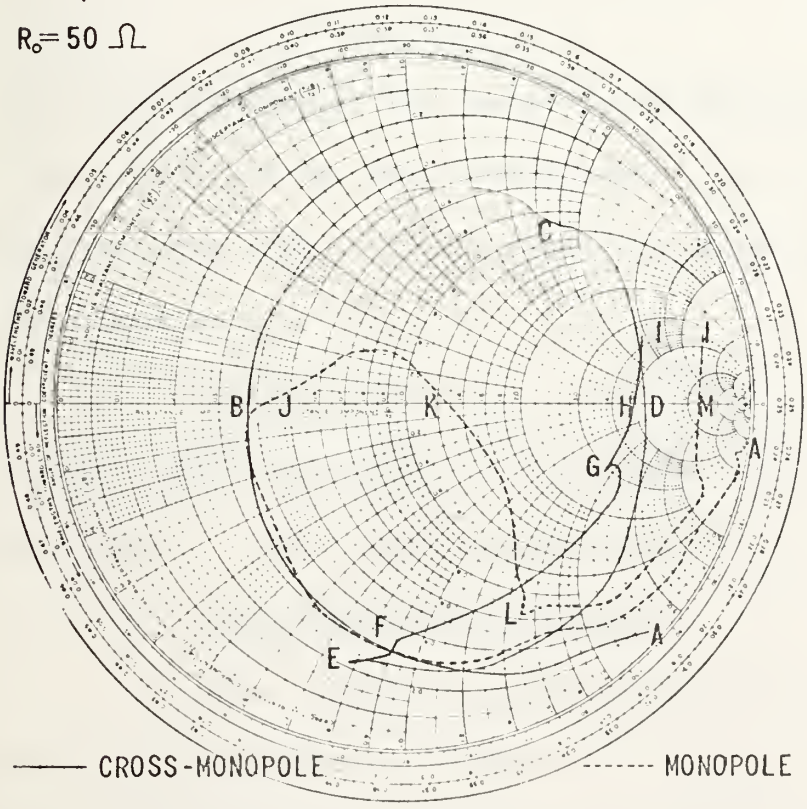

POINT	FREQUENCY
A	2.00 G.HZ.
B	3.01
C	4.34
D	5.30
E	8.00
F	8.70
G	10.80
H	11.36
I	12.00
J	5.46
K	6.91
L	8.50
M	11.36

—— CROSS-MONOPOLE ------ MONOPOLE

Figure 52

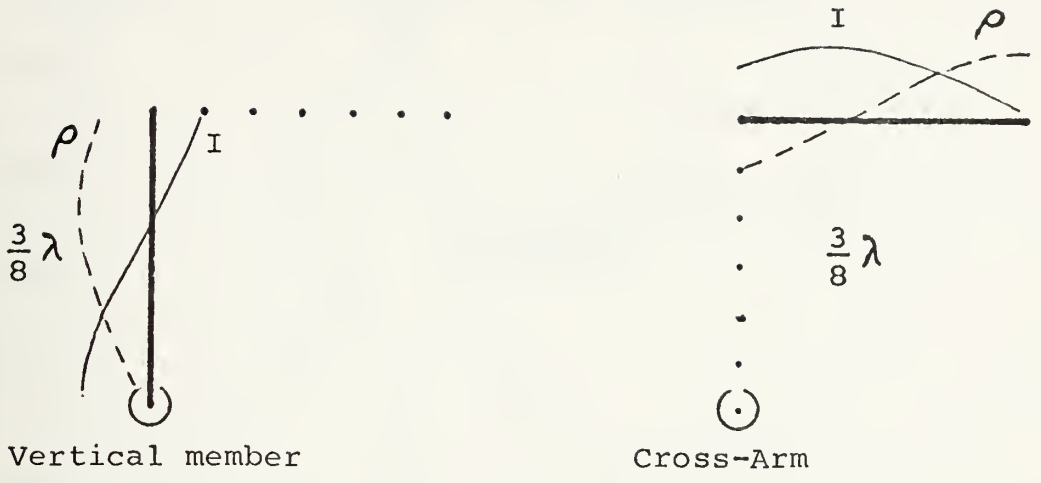

Figure 53

Current and charge distributions on cross-monopole Case 2C at 8.70 GHz

At this frequency, the coupling between the cross members near the junction has little effect on the impedance characteristics, the major effect resulting from the three-quarter standing wave.

Other impedance perturbations indicated in Figure 52 are characteristics of the measuring system, as previously discussed, rather than the wire structure.

6. Cross-Monopole Case 2D

The impedance characteristics of cross-monopole Case 2D are shown in Figure 54. This structure is composed of a 24 mm vertical member loaded with two orthogonally

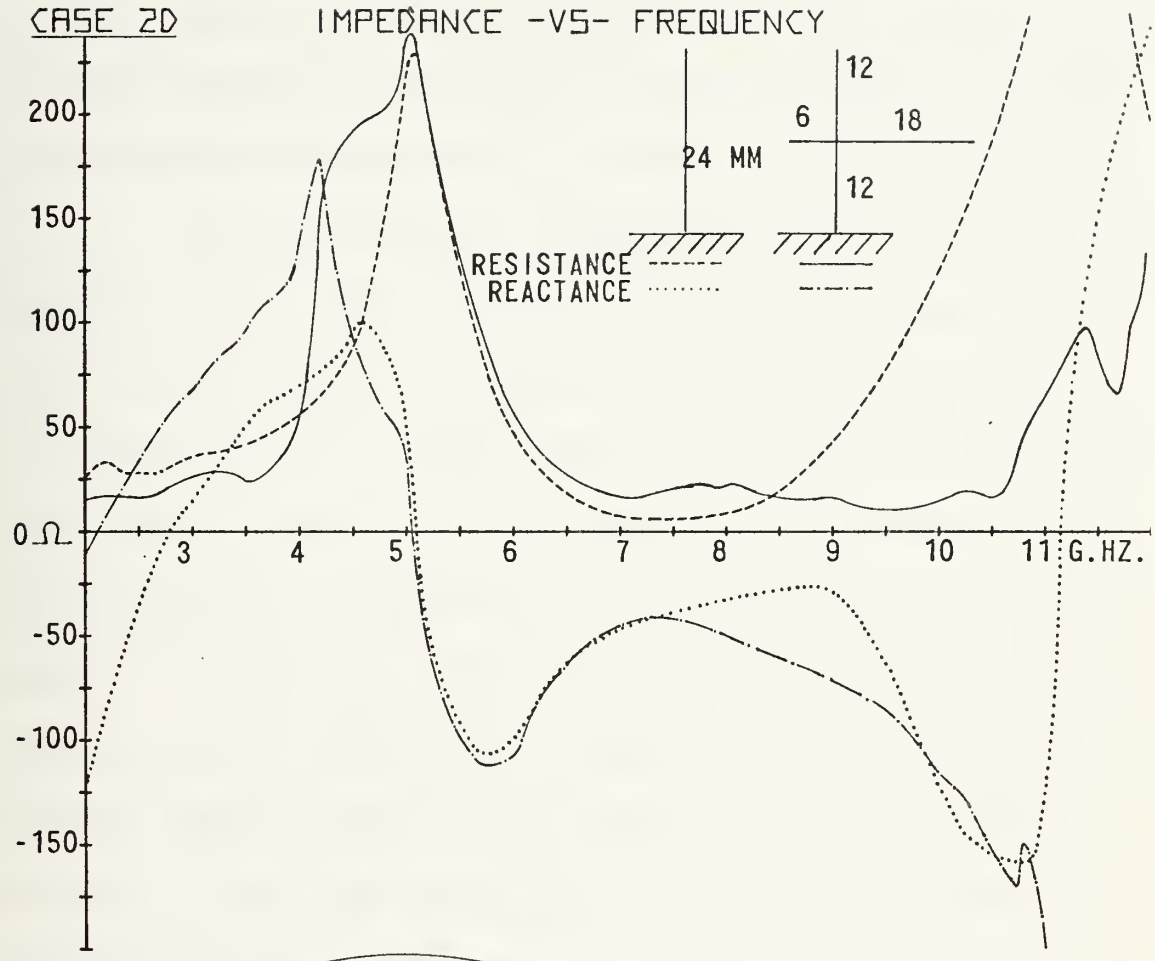

$R_o = 50\ \Omega$

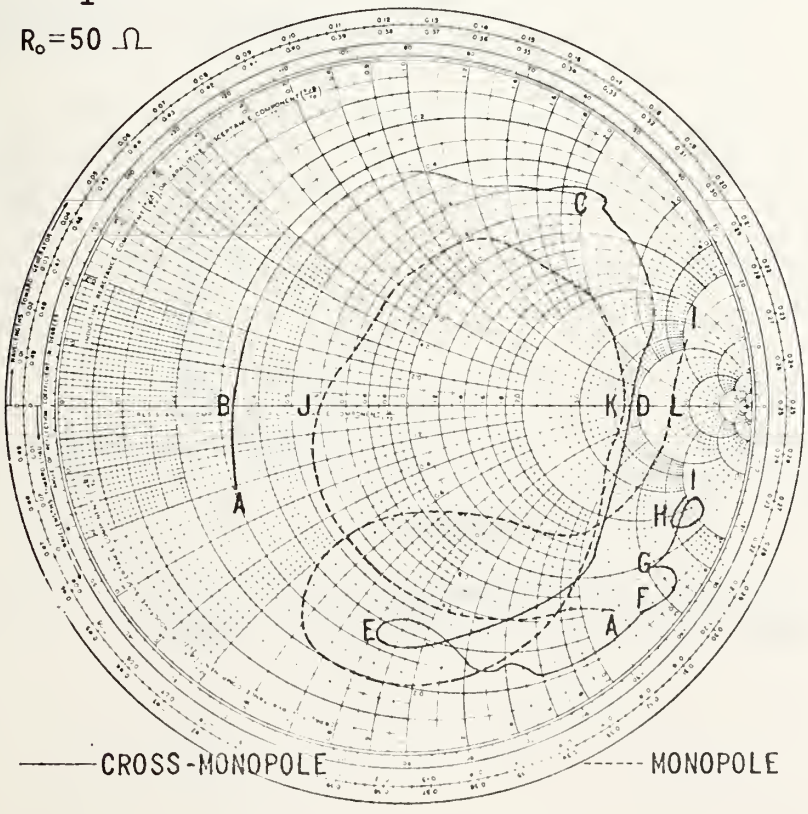

POINT	FREQUENCY
A	2.00 G.HZ.
B	2.12
C	3.73
D	5.07
E	7.31
F	10.30
G	10.80
H	11.80
I	12.00
J	2.78
K	5.09
L	11.14

——— CROSS-MONOPOLE ------ MONOPOLE

Figure 54

mounted arms 12 mm from the ground plane. This structure is the same as Case 2A but with the cross-arm offset by 6 mm providing one 18 mm and one 6 mm arm.

The structure is resonant at 2.12 GHz and anti-resonant at 5.07 GHz. These characteristics relate to a simple 24 mm monopole. There is a sharp perturbation in the impedance at 3.73 GHz. From Figure 40, it is seen that this frequency relates to the quarter-wave resonance of an 18 mm monopole. Consequently, it is assumed that a similar resonance is set up in the 18 mm arm of the cross at this frequency with strong mutual coupling between it and the vertical member producing the frequency lock-in effect. The associated standing wave patterns in the structure are sketched in Figure 55.

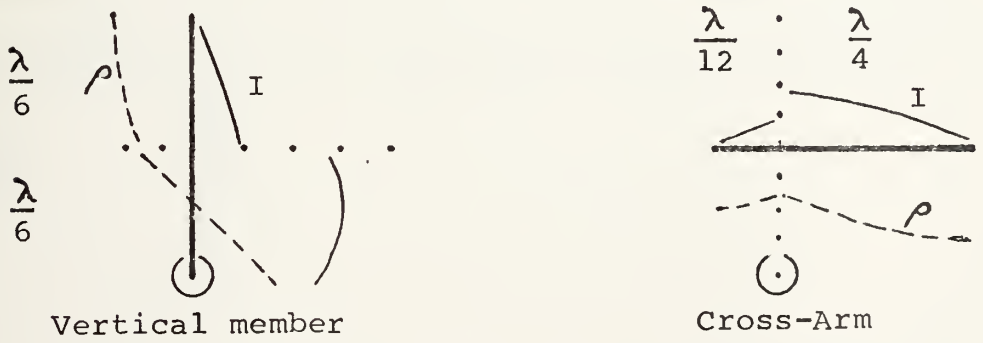

Figure 55

Current and charge distributions on cross-monopole Case 2D at 3.73 GHz

At this frequency, the 6 mm arm is electrically very short; therefore, the current distribution in this member is nearly linear, the current drawn from the junction is minimum, and coupling with the vertical member is slight. However, the upper vertical 12 mm member is one-sixth wavelength long at this frequency. Hence, although not resonant, the current distribution in this member is nearly sinusoidal. The junction location is again, neither a minimum nor maximum in the current and charge distributions.

A small unlabeled perturbation occurs at 9.00 GHz. This anomaly may be associated with the three-quarter wave resonance of the 24 mm vertical member. At this frequency, neither the 6 mm nor the 18 mm arm is a multiple of a quarter wavelength although nearly so; therefore, neither resonates. However, both draw current from the vertical member. The associated standing wave distributions are shown in Figure 56.

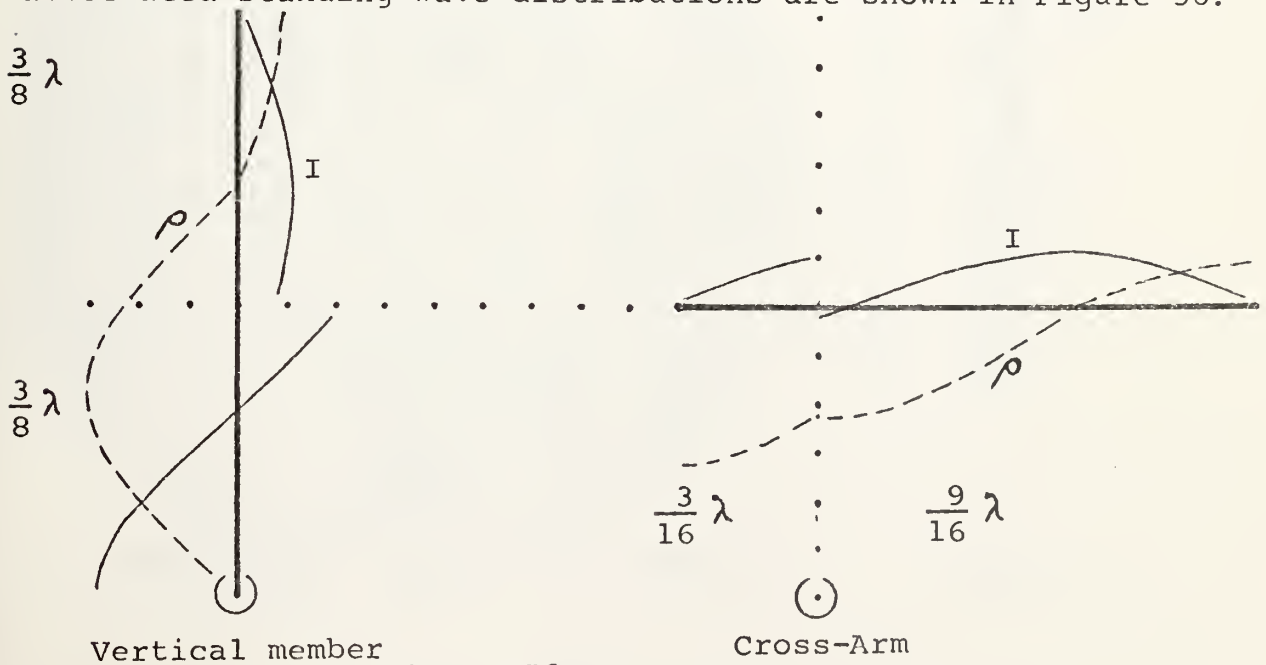

Figure 56
Current and charge distributions on Cross-monopole Case 2D at 9.00 GHz

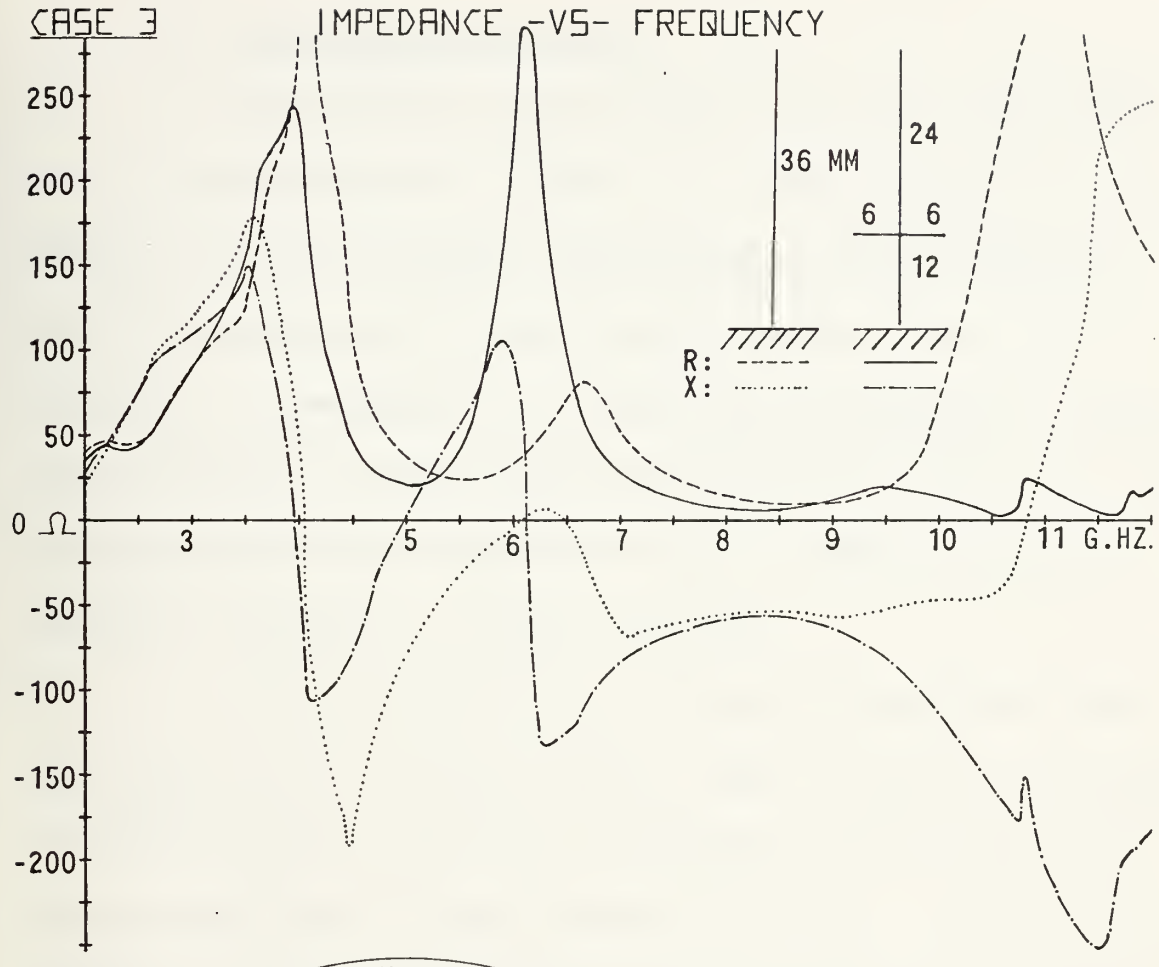

$R_o = 50\ \Omega$

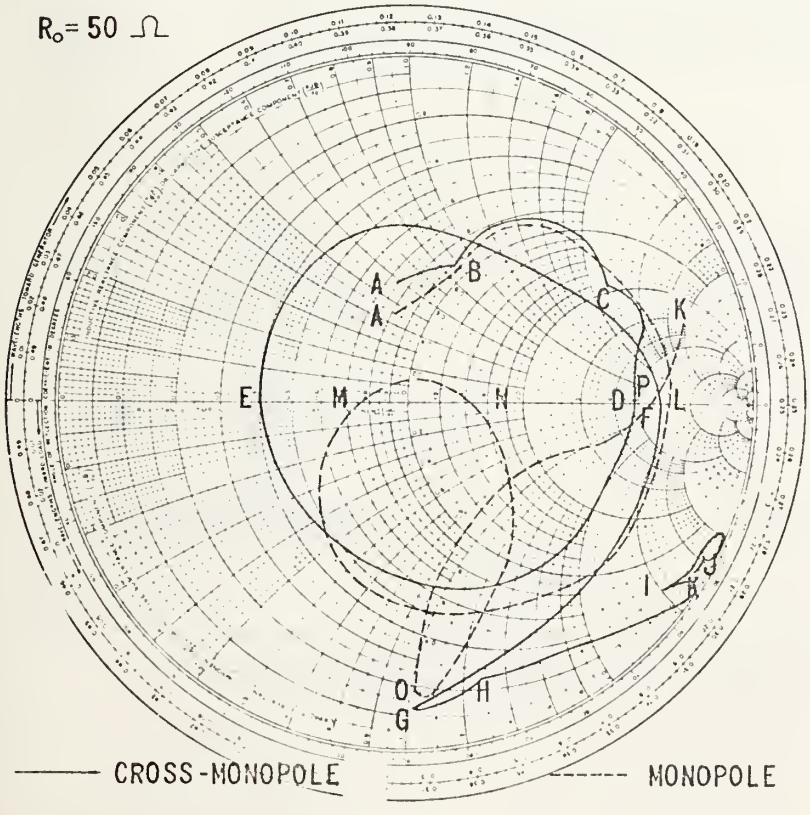

POINT	FREQUENCY
A	2.00 G.HZ.
B	2.16
C	2.93
D	3.95
E	4.98
F	6.12
G	8.50
H	9.00
I	10.80
J	11.80
K	12.00
L	4.05
M	6.07
N	6.49
O	8.50
P	10.86

——— CROSS-MONOPOLE ------ MONOPOLE

Figure 57

7. Cross-Monopole Case 3

The impedance characteristics of cross-monopole Case 3 are reproduced in Figure 57. The structure is composed of a 36 mm vertical member with a 12 mm cross-arm mounted symmetrically 12 mm from the ground plane. The structure is resonant at 4.98 GHz and antiresonant at 3.95 and 6.12 GHz. An examination of Figure 40 reveals that these characteristics are associative with a simple monopole of length in excess of 36 mm as expected.

The perturbation at 2.93 GHz is associated with the quarter-wave resonance of the upper vertical 24 mm member. At this frequency, there is a standing quarter wave on the 24 mm member with current maximum and charge minimum at the junction. The distributions on the structure are sketched in Figure 58.

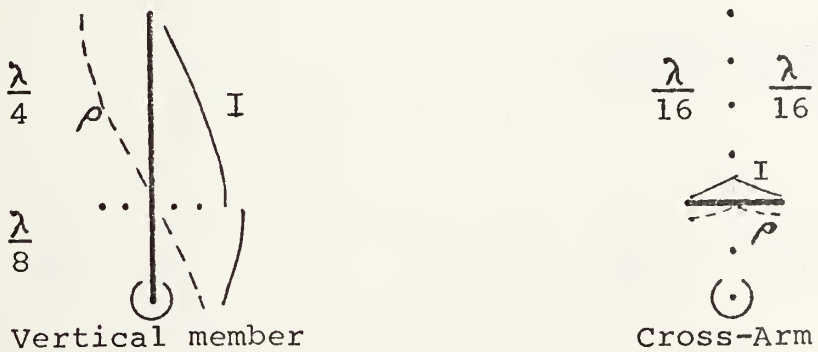

Figure 58

Current and charge distributions on cross-monopole Case 3 at 2.93 GHz

The 6 mm arms, being electrically short, draw little current and do not resonate. Hence, little coupling occurs near the junction.

The impedance perturbation at 9.00 GHz is related to the three-quarter wave resonance in the same upper vertical 24 mm member of the cross. The associated standing wave distributions are shown in Figure 59.

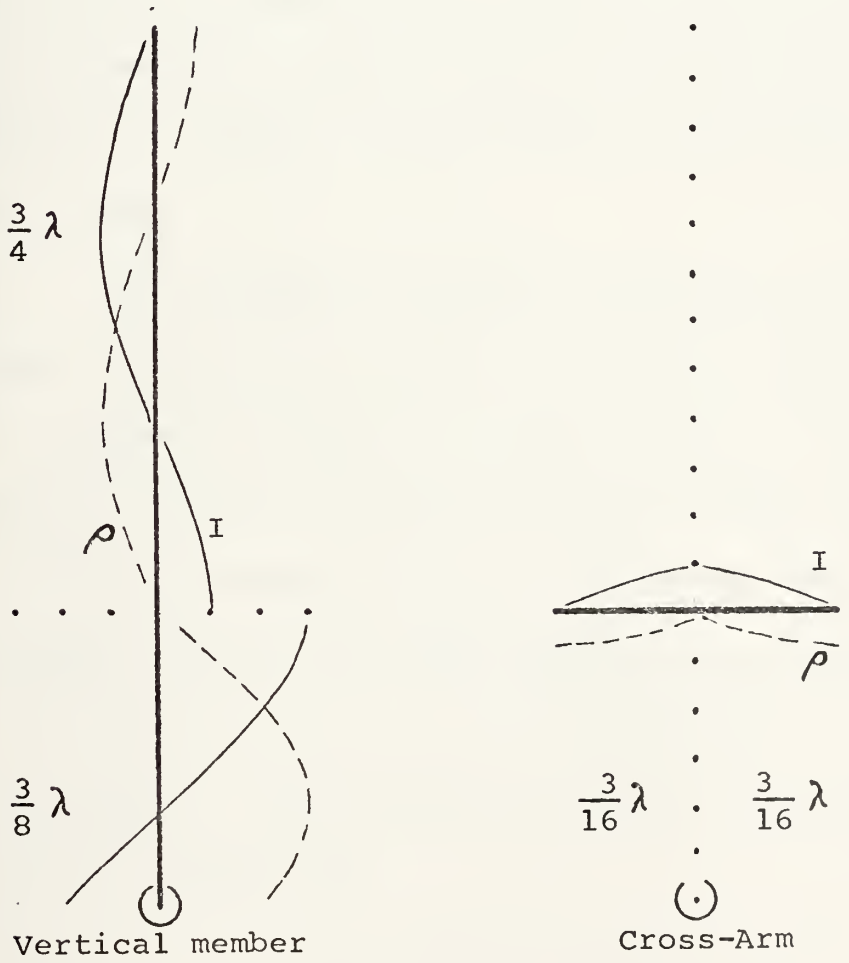

Figure 59

Current and charge distributions on cross-monopole Case 3 at 9.00 GHz

The junction is located at a current maximum and voltage minimum at this frequency. The 6 mm arms are nearly a quarter wavelength long; hence, draw significant current and couple strongly with the vertical member near the junction.

8. Cross Monopole Case 4

The impedance of cross-monopole Case 4 is shown in Figure 60 along with the simple monopole of equal height. The structure is composed of a 30 mm vertical member with a 24 mm cross-arm centered 18 mm from the ground plane. The structure is resonant at 8.44 GHz and antiresonant at 4.53 and 8.94 GHz.

The anomaly at point C in Figure 60, 3.73 GHz, is near the frequency at which an 18 mm monopole is quarter-wave resonant. Although the lower section of the vertical member is a quarter-wavelength long, boundary conditions forbid true resonance to occur. Therefore, the junction is at neither current nor charge maximum nor minimum. The current fed to the junction is divided between the upper three members. The associated standing waves on the structure are shown in Figure 61.

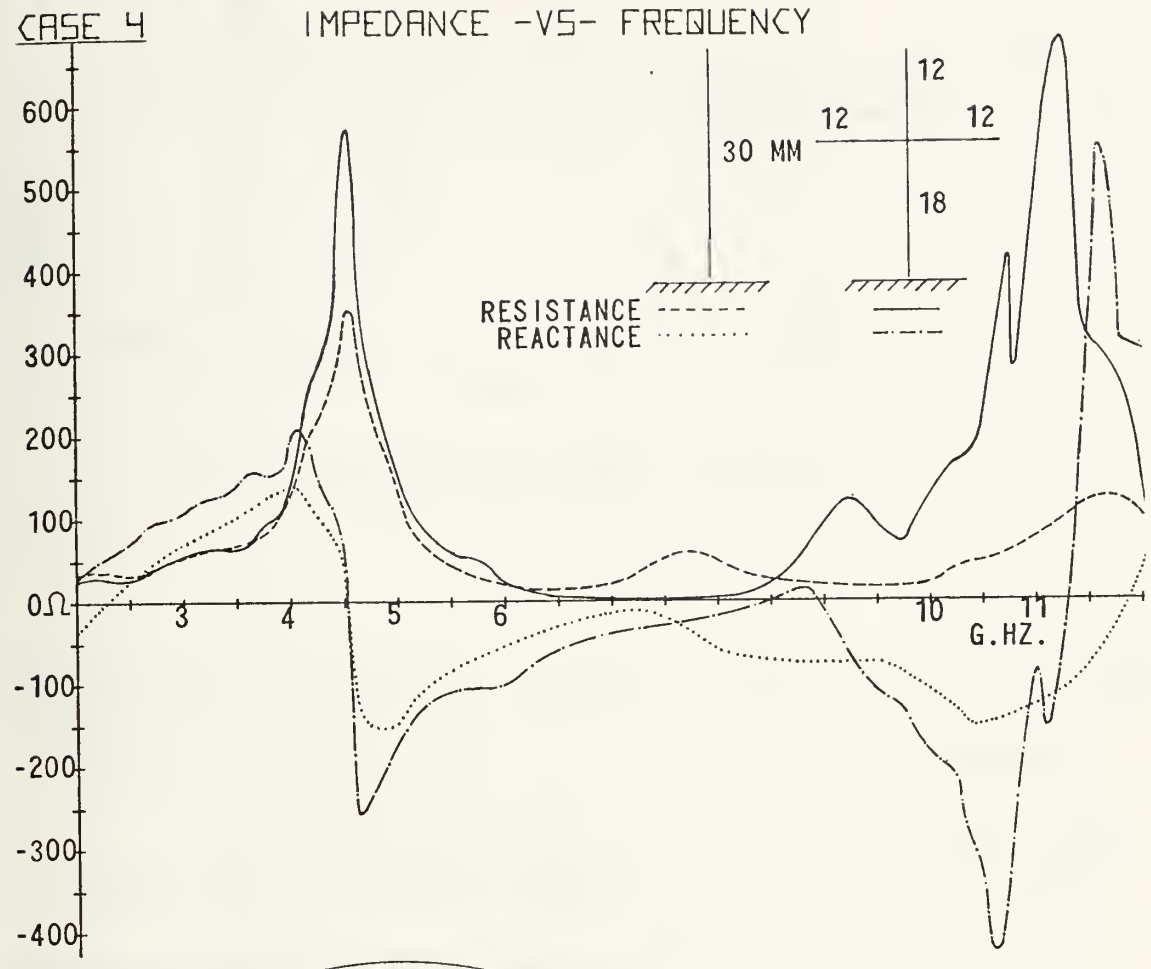

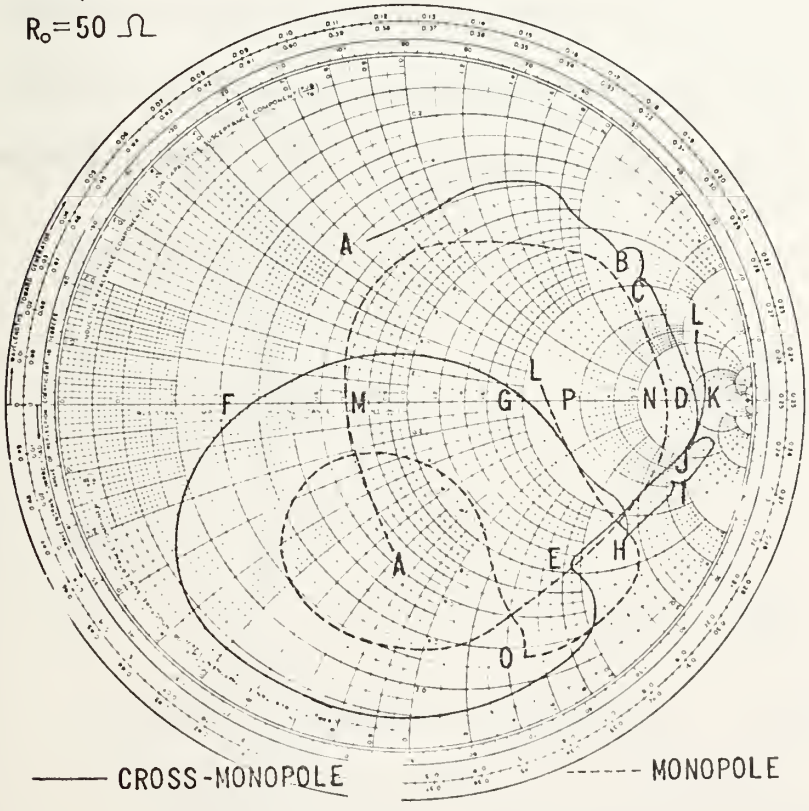

POINT	FREQUENCY
A	2.00 G.HZ.
B	3.33
C	3.73
D	4.53
E	5.58
F	8.44
G	8.94
H	9.75
I	10.25
J	10.80
K	11.30
L	12.00
M	2.29
N	4.52
O	9.25
P	11.86

Figure 60

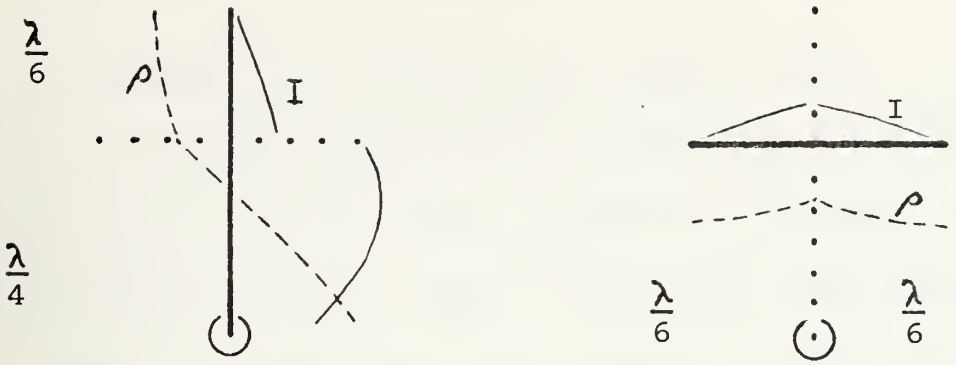

Figure 61

Current and charge distributions on cross-monopole Case 4 at 3.73 GHz

The junction is acting as a point of wave reflection at this frequency and coupling near the junction is only moderate.

Coupling is enhanced, however, at 5.58 GHz, point E in Figure 60. At this frequency, the 12 mm arms of the cross are quarter-wave resonant and are located on the vertical member at a current maximum/charge minimu. The standing waves on the structure are shown in Figure 62.

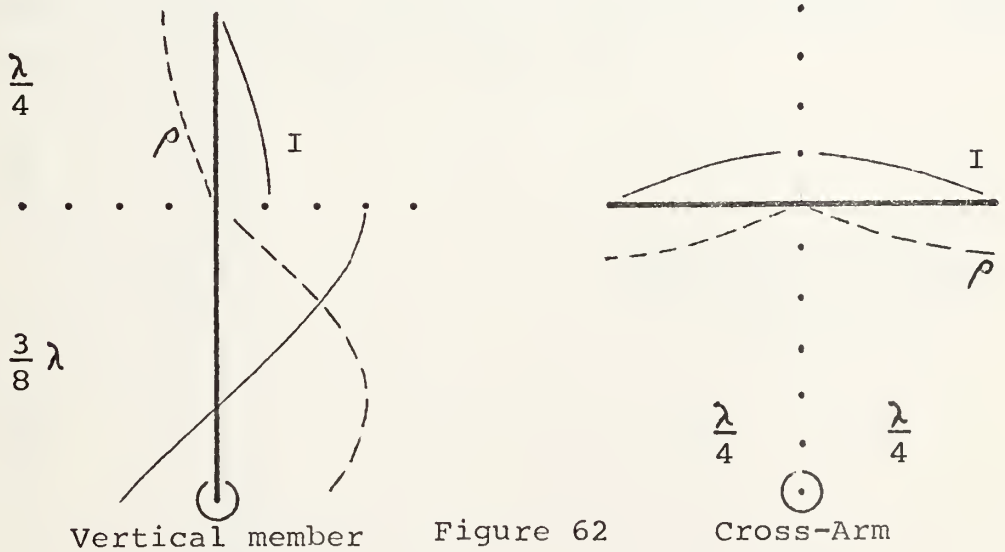

Figure 62

Current and charge distributions on cross-monopole Case 4 at 5.58 GHz

The current into the junction from the lower vertical member is a maximum and is divided between the three 12 mm members; the junction sees a short circuit as it looks into each of the three members. Hence, the current magnitude into the base of the structure peaks exactly at 5.58 GHz causing a sharp dip in the reflection coefficient. This frequency lock-in effect is accompanied by strong coupling between the members near the junction of the cross.

The anomaly at 9.75 GHz indicates three-quarter wave resonance in the lower vertical 18 mm member. At this frequency, the 12 mm members are half-wave antiresonant. The junction sees an open circuit into these three upper members. Hence, the 12 mm members draw only a small amount of current and the junction region provides a reflection point to support the standing wave in the lower member. There is capacitive coupling near the junction. The distributions are sketched in Figure 63.

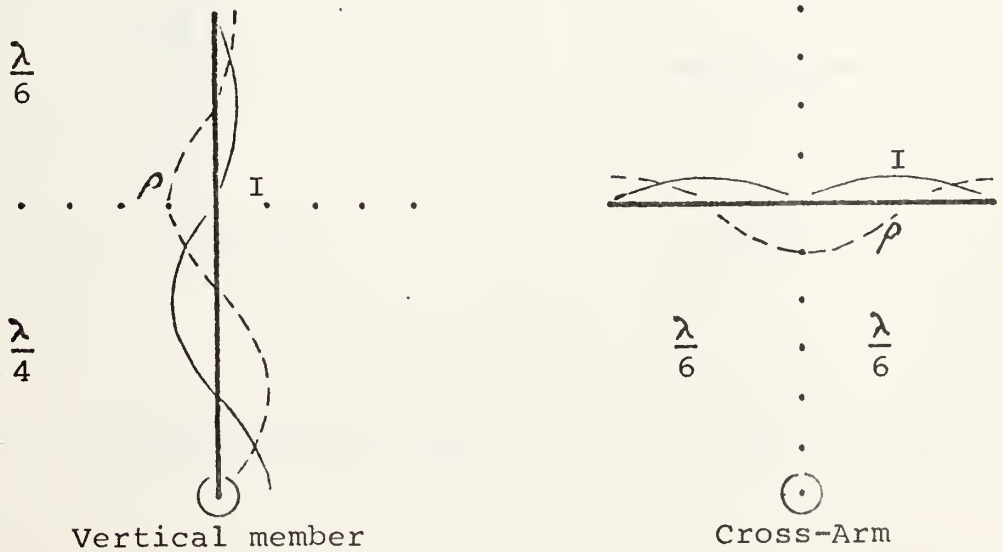

Figure 63
Current and charge distributions on cross-monopole Case 4 at 9.75 GHz

9. Cross-Monopole Case 5

The impedance characteristics of cross-monopole Case 5 are reproduced in Figure 64. The cross is composed of a 42 mm vertical member with a 24 mm cross-arm centered 18 mm above the ground plane. The structure is resonant at 3.79 and 8.41 GHz, and antiresonant at 3.52, 5.02, and 8.95 GHz; the characteristics of a simple monopole considerably longer than 42 mm.

The impedance perturbation at 5.32 GHz is related to the quarter-wave resonance of the two 12 mm arms. At this frequency, the junction sees a short circuit when looking into the arms and an open circuit into the 24 mm upper vertical member which is half-wave antiresonant. The standing wave distributions are shown in Figure 65.

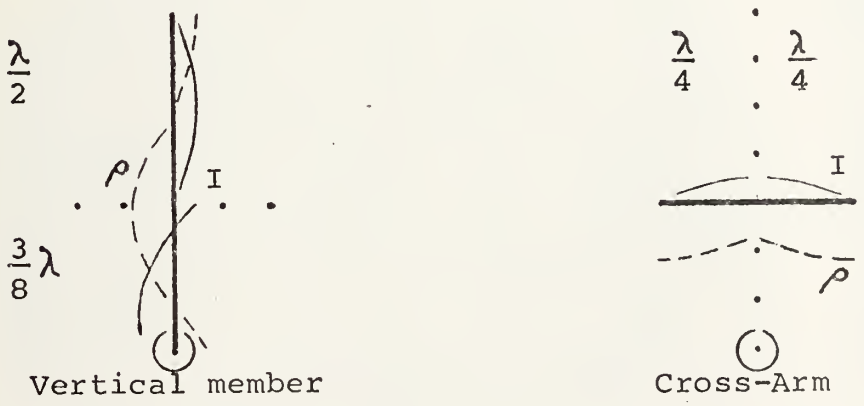

Figure 65

Current and charge distributions on cross-monopole Case 5 at 5.32 GHz

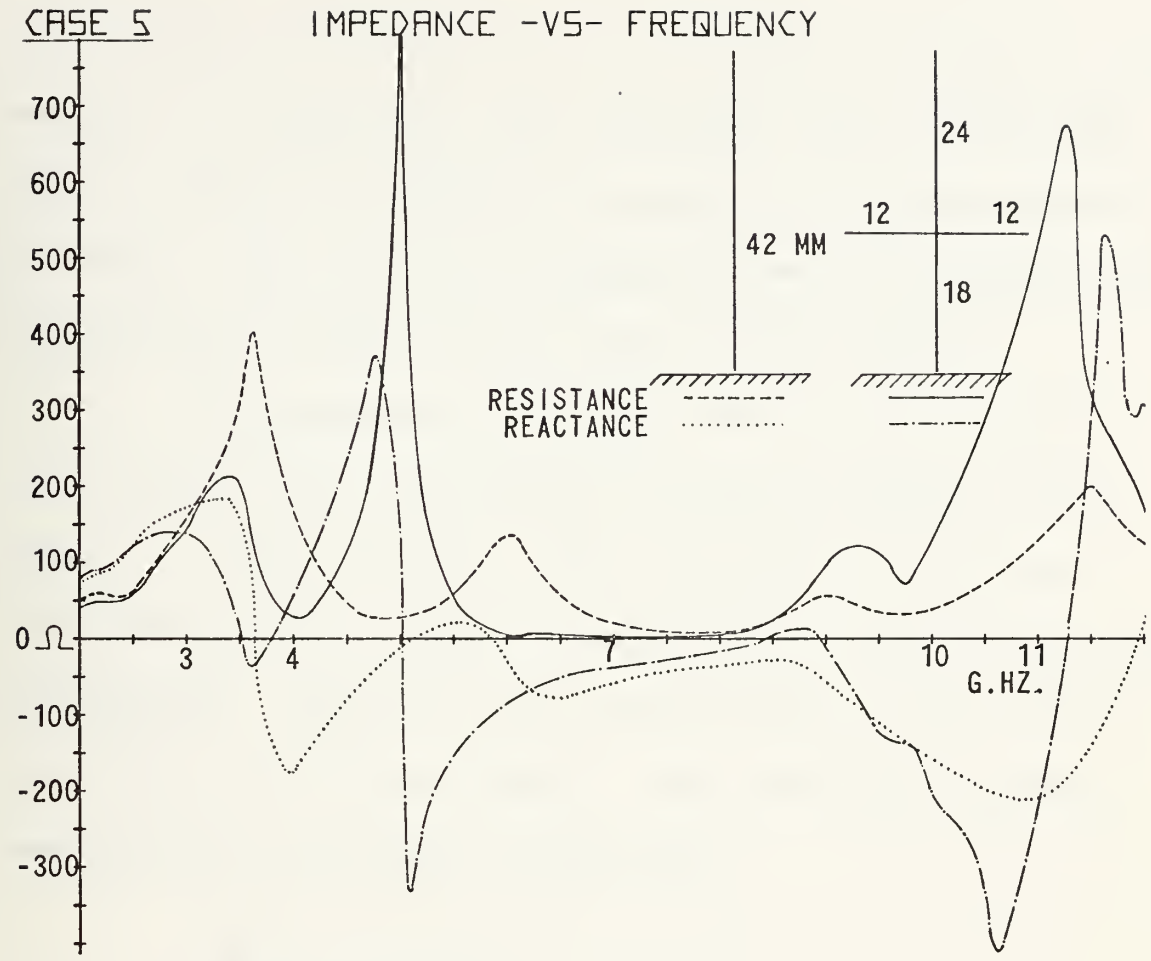

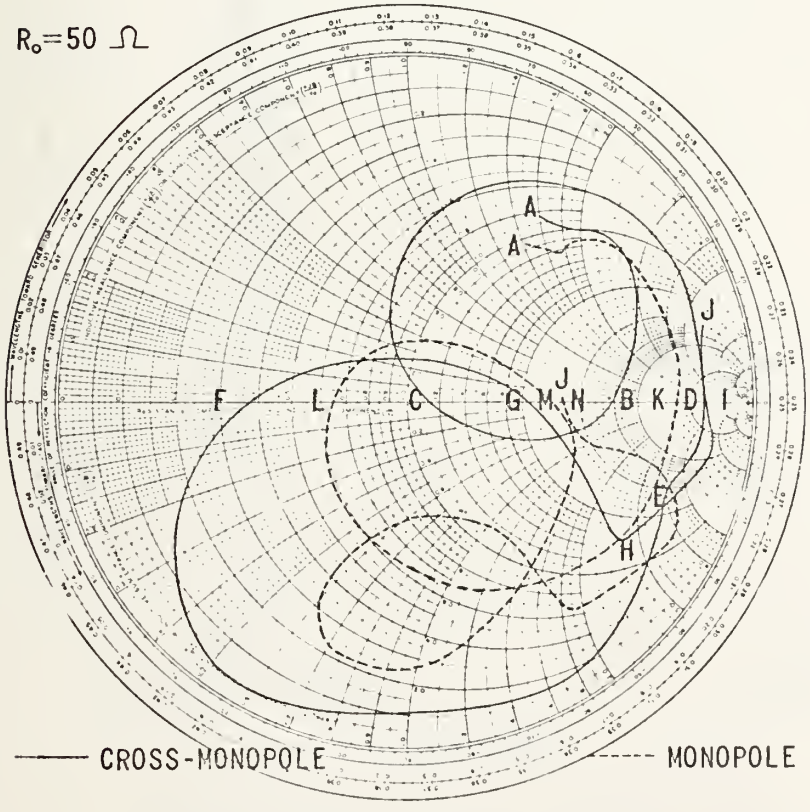

POINT	FREQUENCY
A	2.00 G.HZ.
B	3.52
C	3.79
D	5.02
E	5.32
F	8.41
G	8.95
H	9.75
I	11.25
J	12.00
K	3.64
L	5.14
M	5.86
N	11.97

Figure 64

The position of the junction is a current minimum and charge maximum. Consequently, even though the arms are resonant, little current is available to support their standing waves. Therefore, there is little coupling between the members near the junction and the lock-in effect is not enhanced.

The perturbation at 9.75 GHz is related to the three-quarter wave resonance in the lower vertical 18 mm member. At this frequency, the 12 mm arms are half-wave antiresonant and the upper vertical 24 mm member is full-wave antiresonant. Therefore, the junction sees an open circuit when looking into these members. The associated standing wave patterns are shown in Figure 66.

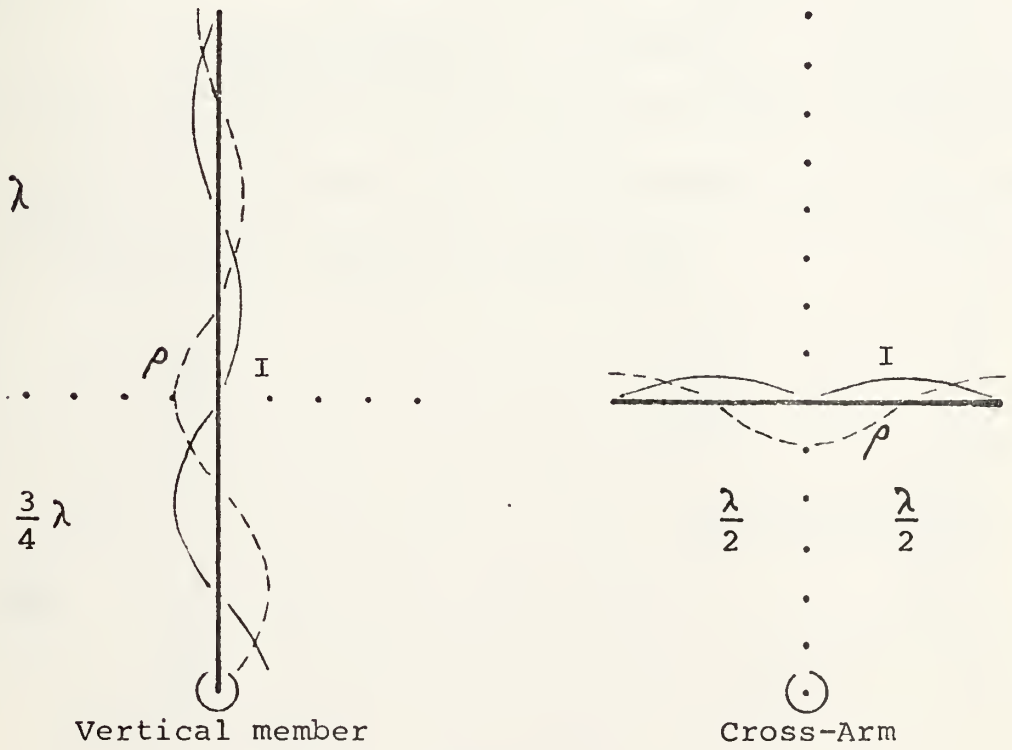

Figure 66

Current and charge distributions on cross-monopole Case 5 at 9.75 GHz

Since the junction is at a current minimum and charge maximum in all members of the structure, there is capacitive coupling; the junction region acting as a point of wave reflection to support resonance in the lower member. Therefore, the perturbation in impedance is caused by a maximization of the current to voltage ratio at the feed point.

10. Cross-Monopole Case 6A

The impedance of cross-monopole Case 6A is reproduced in Figure 67. The cross is composed of a 21 mm vertical member with one 6 mm and one 12 mm arm attached colinearly, orthogonal to the vertical member, 9 mm from the ground plane. The resonant frequency of the structure is 2.70 GHz and the antiresonant frequency is 5.69 GHz.

The perturbation in impedance linearity at 3.38 GHz is associated with the quarter-wave resonance of the vertical 21 mm current path. The standing wave patterns on the structure are shown in Figure 68.

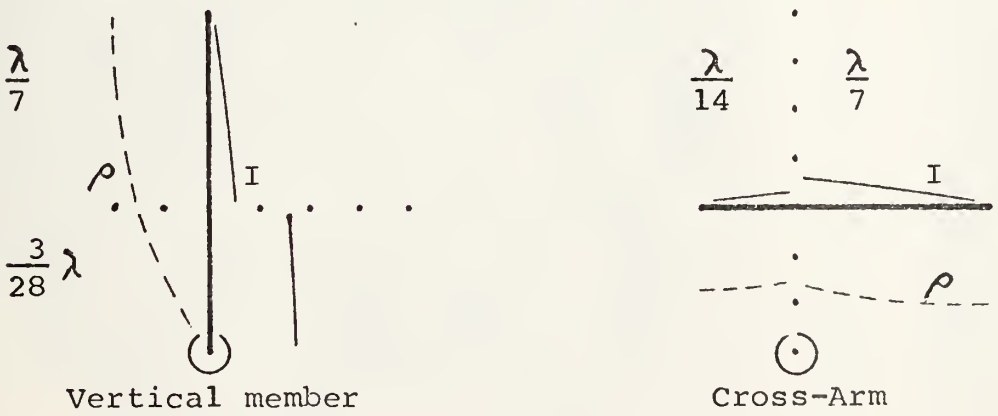

Figure 68

Current and charge distributions on cross-monopole Case 6A at 3.38 GHz

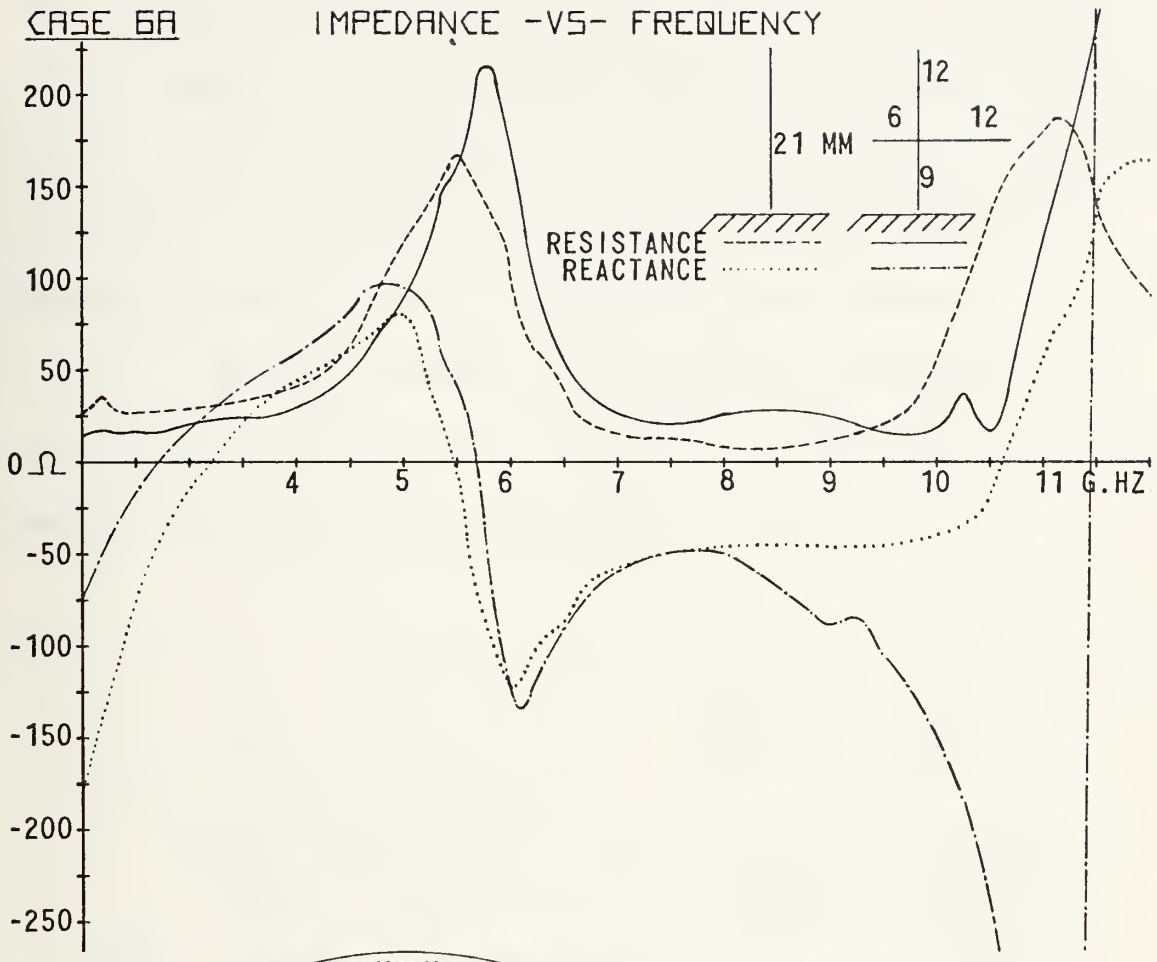

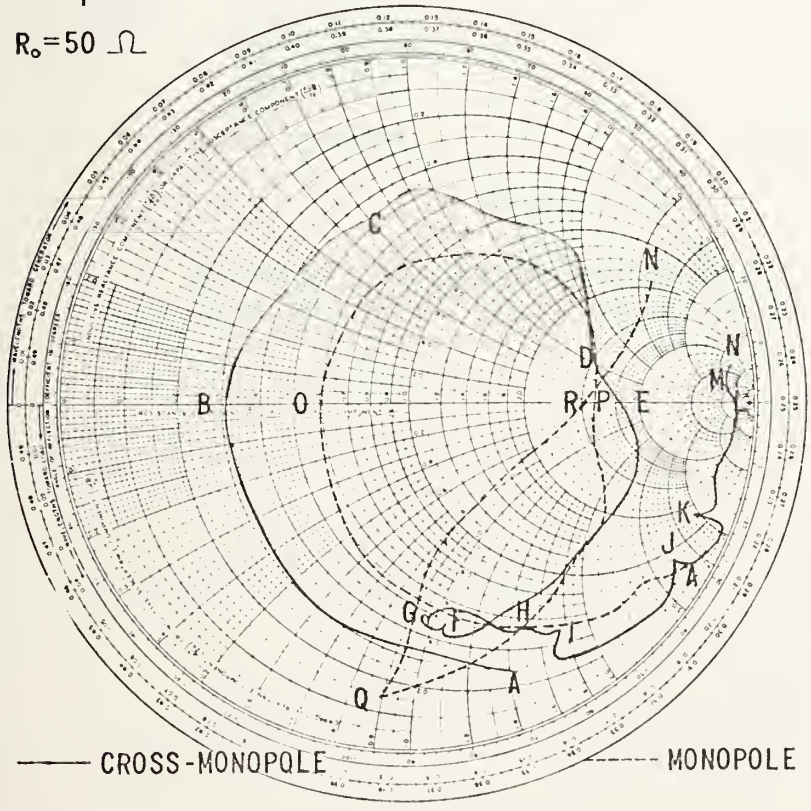

POINT	FREQUENCY
A	2.00 G.HZ.
B	2.70
C	3.38
D	5.44
E	5.69
F	7.36
G	7.75
H	8.70
I	9.00
J	10.25
K	10.80
L	11.47
M	11.80
N	12.00
O	3.21
P	5.47
Q	8.50
R	10.60

—— CROSS-MONOPOLE ----- MONOPOLE

Figure 67

The 6 mm arm is electrically very short; hence, draws very little current. The 12 mm arm and the 12 mm upper vertical member share the remaining current between them. Since the junction is at neither a current nor charge maximum nor minimum, coupling at the junction is only moderate.

The perturbation at 5.44 GHz is related to the quarter-wave resonance of the 12 mm arm and upper vertical member. The wave forms are shown in Figure 69.

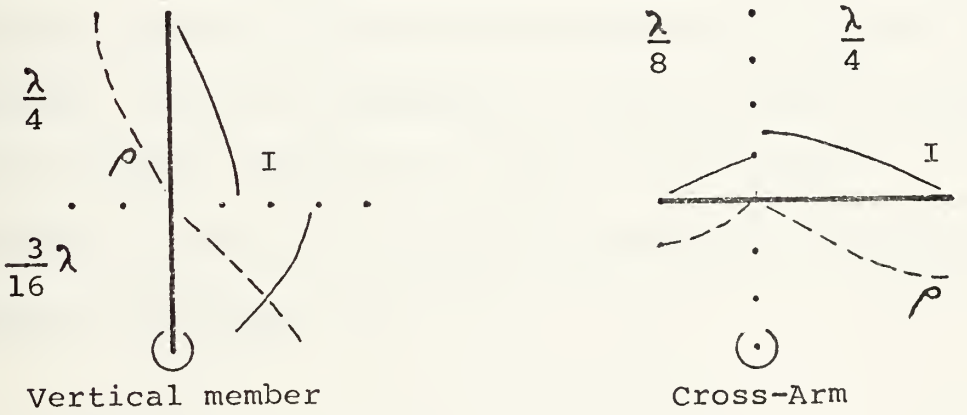

Vertical member Cross-Arm

Figure 69

Current and charge distributions on cross-monopole Case 6A at 5.44 GHz

The 6 mm arm is electrically short at this frequency; therefore, it draws little current from the junction. The 12 mm members couple strongly at the junction, their natural resonant frequency being equal to the driven frequency. The frequency lock-in effect is moderate but not maximum since the standing wave conditions at the feed point of the structure are not ideal.

The impedance nonlinearity at 10.80 GHz is associated with the quarter-wave resonance of the 6 mm arm with the related half-wave antiresonance of the two 12 mm members. The driven frequency of the structure is equal to the natural frequency of three of its members. A qualitative sketch of the standing wave distributions is presented in Figure 70.

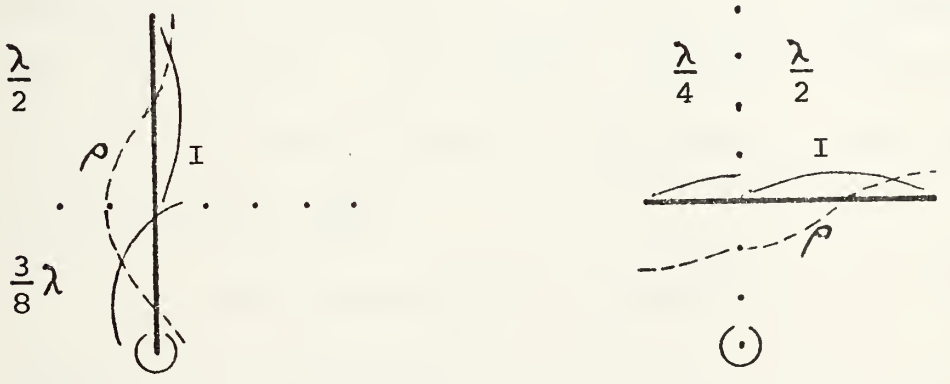

Vertical member

Cross-Arm

Figure 70

Current and charge distributions on cross-monopole Case 6A at 10.80 GHz

The junction is a point of minimum current and maximum charge. The junction sees an open circuit when looking into the 12 mm members but a short circuit into the 6 mm arm. However, the junction conditions do not provide much current to feed the 6 mm short circuit; therefore, even though the 6 mm arm is quarter-wave resonant, coupling is slight in the junction region.

11. Cross-Monopole Case 6B

The impedance characteristics of cross-monopole Case 6B are reproduced in Figure 71. The cross is made of a 42 mm vertical member with one 12 mm and one 24 mm arm attached colinearly, orthogonal to the vertical member, 18 mm from the ground plane. The dimensions of this structure are exactly double those of Case 6A shown in Figure 67. The structure is resonant at 4.09 GHz and antiresonant at 3.95 and 4.70 GHz. As expected, these characteristics are related to a simple monopole considerably longer than the 42 mm vertical member.

The non-linearity in impedance at 2.80 GHz is related to the quarter-wave resonance in the 24 mm arm and upper section of the vertical members. At this frequency, the 12 mm arm is electrically short; therefore, draws little current which is nearly linearly distributed along its length. The standing wave patterns are shown in Figure 72.

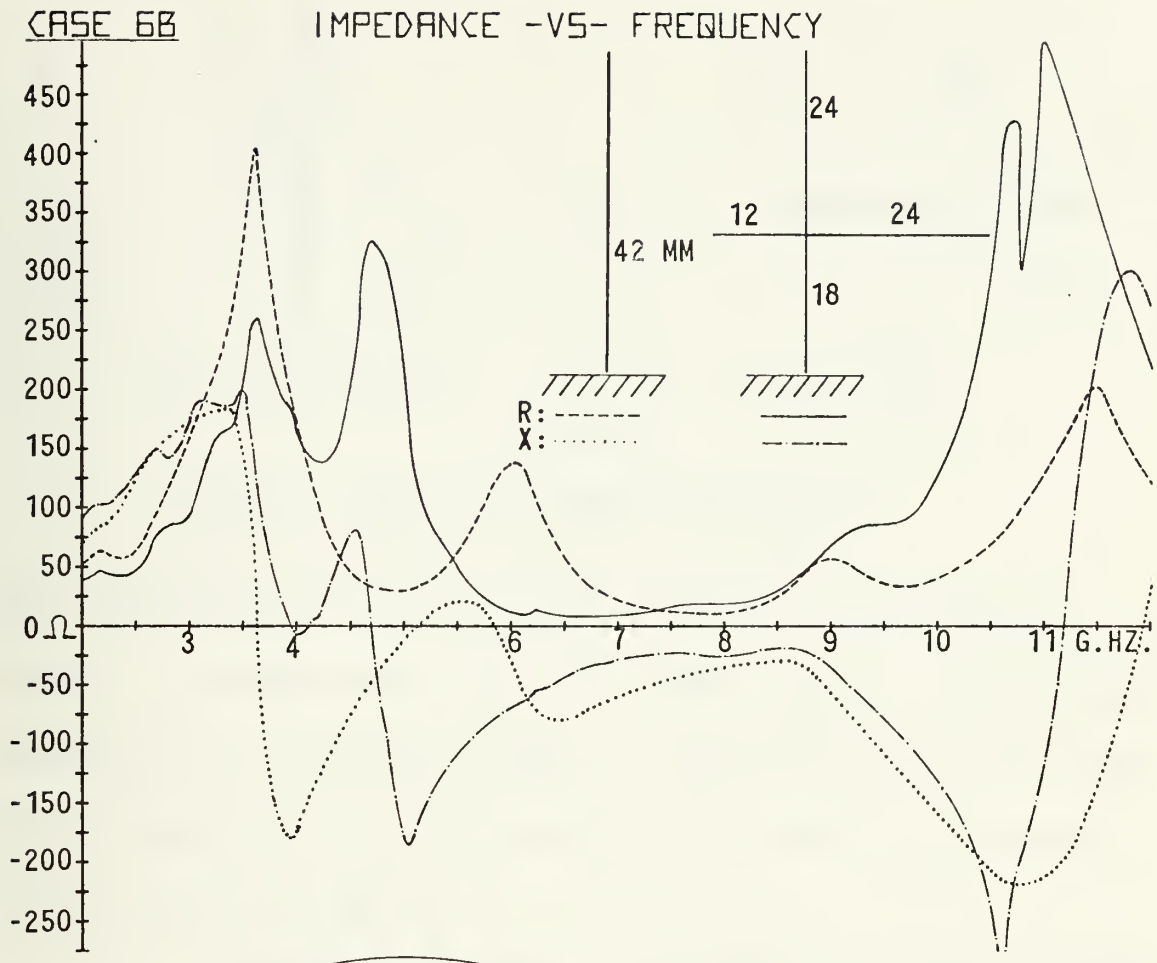

$R_o = 50\ \Omega$

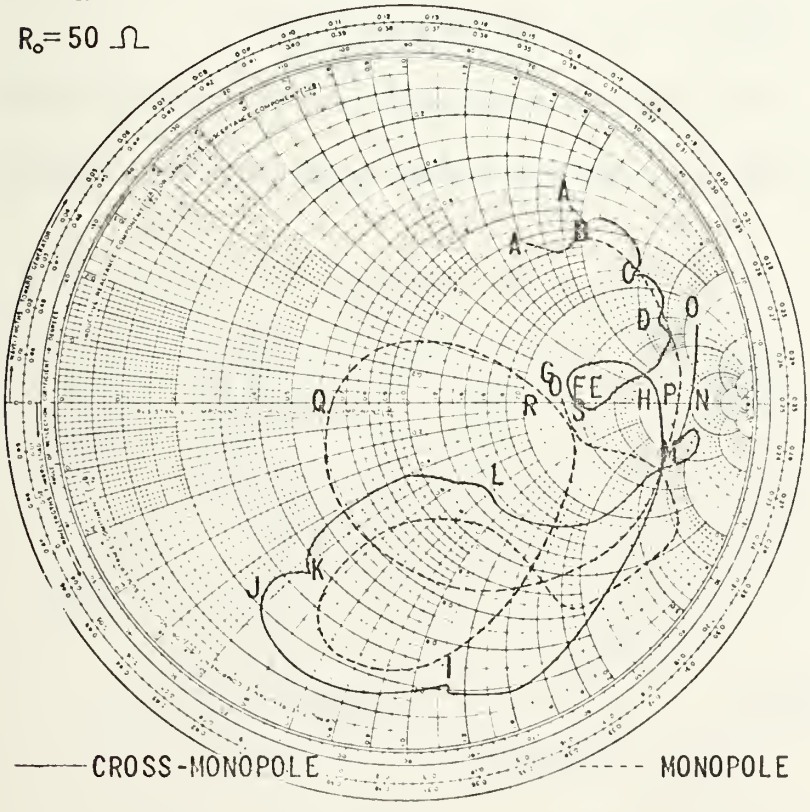

POINT	FREQUENCY
A	2.00 G.HZ.
B	2.17
C	2.80
D	3.38
E	3.95
F	4.09
G	4.25
H	4.70
I	6.21
J	7.13
K	7.76
L	9.00
M	10.80
N	11.19
O	12.00
P	3.64
Q	5.14
R	5.86
S	11.97

——— CROSS-MONOPOLE ----- MONOPOLE

Figure 71

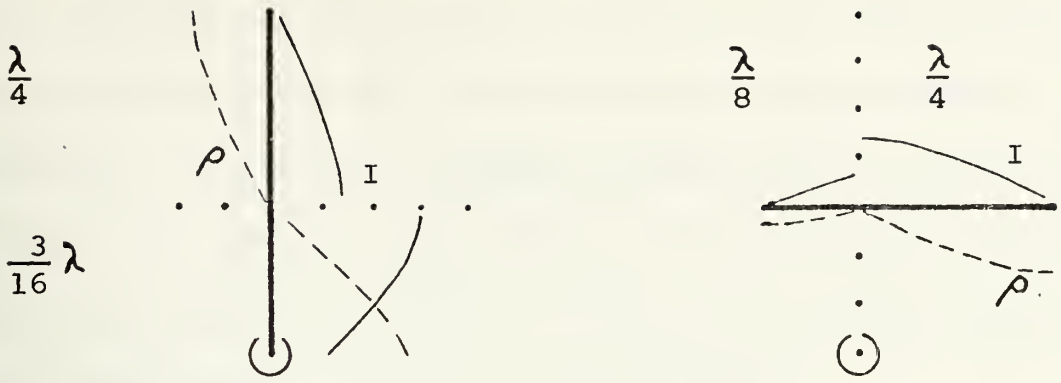

Figure 72

Current and charge distributions on cross-monopole Case 6B at 2.80 GHz

The junction is a point of maximum current and minimum charge. Consequently, there is strong coupling between the members in the junction region. The reflection coefficient at the feed point is minimized and the familiar frequency lock-in effect results.

The perturbation at 9.00 GHz is related to the three-quarter wave resonance of the 24 mm members. The associated standing waves are as represented in Figure 73.

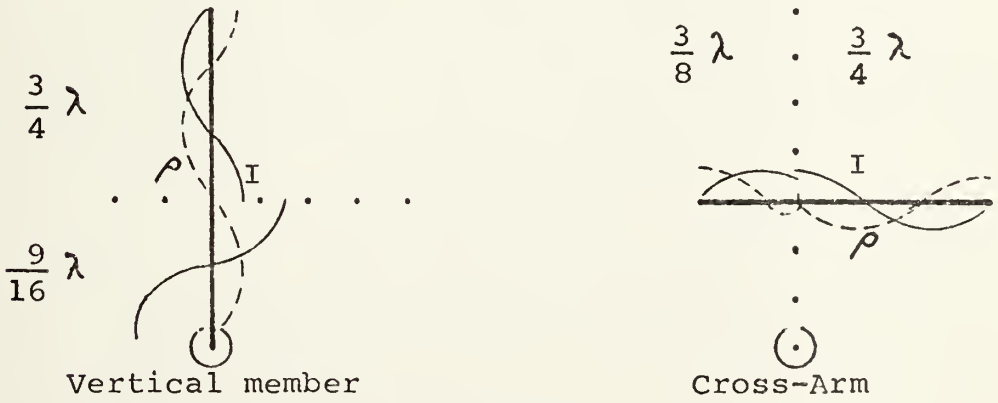

Figure 73

Current and charge distributions on cross-monopole Case 6B at 9.00 GHz

The junction, in this case, is a point of maximum current and minimum charge with two of the three upper members resonant. Therefore, coupling is maximized in the junction region. In general, the resonance characteristics of cross-monopole Case 6B are similar to those of 6A since the wire structure member lengths are proportional.

VII. CONCLUSIONS

The conditions which generate a local minimization of the reflection coefficient at the feed point of a cross-monopole antenna and the observable perturbation in impedance linearity with frequency are maximum current and minimum charge at the cross junction on the base member and one or more other members of the cross. At this para-resonant frequency, current flow into the upper members is maximized producing the frequency lock-in effect. This effect is permitted if the coupled members are a quarter or three-quarters of a wavelength long.

Less enhanced effects occur when the vertical member, the upper section of the vertical member, or either arm of the cross has linear dimensions consistent with quarter wave or three-quarter wave resonance, even though the other members are not resonant. Also, if all upper members of the cross are antiresonant and the lower section of the vertical member is resonant, minor effects will occur.

In each case, the intensity and sharpness of the impedance perturbation is a function of the coupling in the junction region.

VIII. RECOMMENDATIONS

Extend the investigation of impedance characteristics at frequencies for which the lower vertical member alone and the lower vertical member plus each arm of the cross-monopole antenna is quarter-wave and three-quarter wave resonant.

Extend the study to more complicated wire structures concentrating on frequency ranges near those expected for frequency lock-in effects.

Extend the study to thick wires from which notches have been cut. It is expected that lock-in effects will occur when these notches coincide with positions of maximum charge/minimum current and maximum current/minimum charge. The results of such a study could result in a simple method for control of the bandwidth of wire antennas.

Develop the unified theory, mathematics, and equivalent circuits for complex wire structures with resonant members.

BIBLIOGRAPHY

1. Burton, R.W., "The Crossed-Dipole Structure of Aircraft in an Electromagnetic Pulse Environment", Proceedings of the Conference on Electromagnetic Noise, Interference and Compatibility Advisory Group for Aerospace Research and Development (AGARD), NATO, pp. 30-1 thru 30-15, Paris, France, October 1974.

2. Burton, R.W. and King, R.W.P., "Measured Currents and Charges on Thin Crossed Antennas in a Plane Wave Field", IEEE Transactions on Antennas and Propagation (to be published).

3. Butler, C.M., "Currents Induced on a Pair of Skew Crossed Wires", IEEE Transactions On Antennas and Propagation, Vol, 20, pp 731-736, November 1972.

4. Chao, H.H. and Strait, B.J., "Radiation and Scattering Configurations of Bent Wires with Junctions", IEEE Transactions on Antennas and Propagation, Vol. 19, pp. 701-702, September 1971.

5. Hewlett-Packard Application Note 117-1, Microwave Network Analyzer Applications, pp. 8.7-8.9, June 1970.

6. Jordan, E.C. and Balmain, K.G., Electromagnetic Waves and Radiating Systems, pp. 202-205, Prentice-Hall, Inc., 1968.

7. King, D.D., "Measured Impedance of Cylindrical Dipoles", Journal of Applied Physics, p. 844, Vol. 17, 1946.

8. King, R.W.P., The Theory of Linear Antennas, pp. 86-87, 152-153, 171-173, Harvard University Press, 1956.

9. King, R.W.P., Transmission Line Theory, pp. 430-437, McGraw Hill, 1955.

10. King, R.W.P. and Wu, T.T., Analysis of Crossed Wires in a Plane-Wave Field, Tech. Rept. No. 653, Division of Engineering and Applied Physics, Harvard University, July 1974.

11. Ramo, S., Whinnery, J.R., and Van Duzer, T.V., Fields and Waves in Communications Electronics, pp. 254-293, Wiley, 1965.

12. Taylor, C.D., Lin, S.M., and McAdams, H.V., "Scattering from Crossed Wires", IEEE Transactions on Antennas and Propagation, Vol. 18, pp. 133-136, January 1970.

INITIAL DISTRIBUTION LIST

		No. Copies
1.	Defense Documentation Center Cameron Station Alexandria, Virginia 22314	2
2.	Library, Code 0212 Naval Postgraduate School Monterey, California 93940	2
3.	Department Chairman, Code 52 Department of Electrical Engineering Naval Postgraduate School Monterey, California 93940	2
4.	Professor R.W. Burton, Code 52Zn Department of Electrical Engineering Naval Postgraduate School Monterey, California 93940	10
5.	Professor R.W. Adler, Code 52AB Department of Electrical Engineering Naval Postgraduate School Monterey, California 93940	1
6.	Professor J.B. Knorr, Code 52Ko Department of Electrical Engineering Naval Postgraduate School Monterey, California 93940	1
7.	Mr. W.M. Chase Naval Electronics Laboratory Center Code 2120 San Diego, California 92152	1
8.	LCDR R.C. Spencer, USN Naval Ordnance Missile Test Facility White Sands Missile Range New Mexico 88002	2

Thesis
S6678 Spencer
c.1
161077
Resonance of electro-
magnetic waves on cross-
monopole wire structures.